MODELLING AND FUZZY LOGIC CONTROL OF NEONATAL OXYGEN THERAPY

by

Edmund Pavel (Paul) Morozoff, P.Eng.

B.A.Sc. University of British Columbia 1989

THESIS SUBMITTED IN PARTIAL FULFILMENT OF THE REQUIREMENTS FOR THE DEGREE OF MASTER OF APPLIED SCIENCES

in the Department

of

Engineering Science

SIMON FRASER UNIVERSITY

December, 1996

National Library of Canada
Acquisitions and Bibliographic Services
395 Wellington Street
Ottawa ON K1A 0N4
Canada

Bibliothèque nationale du Canada
Acquisitions et services bibliographiques
395, rue Wellington
Ottawa ON K1A 0N4
Canada

Your file Votre référence

Our file Notre référence

0-612-24210-2

Canada

APPROVAL

Name: Edmund P. Morozoff

Degree: Master of Applied Science

Title of

Thesis: MODELLING AND FUZZY LOGIC CONTROL OF NEONATAL OXYGEN THERAPY.

Examining Committee:

Chairman : Dr. Jim Cavers
School of Engineering Science, SFU

Dr. Mehrdad Saif
Senior Supervisor
Assistant Professor
School of Engineering Science, SFU

Dr. Tom Richardson
Supervisor
Associate Professor
Department of Kinesiology, SFU

Dr. Tom Calvert
External Examiner
Professor
Department of Kinesiology and School of Engineering Science, SFU

Date Approved: Dec. 20/96

ABSTRACT

Adequate tissue oxygenation can be impaired in neonates who have under-developed lungs. Systemic arterial blood oxygen saturation (SaO_2) is an indicator of tissue oxygenation and its low level can result in tissue damage associated with hypoxemia. Retinopathy of prematurity and bronchopulmonary dysplasia are diseases associated with exposure to high inspired oxygen levels. Oxygen therapy is the administration of an air/oxygen gas mixture in an effort to regulate arterial oxygen levels and thus control tissue oxygenation. The blood oxygen saturation level from a pulse oximeter, SpO_2, indicates SaO_2 and an automatic SpO_2 controller is recommended as an assistant to nursing staff. A computer driven model of the neonate's oxygen transport system, accommodating bi-directional gas flow in the pulmonary system and pulmonary/cardiac shunts in the circulatory system, was developed for testing several algorithms. Programs modelling one hour of physical behaviour of three types of neonates are produced. Manual control is based on clinical observations and a PID controller's gain values are selected from empirical data. Two fuzzy logic based controllers are designed - non-linear (FL) and non-linear with artifact detection (FLA). All four algorithms were run through the neonate models and distributions of time spent by the models at various SpO_2 levels were used as a comparison method. The PID algorithm provided better control than manual mode and the FL controller was better than both. The FLA controller was slightly better than FL control. In summary, a fuzzy logic controller with artifact detection provided better oxygen therapy for software neonatal models than standard fuzzy logic, PID or manual control.

Acknowledgements

The first people I must acknowledge are Dr. John Smyth and the excellent clinical staff of the Special Care Nursery at British Columbia's Children's Hospital. Dr. Smyth first promoted this work in 1989 and has provided assistance every since. I would also like to thank Dr. Mehrdad Saif for the time, effort and continuous support he gave me as my senior supervisor. Most importantly, I thank my wife, Cary, who has always provided love and understanding.

Table of Contents

Table of Contents Cont'd

Table of Contents Cont'd

List of Tables

List of Figures

List of Figures Cont'd

List of Figures Cont'd

List of Figures Cont'd

Preface

At the age of 16 my engineering career began as a millwright's helper in the sawmills of the Canadian westcoast. Men with blackened sausage shaped fingers working together in harsh conditions to maintain machines the size of small forests. These initial experiences led me into civil and structural engineering where the scale of my projects - highways, airport runways and farmland drainage - remained relatively large. Even later, after graduating with my electrical engineering degree, my first project involved automatic ship steering systems.

It was not until 1989, at British Columbia's Children's Hospital, when I could hold the physical scope of my work in the palm of my hand. Ironically, however, the physical size of the focus of my efforts had reduced but the implications of the end result had exploded. A neonatologist once said to me, "I love my work, on average I get a 75 year return on each investment". I believe that this quote best describes the unlimited potential associated with assisting a new life.

1.0 INTRODUCTION

Ventilated neonates with under-developed lungs may require elevated levels of inspired oxygen to maintain adequate tissue oxygenation. The process of administering air/oxygen gas mixtures is known as oxygen therapy and this thesis is about its automation as applied to a software model of the neonate. During the course of oxygen therapy, elevated levels of blood oxygenation, hyperoxemia, must be avoided or the risk of chronic lung disease or retinal damage is increased. Low levels of blood oxygenation, hypoxemia, may lead to permanent brain tissue damage and, in some cases, mortality.

Arterial blood oxygen saturation, SaO_2, represents the percent of hemoglobin bonded with oxygen and is an indirect indication of tissue oxygenation. The output signal from a pulse oximeter, SpO_2, correlates well with SaO_2 and is often used by clinical staff in the process of oxygen therapy. Medical staff use blood gas analysis to correlate existing arterial partial pressures of oxygen, PaO_2 (another indicator of tissue oxygenation), to current SpO_2. With this information, staff must then determine a safe range of SpO_2, normoxemia, for each infant. Once a safe range of SpO_2 is defined, medical staff will administer a fractional inspired oxygen level, FiO_2, using automatic or manual means. Figure 1 presents a generic system block diagram of the oxygen therapy process. Chapter 2 discusses, in detail, the manual oxygen therapy procedure and its associated difficulties.

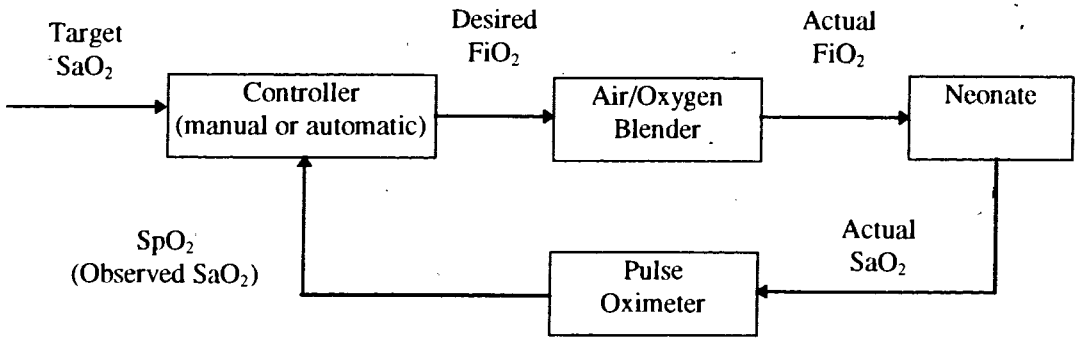

Figure 1. System Block Diagram

Previous attempts by the author to automate SaO_2 control have been impaired by the difficulties associated with co-ordinating subjects, parental consent, nursery and technical staff. Another problem associated with clinical trials is the inability of the controller to stress test itself with live patients. Figure 2 is a simplified diagram of the neonatal oxygen transport system and a computer model of it is proposed in Chapter 3 as a means of alleviating these problems. Commercial software was used to implement the model for a personal computer. A four compartment adult respiratory model which accommodated bi-directional gas flow was developed. The adult cardiovascular system was designed with 11 mixing and four delay compartments. These two models were linked together to produce an adult model of the oxygen transport system and output values for the partial pressure of oxygen in the alveoli (PAO_2) and SaO_2 were validated with current physiological data.

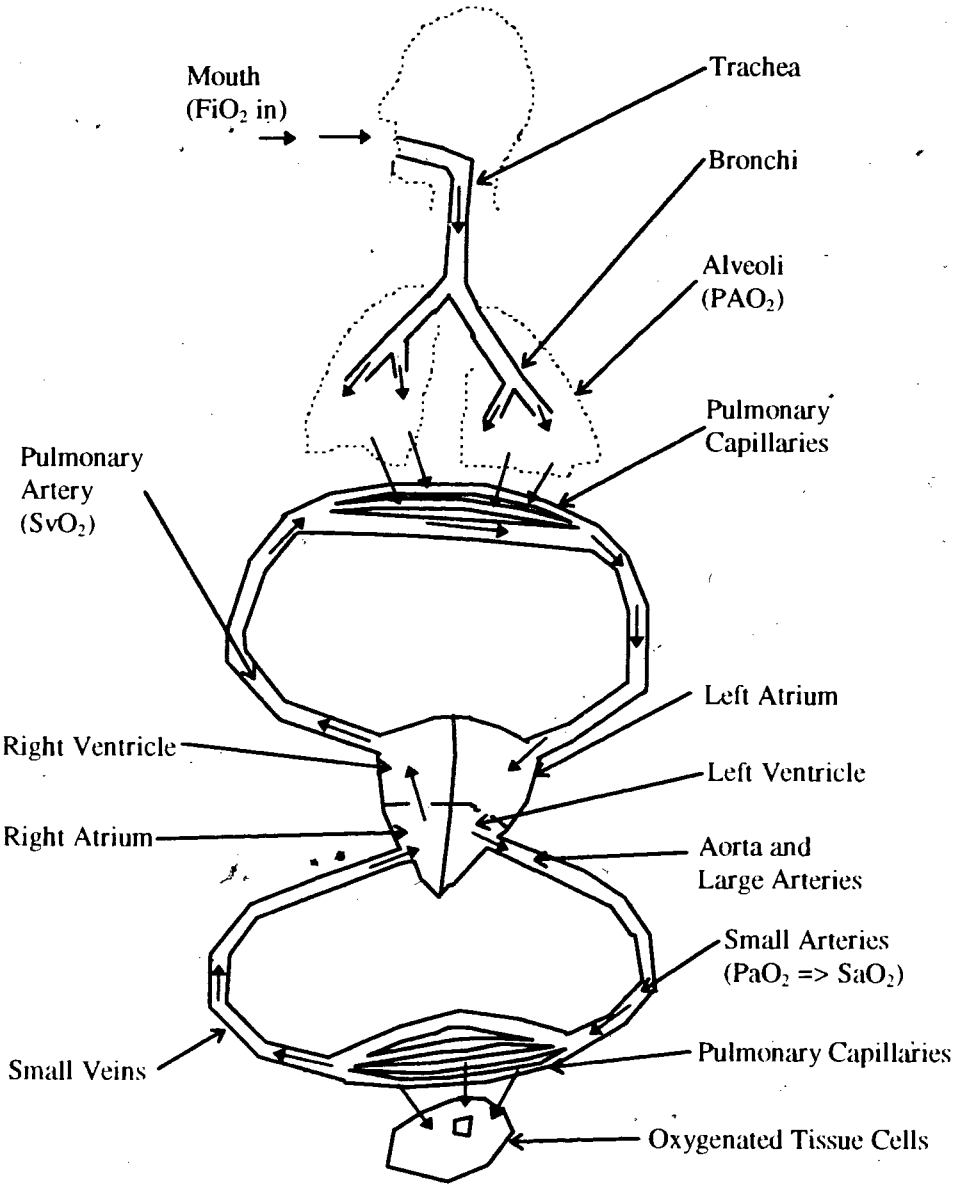

Figure 2. Oxygen Transport System - *solid arrows represent oxygen flow.*

The adult model was then adapted to represent a neonate using a combination of physiological scaling (allometric) equations and empirical data for its parameters. Dynamic shunting conditions were analysed. Models of the air/oxygen blender and pulse oximeter were also produced. The pulse oximeter model included sensor noise and motion disturbances that

could be controlled by a supervisory program. Models for the air/oxygen blender, neonate and pulse oximeter - actuator, plant and monitor respectively - were linked together and controlled by one of three supervisory test scripts. Each script represented a one hour duration for a specific type of neonate: stable but active; unstable and inactive; unstable, inactive and changing oxygen affinity.

Chapter 4 describes the design and implementation of four controllers - manual, proportional-integral-differential (PID), fuzzy logic and fuzzy logic with artifact detection. Manual mode attempts to keep the neonatal models at target but more emphasis is often placed by clinical staff on keeping the patient within normoxemia. The other control algorithms attempt to hold the models to a specific target point.

The results from each controller applied to each type of neonatal model are presented, compared and discussed in Chapter 5. Target performance is defined as the percentage of experiment duration spent at +/- 0.5% SpO_2 of target and +/- 1.5% SpO_2 of target. Normoxemic performance is defined as the percentage of experiment duration spent within normoxemia (90% to 95% SpO_2). Summary and conclusions are presented in Chapter 6 followed by the appendices and list of references.

2.0 OXYGEN THERAPY FOR PRE-TERM INFANTS

2.1 Introduction

Oxygen therapy is the process of administrating blended air/oxygen gas in an effort to maintain a patient's tissue oxygenation at safe levels. The mixture of air/oxygen gas, or fractional inspired oxygen, FiO_2, is often manually set by clinical staff using a mechanical gas blender while a pulse oximeter output, SpO_2, is used by them to observe the patient's systemic arterial blood oxygen saturation, SaO_2. The reading from the pulse oximeter, SpO_2, correlates well with SaO_2 which is often used as an indirect assessment of systemic arterial oxygen tension, PaO_2. Intermittent blood gas testing is done on the patient to correlate SpO_2 readings with arterial oxygen tension and, indirectly, tissue oxygenation.

Preterm babies are infants born before the normal 39 to 40 week human gestation period. Those born before 35 weeks gestation often require oxygen therapy as a result of their under developed lungs. A low blood oxygen saturation level increases the infant's risk of hypoxemia. Prolonged periods of high SpO_2 levels (hyperoxemia) may induce complications such as retinal damage and chronic lung disease. Clinical staff have two problems to solve when administering oxygen therapy to preterm infants. The first problem is the definition of hypoxemia and hyperoxemia for each patient; safe upper and lower SpO_2 limits must be prescribed. The second problem is to keep the patient within the prescribed safe blood oxygen saturation limits (normoxemia).

This chapter first describes the mechanisms of oxygen transport in ventilated pre-term babies. Next it states how oxygen therapy is manually administered to prevent hypoxemia and hyperoxemia. A description of the hazards (and how each hazard occurs) associated with this therapy is presented. Since varying levels of inspired oxygen at constant ventilation may lead to physiological damage in pre-term babies, the author reviews automatic oxygen therapy as a means of limiting these disorders.

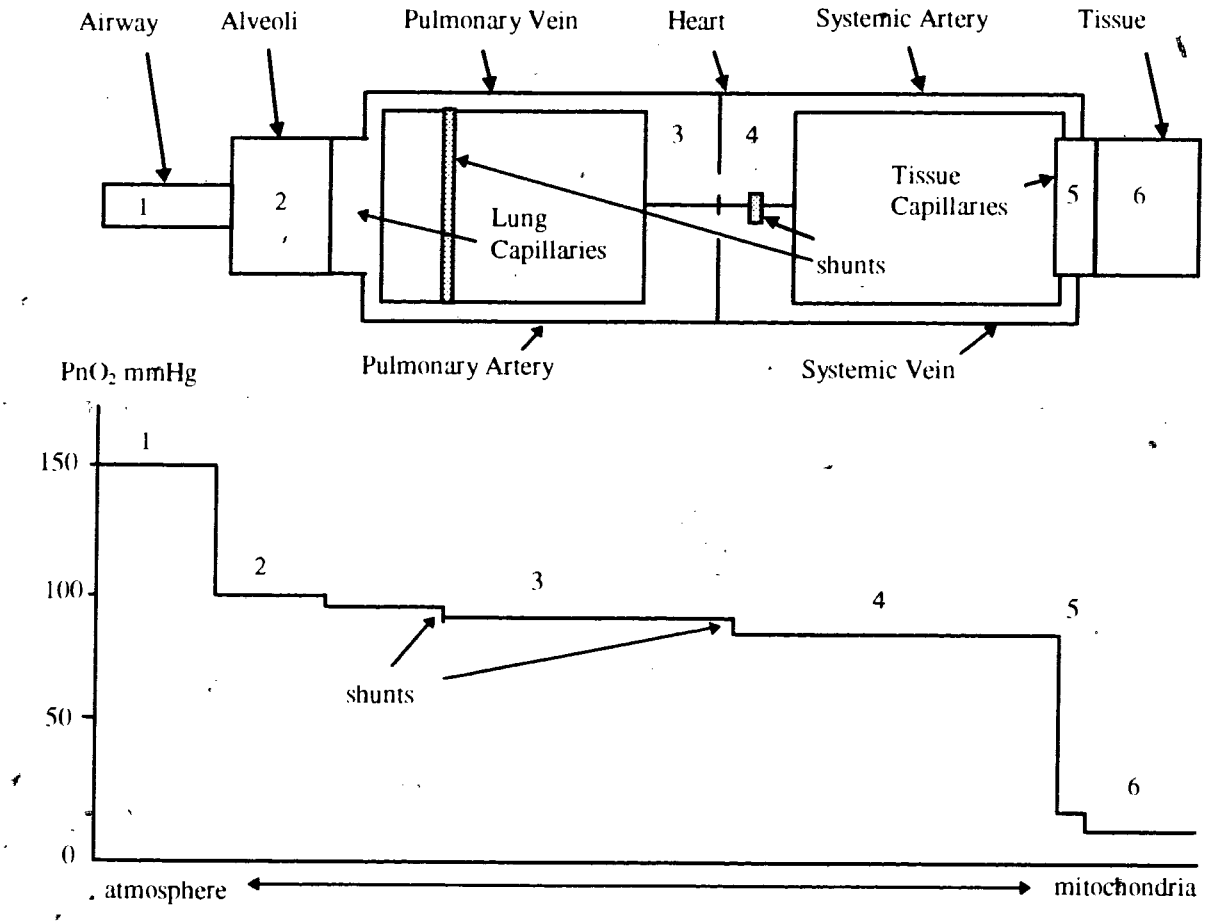

Figure 3. Oxygen Cascade - *PnO_2 represents the partial pressure of oxygen at the "nth" compartment, n = 1 to 6.*

2.2 Oxygen Transport in Neonates

Figure 3 is a simplified diagram of the human oxygen transport system with the removal of oxygen as CO_2 omitted for simplicity. This oxygen cascade has been divided into six compartments and each drop in oxygen partial pressure represents a compartment transition.

Airway

Compartment 1 consists of the mouth, endotracheal tube and bronchial tubes where PiO_2, the partial pressure of inspired oxygen, is usually about 150 mmHg for an FiO_2 of 0.21 (normal room air). The FiO_2 level can be related to the partial pressure of inspired oxygen as a function of the barometric pressure (PB) and partial pressure of water (PH_2O) as follows:

$$PiO_2 = (\%FiO_2/100) * (PB - PH_2O) \qquad (2.1)$$

Alveoli

The second compartment is made up of the alveoli where oxygen pressure (PAO_2) is usually about 50 mmHg lower than the previous compartment due to the diffusion of oxygen into the blood and the additional partial pressure of CO_2 returning from the tissue. Oxygen diffuses through the alveoli membrane into the next compartment since the pulmonary capillary blood contains a lower oxygen partial pressure.

Capillaries and Pulmonary Venous Blood

Tissue capillaries surrounding the alveoli make up the third compartment. Oxygen is present in the blood in two forms - dissolved in the plasma and erythrocyte water and reversibly bound to hemoglobin molecules. The amount of oxygen dissolved in the blood is directly proportional to its partial pressure, PO_2, but is relatively small because oxygen is relatively insoluble in water. Most oxygen is bound to hemoglobin in the capillary blood as a function of the partial pressure of oxygen. As pulmonary arterial blood flows through the lung capillaries, oxygen diffusing from the alveoli binds to capillary blood hemoglobin and is then transported to the pulmonary venous system and then to the left atrium of the heart.

Systemic Arterial Blood

The next compartment consists of the systemic arterial system where blood leaves the left ventricle of the heart. For the sake of simplicity, it will be assumed by the author that very little oxygen is lost to tissue within the pulmonary venous blood and left atrium. PaO_2 and SaO_2 will refer to arterial oxygen tension and blood oxygen saturation respectively for the systemic arterial blood circulation. In the normal newborn, 98% of the oxygen in blood flowing out of the heart into the systemic circulation is bound to the hemoglobin. The oxygen dissolved in the plasma and erythrocyte water has a partial pressure defined as PaO_2 which is related to the blood (hemoglobin) oxygen saturation (SaO_2) by the oxygen dissociation curve shown in

Figure 4. The SaO_2 is the ratio of bound hemoglobin to total hemoglobin in the blood represented as a percentage. A mathematical model for this curve is (Severinghaus,1979):

$$SaO_2 = (((PaO_2^3 + 150\ PaO_2)^{-1} * 23{,}400) + 1)^{-1} \qquad (2.2)$$

The slope and position of the oxygen dissociation curve represents the affinity of oxygen to the blood hemoglobin. A left shifted steep curve is typical of neonates and illustrates a high oxygen affinity (Hay, 1979). In other words, a low PaO_2 is required to drive the hemoglobin to saturation. This feature is very appropriate at the lung compartment, but not necessarily so at the tissue. When the oxygenated blood reaches the tissue, O_2 must be unloaded and a right shifted, less steep curve would be better suited. In other words, a lower Hb-O_2 affinity at the tissue would mean that at relatively high PaO_2 values O_2 would be released. The dashed line in Figure 4 illustrates an SaO_2 value of 97% for neonates, or adults, with a PaO_2 of 100 mmHg.

Neonate blood is made up of fetal hemoglobin (HbF) until about eight weeks of gestation when adult hemoglobin (HbA) appears (Wood, 1973). At 30 weeks gestation the change to HbA from HbF accelerates. For adult hemoglobin the oxygen dissociation curve can be affected by several factors such as temperature, blood pH and 2,3-diphosphoglycerate (DPG) concentration. A right shift can be the result of an increased temperature, increased 2,3-DPG concentration or a decrease in pH. However, in preterm infants, research has shown that pH

and 2-3 DPG have little direct affect on the dissociation curve but the percentage of HbA does (Bard, 1979).

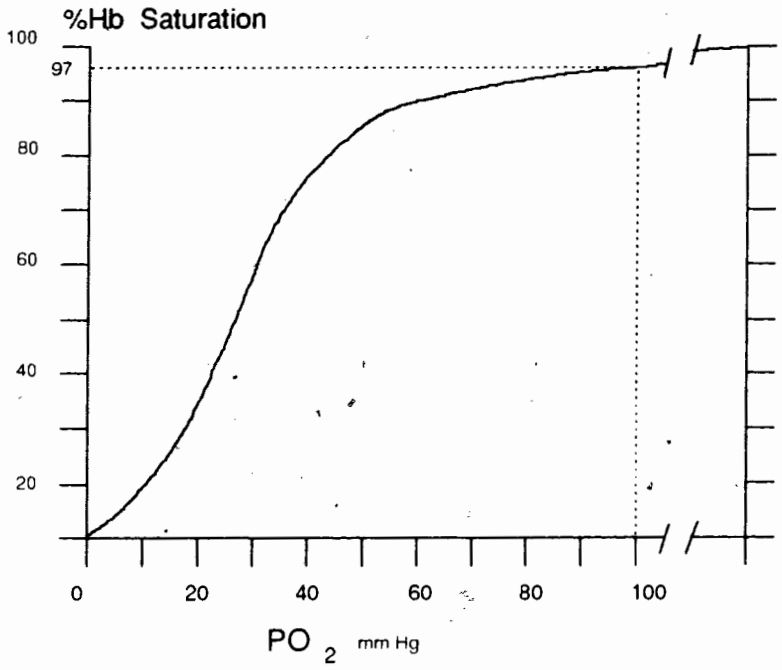

Figure 4. Oxygen Dissociation Curve

Tissue and Mitochondria

As arterial blood enters capillaries surrounded by tissue with low interstitial fluid PO_2 (as a result of oxygen consumption), oxygen dissolved in the blood plasma enters the tissue resulting in a drop in the plasma PO_2. This drop in pressure results in a diffusion of O_2 out of the erythrocyte which in turn results in the release of O_2 bound to hemoglobin as a function of the

oxygen dissociation curve. The oxygen that diffused into the interstitial fluid moves into cells along a concentration gradient generated by cellular oxygen consumption.

Even with a high Hb-O_2 affinity, oxygen is still released from the hemoglobin because of the presence of CO_2 at the tissue. The Hb-CO_2 affinity is much higher than that of Hb-O_2 and since there is a large CO_2 partial pressure gradient between the erythrocyte water and the plasma at the tissue, the CO_2 successfully competes with the oxygen for hemoglobin binding sites. Thus the CO_2 returning from the tissue helps drive some of the oxygen from the hemoglobin and into the blood plasma at the capillaries. In neonates, the blood returning from this compartment usually has a saturation level of about 75% (Dudell, 1990), but this value is a function of the infant's dissociation curve. In other words, an SvO_2 of 75% may be associated with a 40 mmHg PvO_2 (partial pressure of oxygen in the systemic venous blood) for one curve, while on another more left shifted curve, the same PvO_2 may represent 85% SvO_2.

2.3 Complications Associated with Oxygen Therapy

The physiology of the preterm infant changes from week to week. For example, lung development is not complete until about 35 weeks gestation and retinal development continues until after birth. This section will discuss complications that can affect the neonate's oxygen transport system.

Apnea

Sporadic and prolonged periods of breathing inactivity are defined as apneic spells and are most common in preterm infants. Factors associated with apneic spells are hypoxia, rapid eye movement (REM) sleep, absence of core-skin temperature difference, upper airway obstruction, inadequate nutrition, fatigue and gastroesophageal reflux (Avery, 1984). Since apnea is the cessation of breathing it has a major affect on SaO_2 if the neonate is not mechanically ventilated. Without a source of oxygen, the tissue PO_2 will drop very quickly.

Sinus Bradycardia

Irregular or low heart rate (< 100 BPM) will slow blood circulation and thus reduce O_2 delivery. About 35% of premature infants display bradycardiac dysrythmias (Fanaroff, 1983, p.576). An irregular heart rate may also have a detrimental effect on some monitoring instrumentation. Sinus bradycardia is associated with defecation, yawning, hiccuping and nasopharyngeal stimulation but is most likely due to the immaturity of the autonomic nervous system and increased vagal tone (Freed, 1984). Episodes of bradycardia have a profound effect on tissue oxygen levels, but the reverse is not necessarily true.

Surfactant Levels

Surfactant in the alveoli lowers surface tension and thus increases lung compliance. This allows the neonate to inspire larger volumes of gas using lower pressures. The increased efficiency in delivering O_2 to the alveoli reduces stress on the patient. Since surfactant

concentration levels consistent with mature lungs does not begin to appear until about 35 weeks gestation (Fanaroff, 1983, p.134), many low birth weight neonates have a low surfactant level requiring that they be mechanically ventilated using pressures that could promote lung damage.

Shunt

Two types of shunt can be considered. The first is the result of a poor match between blood circulation and ventilated areas of the lung - an area of lung with poor ventilation may have good circulation, or, a well ventilated lung region may have inadequate circulation. This type of shunt is shown in Figure 3 as a pulmonary arterial-venous connection bypassing the capillaries.

The second type of shunt is within the heart as indicated in Figure 3 between the right and left ventricles. Within the mother's uterous, the neonate receives its oxygen by sharing its circulatory system with the mother; oxygenated blood enters the neonate via the umbilical chord. Two cardiac right-to-left shunting mechanisms assist in moving the oxygenated blood through the systemic system (Scarpelli, 1975, p.117). These shunts through the ductus arteriosus and foramen ovale are a means of by-passing the pulmonary circulation. During the neonate's first breaths, these shunts begin to close; with eventual full closure in most infants. Some neonates, about 8 per 1000, maintain the opening between the two hearts and thus blood bypasses the lungs and does not become oxygenated (Freed, 1984). In this condition, known as a right to left cardiac shunt, elevating FiO_2 levels has little or no effect on SaO_2.

Oxygen Affinity ($Hb\text{-}O_2$ Dissociation Curve)

As stated earlier, adult hemoglobin-O_2 affinity is a function of temperature, blood pH and 2,3 DPG concentration. The body temperature of neonates is usually controlled by an incubator and set at 37^0 C. A neonate's O_2 affinity is a function of its HbF/HbA content and not directly 2,3 DPG and blood pH (Bard, 1979). There is an indirect link, however, since HbA is effected by these factors the implication is that 2,3 DPG and pH will have an effect on oxygen affinity as a function of the percentage of HbA in the fetal blood. The fetus appears to respond to hypoxemia by both an increase in HbF synthesis and its red cell mass thus controlling its O_2 affinity. In the neonate, however, complications such as blood transfusions will affect the percentage of HbF and HbA and thus affect the O_2 affinity.

Another problem associated with oxygen therapy is due to the non-linear nature of the $Hb\text{-}O_2$ dissociation curve. In other words, the relationship between the SaO_2 and PaO_2 is not constant or a straight line. As illustrated in Figure 4, the dissociation curve is steep and relatively linear below 40 mmHg and flat and linear above 60 mmHg. Between 40 and 60 mmHg, however, the two segments meet to form what is referred to as the "knee" of the curve. It is very difficult to maintain PaO_2 levels in an infant within the "knee" because any slight drop in PaO_2 as a result of shunt, bradycardia, etc. may drive the infant into the steep part of the curve producing large drops in blood oxygen saturation.

2.4 Oxygen Therapy

2.4.1 Monitoring Device

Originally, PaO_2 levels in neonates were determined by blood gas analysis. As technology moved along, instrumentation was developed by industry that could continuously monitor PaO_2, and later, SaO_2. Bancalari (1987) showed that there was no correlation between continuous monitoring and a reduction in mortality or incidence of retinopathy of prematurity in low birth weight infants - babies weighing less than or equal to 1500 gms. He and Flynn later showed that there was a correlation between retinopathy of prematurity (ROP) and elevated levels of PaO_2 (Flynn and Bancalari, 1992). As a result most, neonatal nurseries monitor infants on supplemental oxygen with continuous PaO_2 or SaO_2 instruments and intermittent blood gas testing.

There is little in the literature to describe an oxygen therapy procedure besides indicating safe ranges of PaO_2. Generally, an optimal PaO_2, or indirectly, an optimal SaO_2 level is determined by hospital staff. A general guideline for PaO_2 levels is 60-80 mmHg or 85-95% for SaO_2 (Hay 1979; American Academy of Pediatrics, 1992). If PaO_2 is under scrutiny, a PaO_2 monitor is connected to the patient and alarm levels are set close to the desired PaO_2.

Since pulse oximetry is non-invasive and more immediate in nature it has become a very popular means of gauging SaO_2 by observing its SpO_2 reading. In most cases SpO_2 correlates very well to SaO_2 within the range of 85% to 95% (Praud, 1989; Bucher 1989). This area is

usually the range of interest with regards to maintaining stable levels of SaO_2 within the patient. Like the PaO_2 monitor, the pulse oximeter is set up to alarm outside a specified range.

Pulse oximeters use the properties of light absorption in oxygenated blood to determine SpO_2. It is based upon the principle that oxygenated and deoxygenated hemoglobin have different absorption spectra. The deoxygenated hemoglobin absorb more light in the 600 to 750 nm wavelength and oxygenated hemoglobin absorbs more light in the 850 to 1000 nm band. An oximeter probe emits light at these two wavelengths through the tissue to a photo-detector where the light absorption by the tissue (and indirectly the hemoglobin) is measured. The ratio of the light absorption at the two wavelengths correlates to the proportion of oxygenated and deoxygenated hemoglobin. Their sensors are very sensitive to ambient light and movement which create erroneous readings known as artifact. The pulse oximeter also must synchronise on the patient's heartbeat since only the light of the pulsating portion of the heartbeat correlates to oxygen saturation; a poor heartbeat signal may also produce artifact and erroneous data (Poets, 1994).

Some literature has suggested using venous blood oxygen saturation (SvO_2) as an indicator of oxygen consumption (Dudell, 1990). Subtracting SvO_2 from SaO_2, an error signal could be produced that would represent oxygen consumption and, indirectly, tissue oxygenation. This technique, however, requires that a catheter be placed in the patient's right ventricle, exposing the patient to infection and possibly complicating the day to day health care that the patient

requires. Another problem is the fact that the venous side of the systemic circulation acts as a reservoir for the blood and there would be a time lag between the SvO_2 at the tissue and that measured at the heart. Research into an indwelling O_2, CO_2 and pH catheter for neonates is promising, but manufacturing and corrosion problems persist (Soller, 1994; Rolfe, 1994).

2.4.2 Actuating Device

A mixture of air and oxygen is produced by feeding each of the two gases into a mechanical air/oxygen blender. The output gas has an oxygen percentage of 21 to 100 percent and is fed into the patient via a ventilator. The blender usually has a mechanical dial within the 21 to 100 percent range which allows the user to set the output gas. Some ventilators have these blenders built into them. As a safety monitor, an O_2 sensor is often placed in line between the blender and ventilator by clinical staff.

The procedure for oxygen therapy is quite straight forward; the clinician adjusts the administered air/oxygen mixture in an effort to maintain stable normoxemia. The alarms on the input device are set using a range close to the target SpO_2. A care giver adjusts the inspired air/oxygen percentage (FiO_2) until the patient is within the prescribed range. As the patient desaturates (becomes hypoxemic) or oversaturates (becomes hyperoxemic) the attendant must carefully adjust the FiO_2 levels. This is not an easy task since the adjustment must be made as a function of the type of problem. For example, in the case of observed oversaturation, patient movement may be causing a false reading and an FiO_2 increase would promote hyperoxemia.

2.4.3 Defining Safe Oxygen Levels

The definition of safe levels of oxygen (normoxemia) is controversial. In the early 1950's with the prevalent use of oxygen in incubators to prevent hypoxemia, there was an epidemic of retinopathy of prematurity which resulted in lower FiO_2 levels prescribed to neonates in the 1960's (Payne, 1984). Along with the resultant reduction in the disease, however, was an increase in infant mortality. Another complication associated with hypoxia and mechanical positive pressure ventilation is known as bronchopulmonary dysplasia (BPD), or more commonly, chronic lung disease. Over the decades the "safe" limit for PaO_2 levels has been changing from 60-100 mmHg to 60-80 mmHg (American Academy of Pediatrics, 1983; 1992). This may have been in response to the increasing number of infants diagnosed with hyperoxemic related diseases such as ROP and BPD. In an effort to reduce hyperoxema even more, recent literature suggests that other safe limits may be as low as 45-60 mmHg (Emond, 1993).

Hypoxemia

The result of low blood oxygen levels are quite obvious. Irreversible brain tissue damage is the result of prolonged periods of hypoxemia. In severe cases damage may lead to death. Infants exposed to severe and continuous hypoxemia increase their risk of conditions such as cerebral palsy or spastic diplegia (MacDonald, 1963).

Bronchopulmonary Dysplasia - BPD

Bronchopulmonary dysplasia occurs among infants who have required high oxygen concentrations and ventilator support (Northway, 1976). It normally follows hyaline membrane disease (also known as respiratory distress syndrome) but may occur in infants without it (Bancalari, 1979). In this condition, there is a destruction of terminal airways with dysplasia and fibrosis. The associated scar tissue build-up reduces effective lung volume. Frequent exposure to prolonged periods of hyperoxemia may contribute to the onset of BPD. Affected infants usually develop chronic respiratory insufficiency with severe cases leading to death (Durbin, 1975).

Carbon Dioxide Retention

As carbon dioxide enters the blood at the lungs about 30% is bound to the deoxyhemoglobin to form the carbamino compound, $HbCO_2$. If the CO_2 is not released at the lungs due to shunting or BPD related complications, the O_2 within the lungs capillaries will have fewer hemoglobin binding sites and thus the blood oxygen saturation will stay low. Prolonged periods of hyperoxemia can promote lung damage which in turn may further impair CO_2 diffusion through the alveoli.

Retrolental Fibroplasia

Retrolental fibroplasia or retinopathy of prematurity (ROP) is a disease affecting retinal blood vessels in premature and term infants and can produce visual impairment and blindness (Payne,

1984). It was first diagnosed in 1941 and in the 1950's and 1960's a relationship between its incidence and high oxygen levels was identified (Terry, 1942; Kinsey, 1956). As a result of these early studies, FiO_2 levels were reduced only to possibly result in an increased infant mortality. Exposure to high levels of PaO_2 (> 80 mmHg) will increase the neonates risk of ROP (Flynn, 1992).

At the fourth month of gestation, vascularization begins at the optic disc and then proceeds outwards where it reaches the nasal periphery at 8 months. The temporal periphery is not vascularized until 1 month after term. At any stage of prematurity and up to one month after term the temporal retina is susceptible to ROP. The primary effect of oxygen (as a result of hyperoxemia) on neonates with an incompletely vascularized retina is retinal vasoconstriction which may be followed by vascular closure. This may eventually lead to complete closure of immature portions of vascularized retina. The secondary effect occurs with a reduction of PaO_2 to normal levels as new vessels form at the damaged area and erupt through the retina surface into the vitreous (Payne, 1984). Also, adjacent to the capillary closure, neovasculation occurs.

2.4.4 Oxygen Regulation

Manual Control

Labile babies are particularly difficult to stabilise. Since these babies tend to desaturate quickly and often, attendants may have to constantly adjust the FiO_2 levels (in some cases 2-3 times a minute). As stated above, the target SaO_2 level is often very close to the "knee" of the

dissociation curve. Since neonates often have a left shifted steep curve, small disturbances can drive the patient into rapid deep desaturation. The nursing staff may react by increasing FiO_2 values, resulting in the baby becoming normoxemic. Unfortunately, however, if the FiO_2 remains increased the infant soon becomes hyperoxemic requiring a decrease in FiO_2. This constant cycling is time consuming and also stresses the baby and nursing staff. The situation is further complicated by nursing staff performing other duties such as suctioning mucus from the infant's lungs and providing physiotherapy.

Associated Therapy

Administering a steroid, such as glucocorticoid, to neonates suffering from BPD can produce marked improvements in their oxygen transport mechanism. These drugs act as anti-inflammatory agents in the lungs. Little research is available to show the long term affects of this type of drug therapy, thus, steroids are generally administered only to critically ill patients. In some cases the steroid is administered to the pregnant mother in an effort to prevent chronic lung disease (Van Marter, 1990).

An artificial surfactant can result in increasing lung compliance which will allow ventilation at lower pressures. Less stress on the patient and a lower risk of lung damage is the result. Surfactant use in preterm infants improves survival rates without increasing the proportion of impaired survivors (Ferrara, 1994). A recent study (Kari, 1994) showed that surfactant therapy

coupled with prenatal steroid therapy decreases pulmonary morbidity and cerebral complications, and increases infant survival.

Vitamin E derivatives are used to scavenge O_2 free radicals from blood. Little data is available but what does exist shows some effect on reducing ROP (Payne, 1984). Administration of morphine to reduce pain and stress on baby seems reasonable but some research shows that morphine depresses all aspects of respiratory activity including rate, minute and tidal volume (Way, 1963). Several commercial drugs are used to assist the ventilation process by acting as bronchodialators. Nitric oxide therapy is very experimental but shows promise since it is a direct pulmonary vasodilator that is deactivated by hemoglobin. In other words, nitric oxide gas will dilate the pulmonary capillaries surrounding the lungs (increasing diffusion due to increased area) but not the rest of the circulation. With scheduled physiotherapy and suctioning of lung mucus, clinical staff can maintain lung compliance and resistance.

Automatic Therapy

The need to automate neonatal oxygen therapy has been identified by the medical community (Flynn, 1992). Previous researchers have been pioneering neonatal oxygen controllers. In England, Beddis (1979) devised a mechanical controller that produced promising results. This type of work lay dormant until Taube (1989), Tehrani(1991) and Morozoff (1991) began their research. Taube's adaptive proportional-derivative-integral (PID) prototype lead to his US

patent. Morozoff built two generations of controllers which followed various control strategies. Chapter 4 contains more details on previous work.

2.5 Summary

A description of the neonatal oxygen transport system is presented. The partial pressure of oxygen drops as it moves from the mouth to the lungs where it diffuses through the alveoli walls and bonds to hemoglobin in the pulmonary capillaries. The percent of hemoglobin bonded with oxygen is known as the blood oxygen saturation, SaO_2, and is related to the partial pressure of oxygen in the blood by the oxygen dissociation curve. Oxygen bonded to the hemoglobin is transported through the circulatory system to the tissue capillaries where a portion is released and enters the tissue.

Frequent and prolonged low oxygen levels in the tissue, hypoxemia, may lead to irreversible brain damage and, in severe cases, mortality. Frequent and prolonged high levels of tissue oxygenation, hyperoxemia, may promote bronchopulmonary dysplasia (chronic lung disease) and retinopathy of prematurity (eye damage). The output of a pulse oximeter, SpO_2, is used as an indicator of SaO_2 which is, in turn, used as an indirect indicator of tissue oxygenation. Normoxemia is defined as the "safe" region of tissue oxygenation and oxygen therapy is the process of maintaining it by the administration of an air/oxygen gas mixture. The reading from a pulse oximeter is often used by clinical staff as a feedback mechanism for manual control of

oxygen therapy. To date, several researchers, including the author have developed automatic oxygen therapy devices which use SpO_2 as an indicator of tissue oxygenation.

3.0 PHYSIOLOGICAL MODEL

3.1 Introduction

Modelling the physiological system affords several advantages in this study. In the past, the co-ordination of human subjects, parental permission, nursery personnel, technical support and functional equipment has been very difficult. On average, a single two or three day test per month could be co-ordinated by the author. A second major advantage to modelling the neonate is related to the stress that he or she can accommodate. Since the neonate must stay within normoxemia, the validation of the prototype controller described in the previous section was based on a limited SaO_2 bandwidth. A model, however, can be repeatedly driven to critical SaO_2 levels as a means of verifying the controller's long term response before field trials with a prototype device. A third advantage of producing a neonatal model is that it provides a platform for further research - not only in the field of SaO_2 control, but also in the study of the effects of changes to physiological parameters such as lung compliance, breathing rate, heart rate, etc.

A simulation may produce the same output as a model, but internally offers no explanation for its data. The model differs from the simulation by attempting to define the mechanisms that produce experimental observations. The depth of detail to which the model explores usually represents its resolution. Designers must define a depth of detail and its associated output since, in most cases, those model details may be difficult to attain. Once a model has been formulated, a computer application may be realised. The depth of the model detail may also effect the

computation time required; higher levels of detail requiring increased computational power. Some models may be so detailed and complicated that, even though they are realisable, they may not be useful for real-time model based control due to their processing power requirements.

A model of the human oxygen transport system from inspired air at the mouth to its consumption in the mitochondria is a complex task. Oxygen, as a gas, is compressible and its pressure through the respiratory system - mouth to alveoli - is a function of resistance, compliance and direction of flow. Once oxygen diffuses through the alveoli walls into the blood stream, its concentration is affected by blood flow, mixing chamber time constants, shunting and consumption rate. In summary there are two subsystem models - respiratory and circulatory.

This chapter describes the design, implementation and testing of models for a neonate's oxygen transport system, an air/oxygen blender and a pulse oximeter. These three components - plant, actuator and monitor - are used to design and test a controller in the following chapter. After the introduction, the model's computer development environment is presented. Next, the respiratory and cardiovascular models are described. These two models are then combined into adult and neonatal models in the following two sections. Air/Oxygen blender and pulse oximeter models are then presented followed by a discussion of various test scripts.

3.2 Development Environment

As a computer engineer, and an experienced computer programmer, the author originally proposed writing the model in the "C++" programming language. In fact, some of the early respiratory models were first written using "C++" on an IBM compatible personal computer (PC). However, after some initial training, the author moved towards using the commercial MATLAB (MathWorks, 1995) software program with its "SIMULINK" feature.

SIMULINK is an icon driven model building software package and provides some components such as summers, multipliers, filters, transfer functions, etc. More importantly, it provides the user with a standard framework to which custom building blocks can be added. The neonatal model requires many custom blocks to accommodate bi-directional gas flow, real-time adjustment of time constants, etc. Another feature of SIMULINK is its packaged input/output (I/O) routines such as graphing and disk file access. A third feature associated with this package is that other researchers familiar with it can take advantage of the model; understanding and editing a custom "C++" driven model would most certainly be more difficult and time consuming.

This model was developed on an IBM compatible '486 133 Mhz PC with 16 Mbytes of RAM. Its operating system was MicroSoft Windows® 3.0 (MicroSoft, 1994). MATLAB version 4.2c.1 was used to drive SIMULINK version 1.3c.

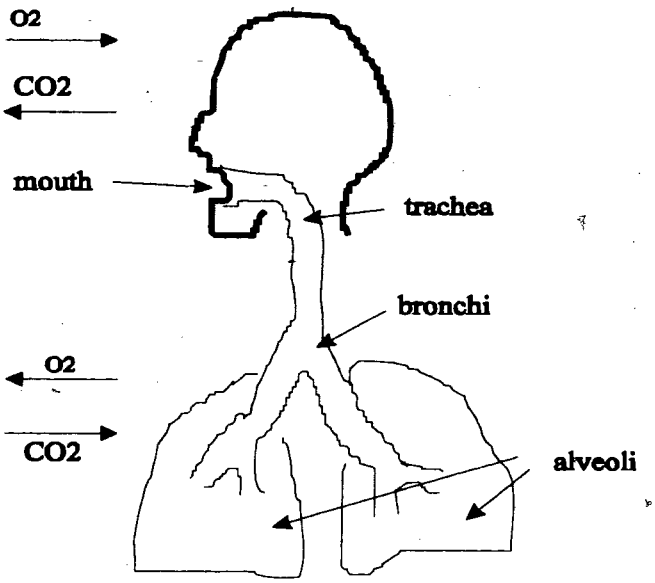

Figure 5. Respiratory System

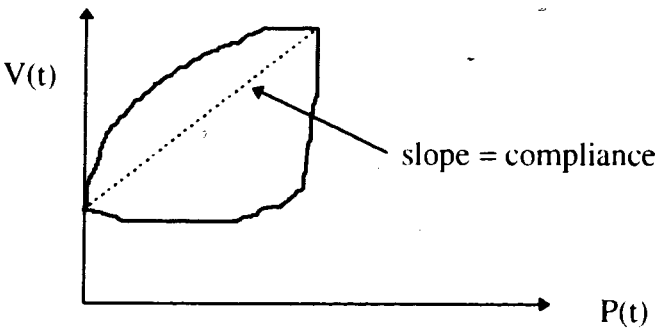

Figure 6. Pressure - Volume Plot - *the plot is for a single breath starting in the lower left hand corner and moving counter-clockwise along the curve. Also note, that this is a positive pressure plot from a ventilated patient.*

3.3 Respiration

The respiratory system is primarily dedicated to the function of oxygen and carbon dioxide exchange. These gases enter and exit at each end of a well structured system as shown in Figure 5. Gas pressure, flow and volume are parameters which describe characteristics of the

respiratory system. The instantaneous respiratory system pressure can be modelled by the following simplified equation (Richardson 1989):

$$P(t) = P_0 + (1/C)V(t) + (R)F(t) \qquad (3.1)$$

where:

P(t) = pressure difference between atmosphere and patient airway

V(t) = lung volume above residual capacity

F(t) = gas flow

P_0 = respiratory system offset pressure

C = respiratory system compliance

R = respiratory system resistance

Compliance is a measure of how "easy" the respiratory system expands. If we plot pressure versus volume for a single breath we will get a circular shaped curve shown in Figure 6. Dynamic compliance is the slope of the curve and is calculated as:

$$C(t) = V(t)/P(t) \qquad (3.2)$$

A common method of estimating the average compliance is to calculate the slope of a straight line from the beginning to end of inspiration as shown by the dotted line in Figure 6.

Resistance is a function of pressure and flow and its dynamic value can be expressed as:

$$R(t) = P(t)/F(t) \qquad (3.3)$$

If we plot a pressure-flow loop for a single breath, an estimate of the average resistance can be calculated from the slope of a straight line between the start and end of inspiration - a procedure similar to the calculation of average system compliance.

Table I. Comparison of Pulmonary Mechanics and Electrical Models

Respiratory System	Electrical Analogue
flow (F)	current (I)
pressure (P)	voltage (V)
resistance (R)	resistance (R)
compliance (C)	capacitance (C)
volume (Q)	charge (Q)

An analogy between an electrical circuit and pulmonary mechanics can be made as shown in Table I (Grodins, 1963, p.16; Milhorn, 1966, p.53). Figure 7 illustrates a respiratory system compartment modelled as a simple RC circuit. Using the electrical analogy we can define the respiratory values as follows:

$$F_1(t) = (P_1(t) - P_2(t))/R \qquad (3.4)$$

$$dQ(t)/dt = F_1(t) - F_2(t) \qquad (3.5)$$

$$P_2(t) = (Q(t) - QU)/C \qquad (3.6)$$

Using $P_1(t)$ from the previous network and $F_2(t)$ from the next and the above equations, the instantaneous pressure, flow and volume - $P_2(t)$, $F_1(t)$ and $Q(t)$ respectively - can be calculated.

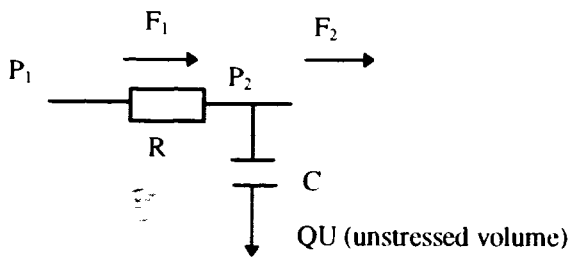

Figure 7. Respiratory RC Network

The first quantitative model of the human ventilation model was developed by Gray (1946) and described ventilation rate, in a feedback loop, controlled by the partial pressure of arterial carbon dioxide, PaO_2 and acidemia (H^+a). This steady state model was further developed (Grodins, 1950; Saito et al., 1960) and a second generation of respiratory models - dynamic models - evolved (Grodins, 1954; Defares, 1960). Respiratory model computer simulations were first explored by Horgan (1965) and Milhorn (1965). Both steady state and dynamic models were limited by constant and uni-directional oxygen flow through the lungs until Yamamoto (1970) introduced a periodic respiratory drive.

Many of the researchers described in the above paragraph modelled the respiratory system using the RC network analogy at varying levels of detail. One researcher, V. Rideout (1991), produced a very good model which has been adapted into the one presented in Figure 8. In this model, for an adult, there are four chambers - mouth, trachea, bronchi and alveoli - each consisting of a resistance-compliance network. His work, was founded on those mentioned in the above paragraph plus that of Jodat (1966), Horgan (1968) and Pedley (1970).

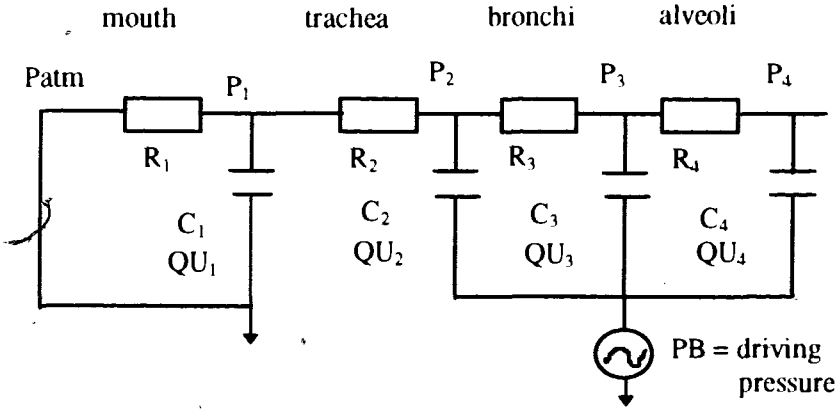

Figure 8. Respiratory System Model. (Modified from V.Rideout, *Mathematical and Computer Modelling of Physiological Systems*. Prentice Hall, Inc. New Jersey, 1991, p.139.)

The model shown in Figure 8, like Rideout's, assumes that resistance and compliance are constant. A more detailed model would include non-linear R(t) and C(t) but would be difficult to implement. Also, it is assumed that the respiratory compartments contain unstressed volumes (QU_1, QU_2, ...), defined as compartment volumes at zero pressure. Another assumption is that the driving pressure of the system (i.e. the breathing apparatus) is sinusoidal in nature and drives a negative pressure in the diaphragm. In the nursery, ventilators are positive pressure devices and, in most cases, not sinusoidal. The author suggests that the SaO_2 waveforms produced from the model and ventilator, will produce little difference since the SaO_2 waveform is heavily filtered by the cardiovascular system's mixing chambers (see below).

Only about two thirds of each tidal volume reaches the alveoli for gas exchange. One portion not involved with gas exchange is called the anatomical dead space volume and it includes the mouth, trachea, bronchi compartments. The model accounts for anatomical dead space by not allowing gas exchange from these compartments with the blood. Alveolar dead space is a function of the pulmonary blood circulation and it is accounted for by a pulmonary shunt in the circulatory model.

The respiratory model was implemented using SIMULINK blocks as illustrated in Figure 9 and the alveoli pressure (P4) was comparable to Rideout's data (1991, p.142). This model only deals with the flow of air and assumes that the total flow out of the alveoli (into the blood) is very small or zero.

After verifying the air transport model, an oxygen transport model was produced by building a model parallel to it. In this case, Rideout (1991, pp.145-146) derives the flow, pressure and volume values of oxygen as a function of the percentage of oxygen in air and the direction of flow - inspiration or expiration. Thus, the model for air transport is used to produce a total flow for each compartment and from these, the flow and volume of oxygen are derived. This model must also deal with the flow of air (and oxygen) in both directions. This is complicated by the fact that oxygen flows out of the model at the alveoli faster during inspiration than at expiration. To account for this, a switching function was produced which derives the compartment's pressure as a function of the direction of total gas flow.

During inspiration the oxygen partial pressure difference between the alveoli (PAO_2) and the pulmonary capillary blood (PcO_2) is high because the lungs are filling with fresh air and de-oxygenated blood is flowing through the lungs. On the pulmonary venous side of the lungs, the partial pressure of oxygen is approximately equal to that in the alveoli. In summary, during inspiration, oxygen flows out of the lungs and into the blood regulated by the circulatory system blood flow. During expiration, oxygen is no longer flowing into the lungs but is still depleted by the pulmonary capillary blood flow resulting in a lowering of the partial pressure of oxygen in the alveoli.

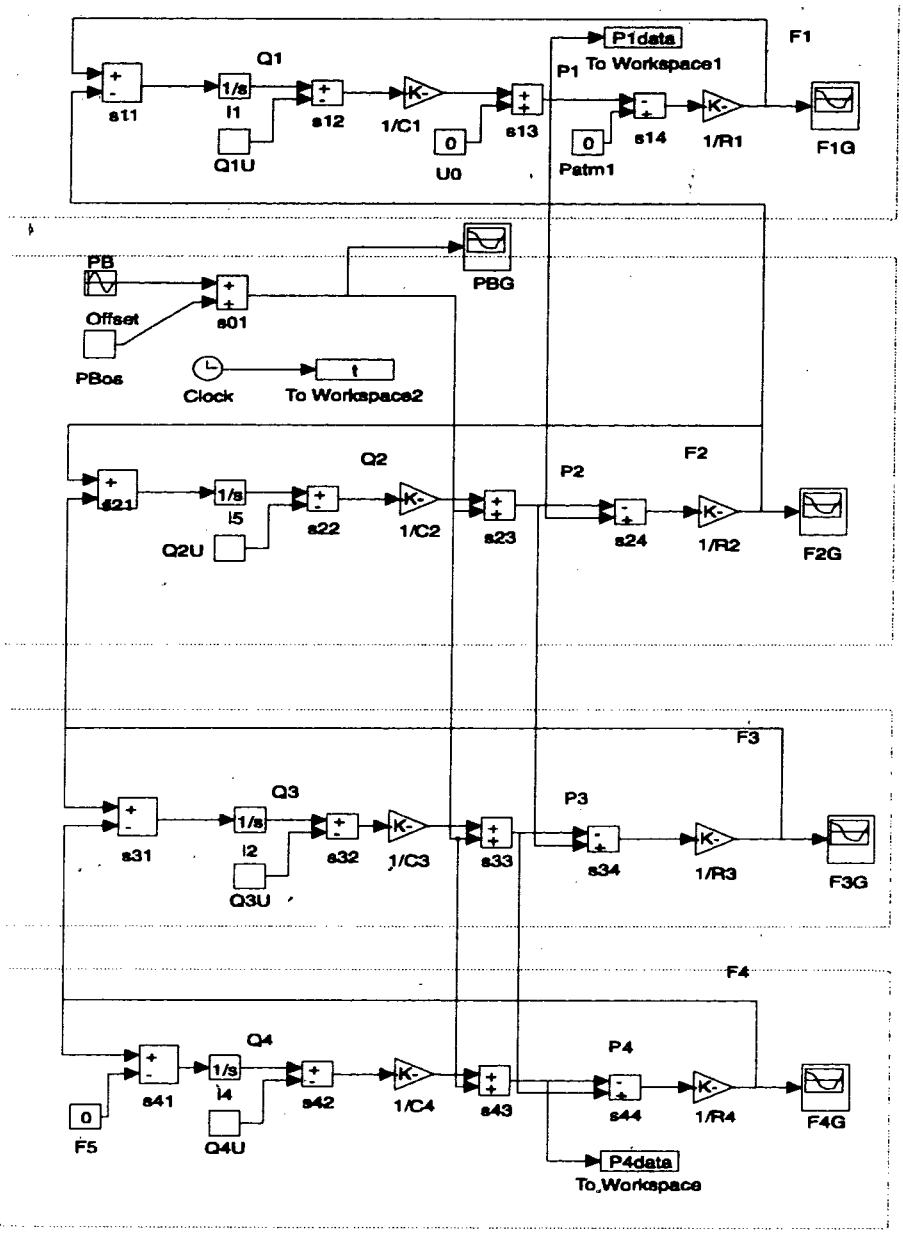

Figure 9. Respiratory System Model Implementation - *Each row of discrete blocks, as outlined by a dashed box, represents a respiratory compartment - from top to bottom, mouth, trachea, bronchi and alveoli. They make up the dynamic equations (3.4), (3.5) and (3.6) associated with an RC model of each compartment.*

Figure 10 represents Rideout's oxygen transport model in the respiratory system of an adult as implemented by the author using the SIMULINK program. This was not a straight forward

task since , due to the discontinuities at zero flow (i.e. between inspiration and expiration), the model engine became unstable. To correct the problem, the author increased the numerical integration step to 0.005 and the numerical integration algorithm to the Adams/Gear technique. Unfortunately, this increased the model's processing time. In summary, Rideout's respiration model for oxygen transport in an adult was implemented with the SIMULINK program. The results were comparable to his published data (Rideout, 1991, p.147).

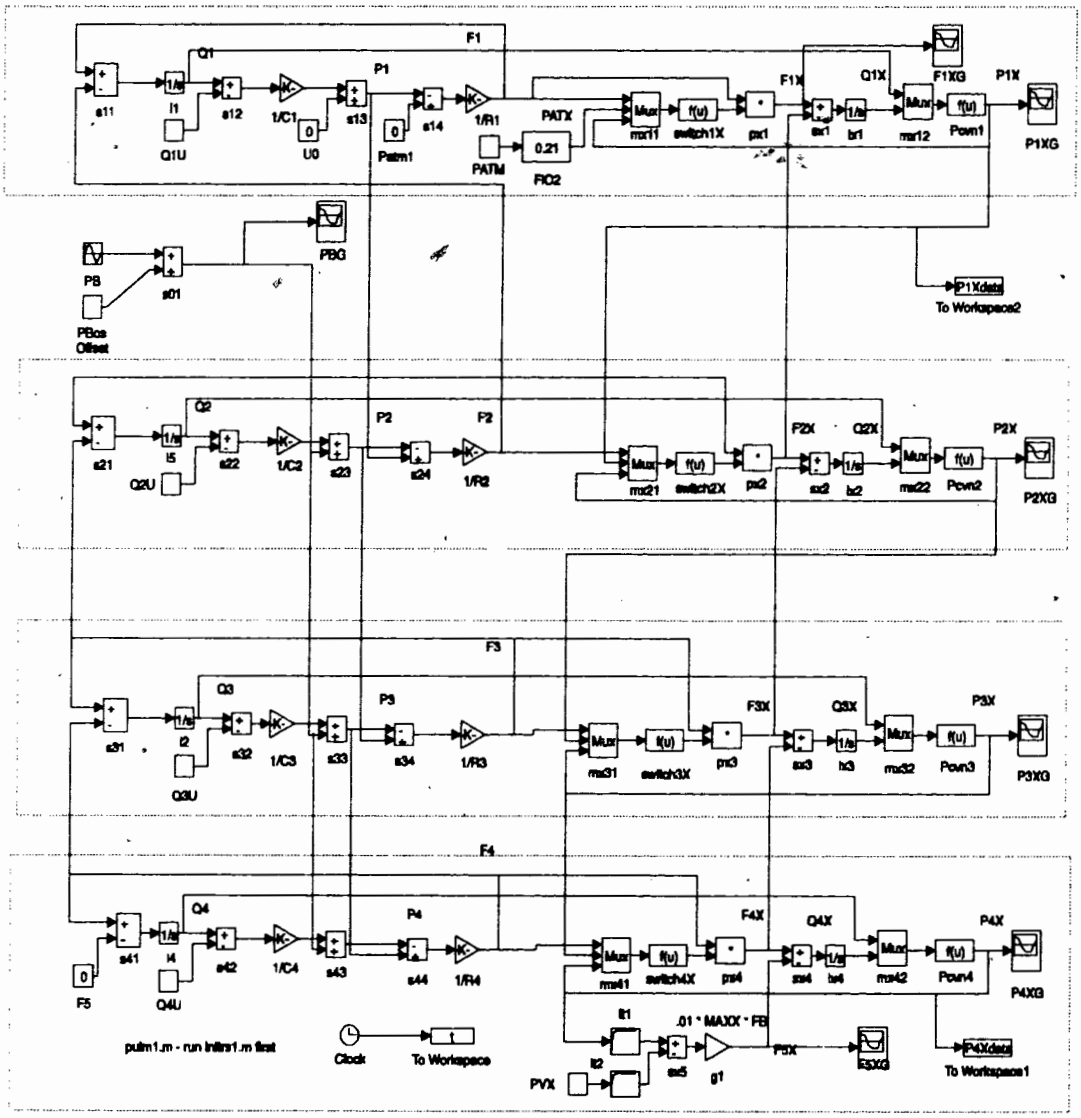

Figure 10. Adult Oxygen Transport Model - *the dashed boxes, from top to bottom represent the four respiratory compartments - mouth, trachea, bronchi and alveoli.*

3.4 Cardiovascular Model

The cardiovascular system consists of the pulmonary capillaries, pulmonary veins, heart, systemic arteries and systemic capillaries. Oxygen bonded to hemoglobin and dissolved in the blood is transported through this circulatory loop shown in Figure 11. This section describes a model for the flow of oxygen from the respiratory system to the tissue where a portion is metabolised.

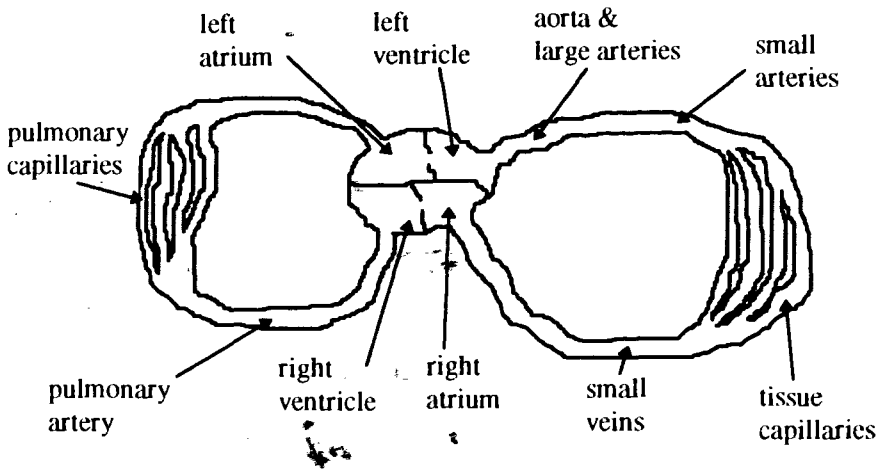

Figure 11. Cardiovascular System

Since the blood, like most fluids, is non-compressible, the compartments shown in Figure 11 can be treated as mixing chambers. The output concentration of a material from a mixing chamber is a function of the flow, volume and input concentration (Sheppard, 1948). Figure 12 illustrates a simple mixing chamber.

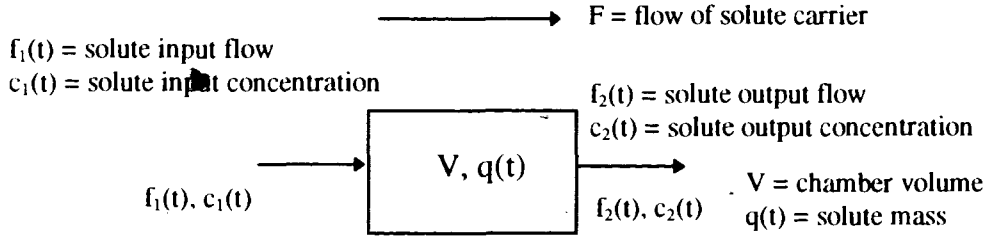

Figure 12. Simple Mixing Chamber

By mass balance:

$$q(t) = \int \{f_1 - f_2\}dt + q(0) \tag{3.7}$$

if:

$$c_1(t) = q(t)/V \tag{3.8}$$

$$f_1(t) = F*c_1(t) \tag{3.9}$$

$$f_2(t) = F*c_2(t) \tag{3.10}$$

then:

$$c_1(t) = (F/V) * \int \{c_1 - c_2\}dt + c_1(0) \tag{3.11}$$

or :

$$dc_1/dt = (F/V) * (c_1 - c_2) = (1/T) * (c_1 - c_2) \tag{3.12}$$

where:

$$T = V/F \tag{3.13}$$

In the frequency domain:

$$C_2 = C_1 * \frac{(1/T)}{(s + 1/T)} \tag{3.14}$$

Equation (3.14) shows that each mixing chamber can be modelled as a simple first order transfer function with a time constant, T, equal to volume divided by flow. A second type of compartment, a connecting compartment, can be modelled as a simple delay function. It represents the transport time of the solute in the blood through a region where the concentrations remain reasonably constant.

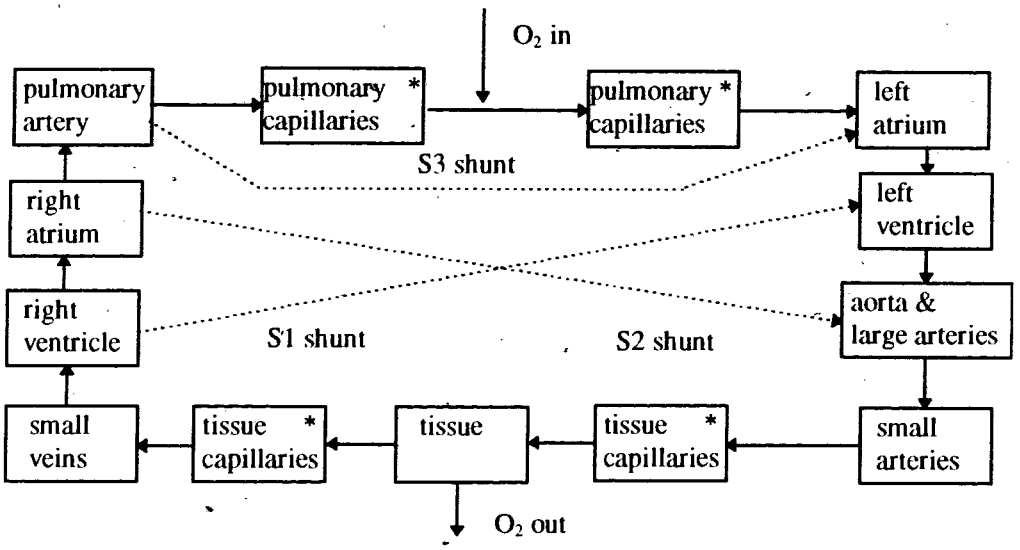

Figure 13. A 13 Compartment Circulatory System Model - *the capillary compartments, as indicated with an asterix are split in half to produce four delay compartments. The rest of the compartments are mixing chambers.*

Figure 13 illustrates a 13 compartment model of the cardiovascular system. There are four delay compartments representing the pulmonary and systemic capillaries. The delays associated with the systemic capillary compartments have been reduced to accommodate the tissue compartment. In earlier versions of the model, the tissue compartment was removed as a means of reducing the simulation's computing time. This model is derived from Rideout's 10 compartment model (1991, p.45) which was designed as a closed loop - including a single shunt - to track solute concentrations input at the right atrium. The first step in building the Figure 11 model was to adapt the 10 compartment model to SIMULINK. This 10 compartment model produced results that were comparable to Rideout's (1991, pp.46-48). The assumptions associated with this model are as follows:

(1) blood flow is non-pulsatile and uni-directional.

(2) all mixing chambers are perfect - instantaneous and complete.

(3) red blood cells travel at the same rate as blood.

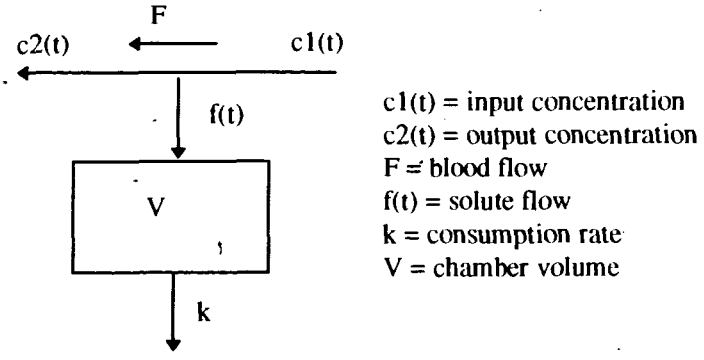

Figure 14. Tissue Compartment Model

The next step in the development process was to add the SaO_2 input and oxygen consumption. A unit step generator was used to produce an SaO_2 input. The tissue compartment transfer function, as shown in Figure 14, was modelled for oxygen consumption as follows:

$$f(t) = F * (c_1(t) - c_2(t)) \tag{3.15}$$

$$V * dc_2(t)/dt = f - (k * c_2(t)) \tag{3.16}$$

therefore:

$$V * dc_2(t)/dt = F * (c_1(t) - c_2(t)) - (k * c_2(t)) = (F * c_1(t)) - c_2(t)*(F + k) \tag{3.17}$$

in the frequency domain:

$$C_2 * (V * s + F + k) = F * C_1 \tag{3.18}$$

therefore:

$$C_2 = \frac{Ti}{s + Ti + k/V} \tag{3.19}$$

where:

$$Ti = F/V = \text{inverse of time constant} \tag{3.20}$$

A third major difference between the 10 and 13 compartment models is that the 13 compartment model has three shunts - a pulmonary shunt (S3) across the lungs; an atrial right-to-left shunt through the foramen ovale (S1); and a right-to-left shunt from the pulmonary artery to the aorta (S2). These shunts were first implemented as a combination of SIMULINK multipliers and additive blocks and once the simulation was started, the percentage of shunt could not be adjusted. Also, when a shunt or change in shunt percentage occurs, the flows through the effected compartments change and, since the time constants are a function of flow, the time constants' values must change.

Figure 15 represents the SIMULINK implementation of Figure 13. Constants, such as Ti, Ki, etc. are set by running the initialisation "initpm1.m" first. At the start of a simulation, the flows and time constants are calculated as a function of the initial shunt values. The initial flows are set to zero by the SIMULINK program and the simulation requires about 3 minutes to reach steady state. This model was tested using a pulse generator to produce an SaO_2 change between the two pulmonary capillary compartments. The dynamic response was comparable to Rideout's data (1991, p.148).

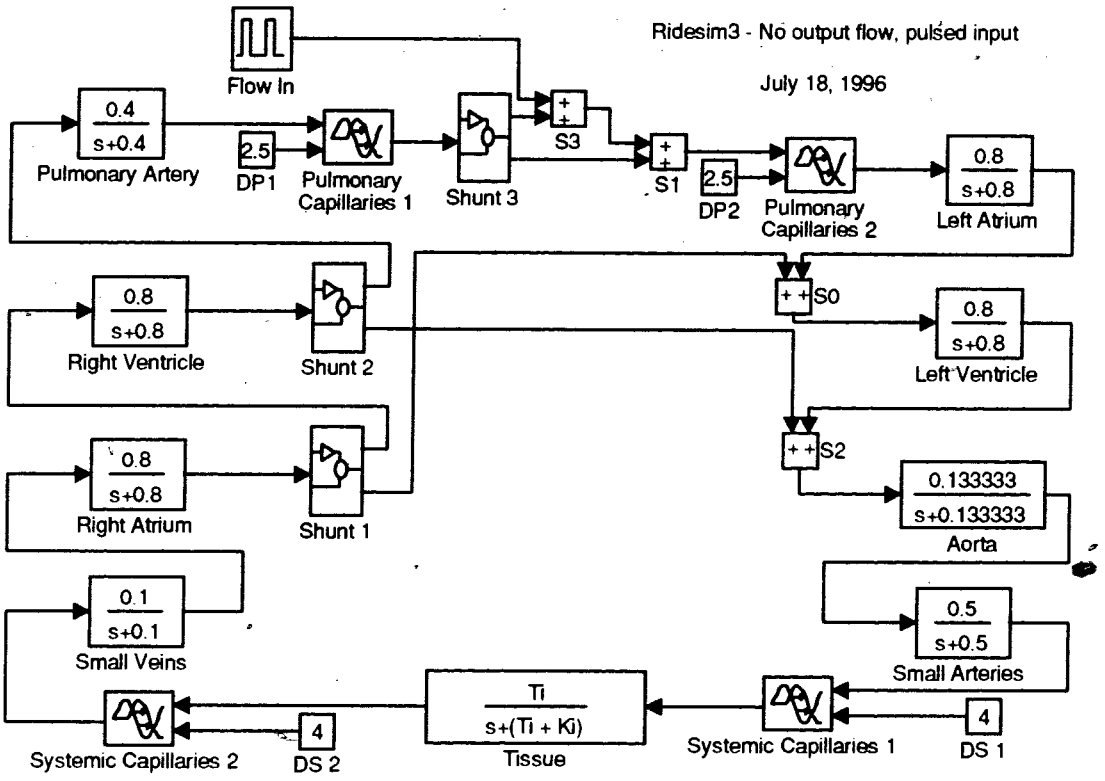

Figure 15. Adult Cardiovascular Model

3.5 Adult Oxygen Transport Model

An adult oxygen transport model consists of merging the respiration and circulation models described in the previous sections. This process was relatively straight forward but produced a model with a substantially increased run time. The respiration model outputs its PAO_2 value to the circulation model which in turn exports its SvO_2 value back to the respiratory system.

A major complication arose when trying to make the shunting values dynamic. Shunt values change during an experiment as a means of emulating the adult's physiological behaviour. At

first, a supervisory program was written by the author to adjust the shunts and compartment time constants. Unfortunately this produced unstable transient responses because SIMULINK sets its integrators to zero whenever the parameters of its library transfer functions are changed. The solution was to redesign the compartments using discrete building blocks such as integrators, summing junctions, etc. SaO_2, SvO_2 and PAO_2 values for a 10% steady state pulmonary shunt are shown in Figure 16. The output flow during this simulation was 4.2 ml/s (250 ml/min.) which is close to the estimated oxygen consumption of a 70 kg. adult with an average blood flow (F) of 100 ml/s (Ross, 1985). Also note that PAO_2 oscillates between 100 and 122 mmHg producing an SaO_2 of 97% and an SvO_2 of 78% which are comparable with physiological data (West, 1985).

Figure 17 is a plot of the SvO_2, SaO_2 and PAO_2 values when a pulmonary shunt (S3) increases from 0.10 to 0.55 at 200 seconds and then is reduced back to 0.10 at 300 seconds. The initial conditions are set before running the simulation. Figures 18 and 19 show the same model parameters for S1 and S2 shunts adjusted following the Figure 17 paradigm. The first 200 seconds in each graph represents the initial start-up transient and are removed. This transient is a function of SIMULINK's delay compartments which cannot be pre-loaded with initial values besides zero. Figure 17 shows a desaturation pulse to 80% which is not as low as the other two plots. This is because the plots in Figures 18 and 19 represent a 10% S3 shunt plus a 55% S2 or S1 shunt, while Figure 17 represents only a 55% S3 shunt.

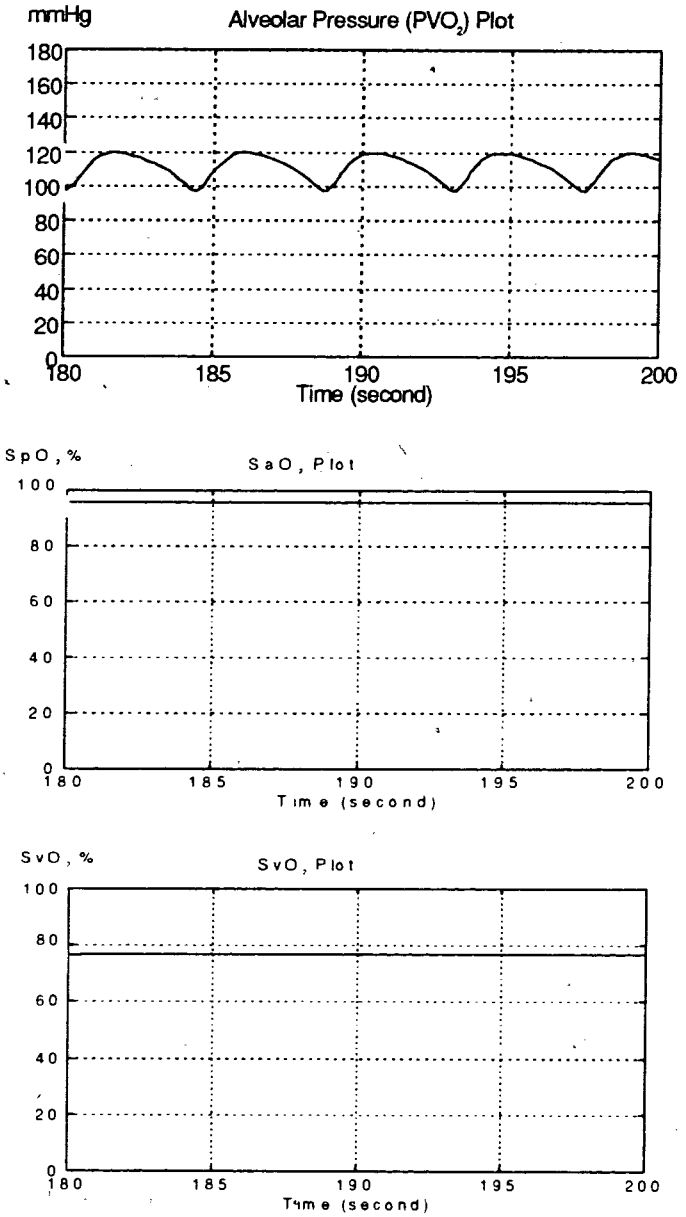

Figure 16. Adult SaO_2, SvO_2 and PAO_2 Plots

These three plots demonstrate the model's non-linearity with a desaturation time constant of about 70 seconds and a saturation time constant of 15 seconds. Physiologically speaking, this makes sense; the body is very slow to desaturate but quick to saturate. This dynamic response to shunting has been collaborated by Wilkinson (1995) who derived SaO_2 curves from lambs

with varying degrees of shunting. Their time constants were 20 and 6 seconds for desaturation and saturation respectively. The ratios of saturation to desaturation time constants for the model and Wilkinsin's work are comparable - about 0.25.

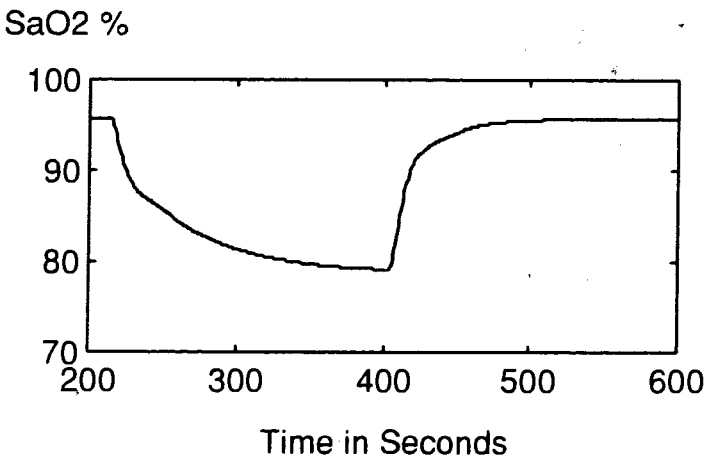

Figure 17. Adult Model S3 Adjustment - *0.10 to 0.55 at 200 sec. and to 0.10 at 400 sec.*

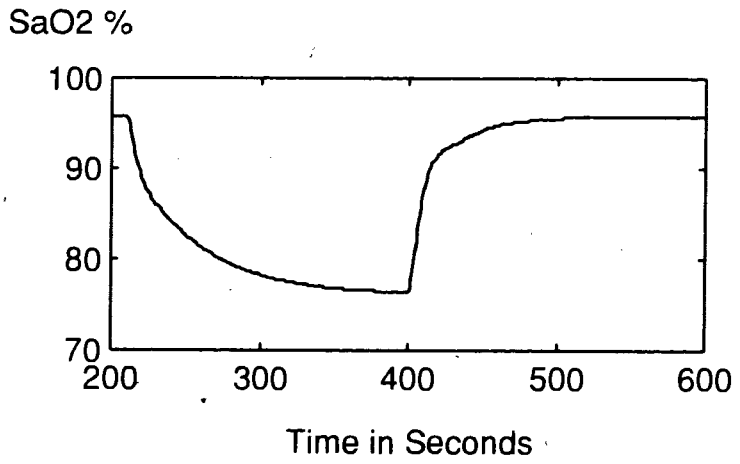

Figure 18. Adult Model S2 Adjustment - *0.10 to 0.55 at 200 sec. and to 0.10 at 400 sec.*

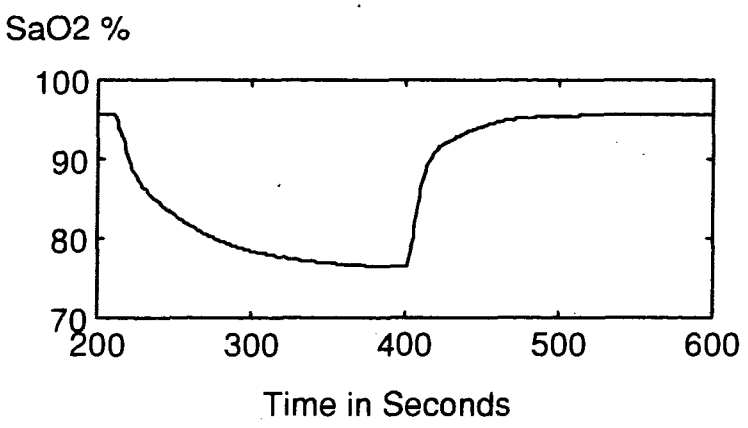

Figure 19. Adult Model S1 Adjustment - *0.10 to 0.55 at 200 sec. and to 0.10 at 400 sec.*

3.6 Neonatal Oxygen Transport Model

There are essentially three major differences between human neonatal and adult physiology. The first, and most obvious, is scale; the magnitude of the neonate's respiratory and circulatory system parameters such as lung volume, resistance, compliance, blood flow, heart chamber volume tend to follow physiological scaling laws (Dawson, 1991).

The second major difference, as described in the previous chapter, is that neonatal hemoglobin has a higher affinity to oxygen than adult hemoglobin. This implies that the neonate will saturate at lower PaO_2 values than the adult. It also implies, however, that the rising edge of the neonatal oxygen dissociation curve is much steeper than the adult's, which can result in larger desaturations when the neonate's PaO_2 moves below the "knee" of the curve.

The third most important physical difference is that the neonate often suffers from one or more simultaneous shunts. It is primarily those shunting events, as observed in the nursery, which produce dangerously low blood oxygen saturation levels in pre-term infants. This section describes how the adult oxygen transport model has been adapted to a neonatal model incorporating differences in scale, oxygen affinity and shunting.

Information with regards to the specific physical parameters used by the model tends to be scarce. A major help, however, is the general observation that within mammals, parameters for a specific age can be extracted from those of an adult mammal bearing the same weight, surface area, etc. (Cook, 1958). For example, the oxygen consumption rate of a 1500 gm human is about the same as that of a full grown 1500 gm rat. This principle will be used to extrapolate parameter values which are unavailable in the literature via empirical means. A second technique the author has used to calculate model parameters is one of proportional scaling where an aggregate sum is available but not its specific break down. For example, a 70 kg adult's total lung compliance, on average, is 0.2183 (cm^4*s^2/gm) with 0.60% for mouth, 1.8% for trachea, 6.0% for bronchi and 91.6 % for alveoli.

Table II lists the various respiratory parameters as calculated from their associated allometric equations (Stahl,1967). The three values of interest for the model are lung compliance, resistance and tidal volume. From Dawson, (1991, p.127), for a 1500 gm mammal we get a total lung volume of 0.102 litres - derived from: 0.068 * M = 0.068 * 1.5, where M is mass in Kg. He also states (1991, p.127) that the tidal volume is generally about 10% of the total lung

volume. This is true for a 70 Kg adult whose total lung volume is about 5 litres and tidal volume is 500 ml (Ross, 1985). Thus for a neonate we can set the tidal volume to 10 ml, which is empirically confirmed (Scarpelli, 1975). The total adult unstressed volume (i.e. volume at rest) is 466 ml which is 93.2% of the tidal volume. Using this relationship, the author estimates the neonate's unstressed volume to be 9.32 ml (93.2% of 10 ml) as listed in Table III. The unstressed volumes of each specific compartment are then calculated as weighted percentages, where the percentage for each compartment is based on the adult model. For example, the adult alveoli unstressed volume is 85.8% of the total, thus the neonate's value is 8.00 ml (0.858 * 9.32 ml).

Empirical values for the total static respiratory resistance are available and have a large range (Cook, 1957; 1958; Polgar, 1961 and 1965; Kraus, 1973). They are, however close to the allometric value from Table II of 18 cm^4*s^2/gm but the writer has chosen a slightly higher value of 25.0 as shown in Table III. Total pulmonary compliance is also varied but a review of the literature prompts the author to use a value of 0.002 cm^4*s^2/gm (Cook, 1958, Scarpelli, 1975, p.155). The allometric value from Table II is a bit higher at 0.0033 cm^4*s^2/gm.

Table II. Allometric Values for the Respiratory System (M = mass in Kg.)

Parameter	Equation	70 Kg Adult	1500 gm. Neonate
Tidal Vol. (ml)	$7.69M^{1.04}$	638	11.7
Total Capacity (ml)	$53.5M^{1.06}$	4832	82.2
Respiratory Rate (bpm)	$53.5M^{-0.26}$	17.7	48.1
O2 Uptake (ml/s)	$0.193M^{0.76}$	4.88	0.26
Compliance (ml/cmH_2O)	$2.10M^{1.08}$	206.5	3.25 (0.0033 cm^4*s^2/ml)
Resistance (cmH_2O*s/L)	$2.44M^{-0.70}$	1.247	18.37 (18.0 dyne*s/ml)
Cardiac Output (ml/s)	$3.117M^{0.81}$	97.3	4.33
Cardiac Rate (/min.)	$241M^{-0.25}$	83.3	218

Table III. Respiratory System Model Parameters - *adult and neonatal values as used in the models.*

Parameter	70 Kg. Adult	1500 gm. Neonate
Total Unstressed Vol. (ml)	466.0	9.32
Mouth Unstressed Vol.(ml)	40.0	0.80
Trachea Unstressed Vol.(ml)	8.0	0.16
Bronchi Unstressed Vol.(ml)	18.0	0.36
Alveoli Unstressed Vol. (ml)	400.0	8.00
Total Resistance (dyne*s/ml)	1.42	25.0
Mouth Resistance (dyne*s/ml)	1.0	14.62
Trachea Resistance (dyne*s/ml)	0.33	4.825
Bronchi Resistance (dyne*s/ml)	0.30	4.385
Alveoli Resistance (dyne*s/ml)	0.08	1.17
Total Compliance (cm^4*s^2/gm)	0.2183	0.002183
Mouth Compliance (cm^4*s^2/gm)	0.0013	0.000013
Trachea Compliance (cm^4*s^2/gm)	0.0040	0.000040
Bronchi Compliance (cm^4*s^2/gm)	0.0130	0.000130
Alveoli Compliance (cm^4*s^2/gm)	0.2000	0.002000
Respiratory Rate (beats/min.)	14	25

Table IV. Circulatory System Model Parameters - *adult and neonatal values as used in the SIMULINK models.*

Parameter	70 Kg Adult	1500 gm Neonate
Average Blood Flow (ml/s)	100	16.70
Oxygen Consumption (ml/s)	24.36	0.20
Total Transport Time (sec.)	39.0	9.0
Pulmonary Capillary Vol. (ml)	800	18.8
Left Atrium Vol. (ml)	125	4.68
Left Ventricle Vol. (ml)	125	4.68
Aorta & Large Artery Vol. (ml)	750	28.22
Small Artery Vol. (ml)	200	7.51
Tissue Capillary Vol. (ml)	800	30.06
Small Vein Vol. (ml)	1000	37.58
Right Atrial Vol. (ml)	125	4.68
Right Ventricle Vol. (ml)	125	4.68
Pulmonary Artery Vol. (ml)	250	9.39

The average blood flow for a 1500 gram neonate, as listed in Table IV, was derived from Dawson's scaling laws (Dawson, 1991). Oxygen consumption is empirically defined by Scarpelli (1975, p.174) at 0.15 ml/s which is lower than Dawson's allometric value of 0.25 ml/s (1991, p.88); an average of 0.20 ml/s has been chosen by the author. The total transport time is from Dawson (1991, p.87) and confirmed by Stahl (1967). The adult volume parameters listed in Table IV are from Rideout (1991, p.46) and Ross (1985, p.121); they are used to scale neonatal values. The neonatal O_2 dissociation curve was extracted from Poet (1991) and is comparable to that of other researchers (Scarpelli, 1975, p.138; Delivoria-Papadopoulos, 1971).

Another assumption made by the author is that the neonatal model represents an infant breathing unassisted. In many cases, neonates weighing 1500 grams are ventilated at pressures of 10 to 25 cmH_2O. The pressure signal generator was moved to the mouth compartment and the output PAO_2 was not changed. In reality, larger input pressures are required to ventilate neonates because the compliance of the ventilator's circuit is significantly higher than the neonate's pulmonary system. In other words, the tubing tends to expand before the lungs. Also, when the patient breaths on his/her own, they use their diaphragm and chest wall muscles to inflate the lungs. Under a ventilator, however, the ventilator must also overcome the static and, in some cases opposing, chest wall and diaphragm resistance. As a means of simplifying the model, an internal pressure generator is maintained and the effects of the ventilator omitted. The driving pressure of the pressure generator has been slightly increased to accommodate the two orders of magnitude reduction in compliance. Figure 20 illustrates the SaO_2, SvO_2, O_2

flow and PAO_2 values for a 10% S3 shunt and an FiO_2 value of 0.21 (room air). This plot shows the PAO_2 in the range of 40 to 90 mmHg which is comparable to published values (Scarpelli, 1975, p.146). Also, the average O_2 flow is about 0.30 ml/s, close to the value defined in Table IV. The neonate model is shown in Figures 21, 22 and 23. Implementation of individual compartments in Figure 22 is identical to that shown in Figure 10. In this model, FiO_2, all three shunts and the dissociation curve can be adjusted during a simulation. Before this model is run, the initialisation program, "initnn1.m" must be run - See Appendix A for a listing.

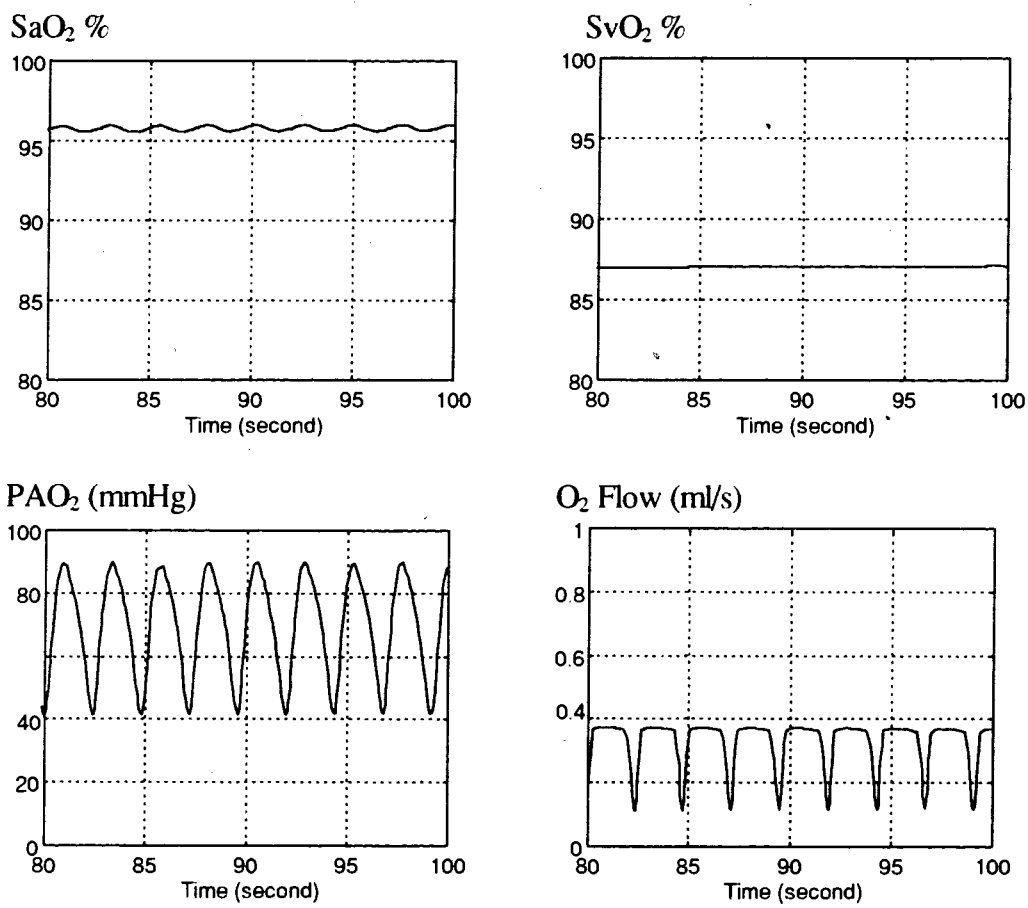

Figure 20. Neonatal Model Output

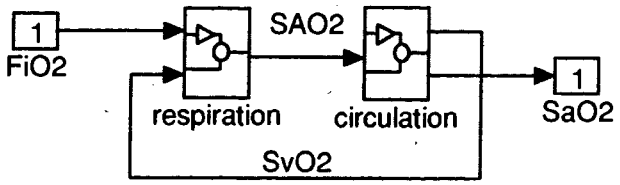

Figure 21. Neonatal Model Overview

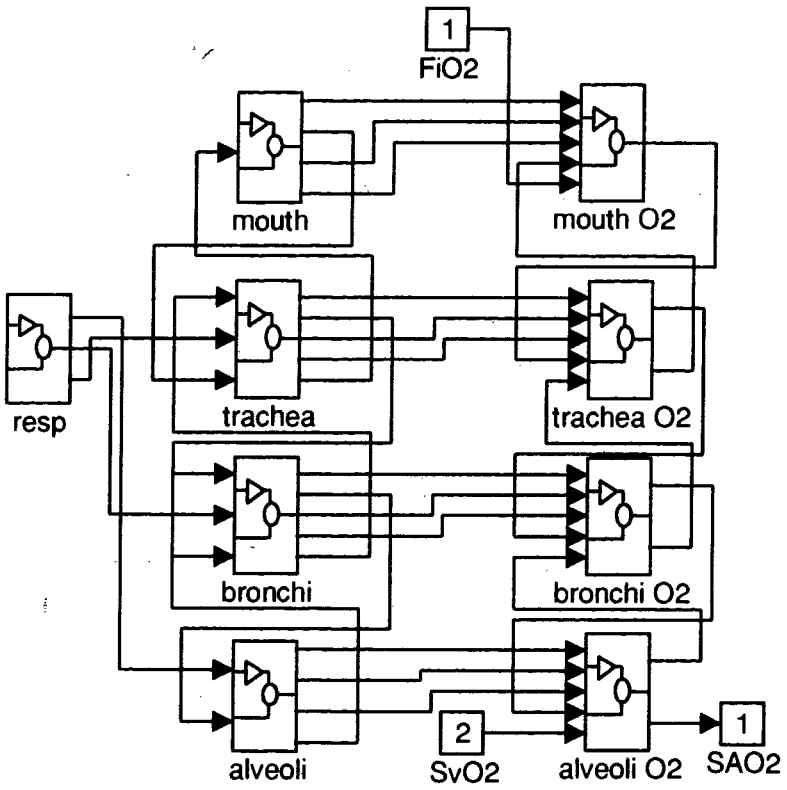

Figure 22. Neonatal Respiratory System Model.

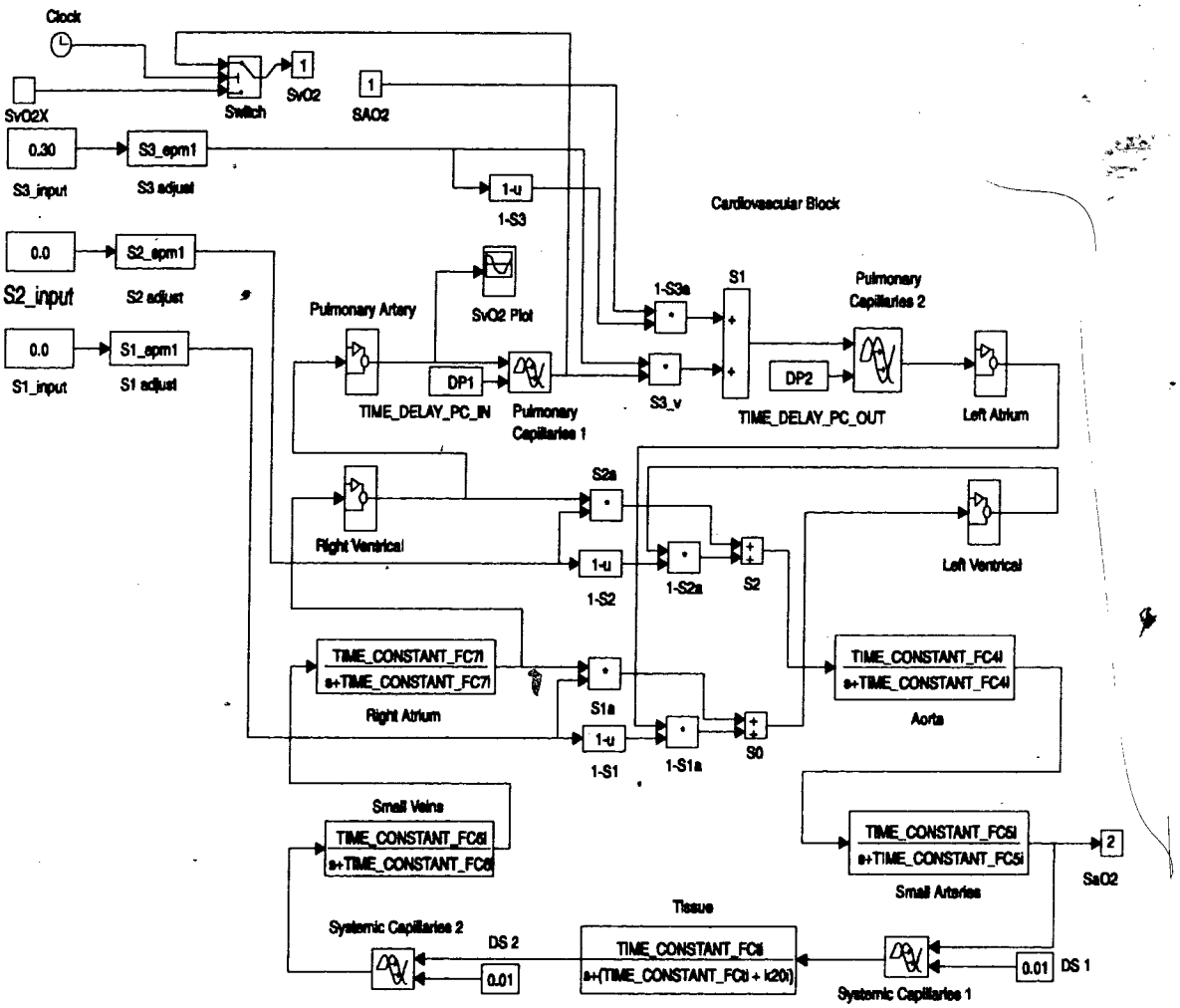

Figure 23 Neonatal Circulatory System Model.

3.7 Air/Oxygen Blender Model

The electro-mechanical air/oxygen blender constructed by the author has a rate limited swing from 0.21 to 1.0 FiO_2 in 5.0 seconds. A prototype blender was modified with a clutched DC motor to adjust the dial and an optical encoder to realise dial position. The clutching mechanism provided a means of accommodating user override. The blender had a 240 degree rotation representing a 79% FiO_2 range. This gave 3 degrees of resolution per 1% FiO_2. With a

16 bit optical encoder providing position feedback, 1200 counts per degree were available. In reality, a 0.2% FiO_2 dial resolution could be produced by the prototype. It is assumed that the model's mixed gas output is instantaneous and of infinite resolution. Figure 24 represents the blender model.

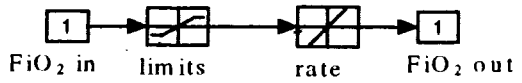

Figure 24. Air/Oxygen Blender Model.

3.8 Pulse Oximeter Model

The pulse oximeter can be subject to two sources of disturbance - sensor noise due to light and motion artifact. Sensor noise is modelled by adding a white noise generator to the input signal and motion artifact is produced by amplifying a pulse generator's signal and adding it to the pulse oximeter's input. This amplification can be controlled by software during a simulation. Figure 25 represents the pulse oximeter model and Figure 26 displays the test output from a 0.2 Hz sine wave input.

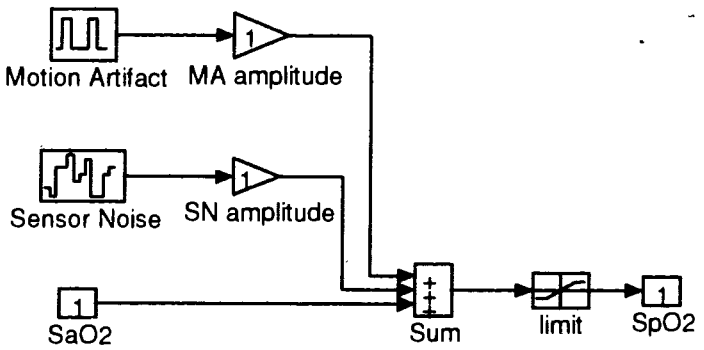

Figure 25. Pulse Oximeter Model

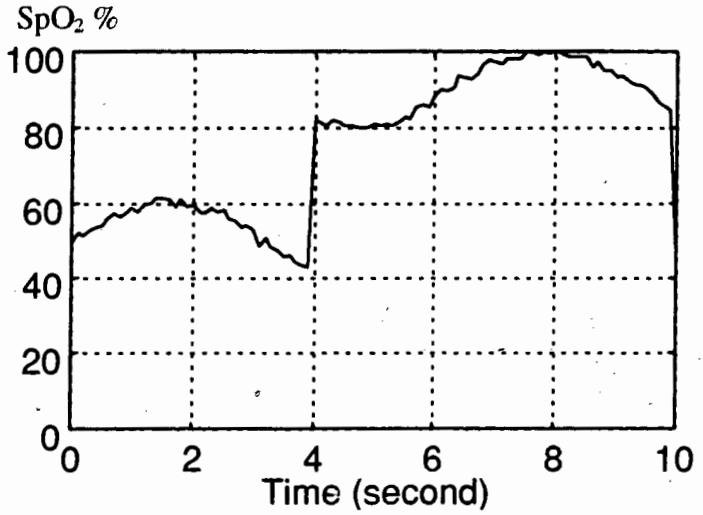

Figure 26. Pulse Oximeter Model Test Output.

3.9 Supervisory Programs

A one hour simulation of a 1500 gm neonate can be produced using the three components - actuator (air/oxygen blender), plant (neonate) and monitor (pulse oximeter) - and a supervisory program, also known as a test script. Each supervisory program is a software routine that reads the clock and at specific times events such as motion artifact, shunting, etc. can be applied to the model.

After reviewing nursery data, collected during previous studies (Morozoff, 1992; 1994), the following conditions have been defined by the author:

(1) Short desaturation pulse: a large desaturation pulse with a 1-2 minute duration. This is a very common occurrence and the pulse is usually caused by a single shunt.

(2) Long desaturation pulse: 10 - 15 minute duration where motion artifact and other shunting conditions can occur.

(3) Positive motion artifact: these are 100% SpO_2 saturations produced by patient motion and tend to be long enough - 10 to 60 seconds - for the controller to begin lowering the FiO_2. In the nursery, under manual oxygen therapy, however, this condition is usually ignored by clinical staff and no oxygen increment is realised.

(4) Negative motion artifact: these are SpO_2 desaturations (usually below 75% SpO_2) produced by patient motion. The duration is 10 - 60 seconds and, like condition (3), usually ignored by clinical staff.

(5) Large desaturation coupled with positive motion artifact: positive motion artifact disguises the desaturation and the controller drops the FiO_2 causing further hypoxemia.

(6) Large saturation coupled with negative motion artifact: opposite of condition (5); this creates a high FiO_2, pushing the infant into saturation.

(7) Long term physiological change: average FiO_2 tends to change as a result of a specific event such as physiotherapy, drug injection, feeding, etc. This can be modelled as a dissociation curve shift or a shunt adjustment.

From the above conditions, three preliminary scripts were produced - baby 1, 2 and 3. See Appendix B for listings of each. Baby 1 represents a generally stable infant with a 20% pulmonary shunt. This baby, however, is quite active and produces many events of motion artifact - conditions (3) and (4). The purpose of baby 1 model is to test a controller's reaction to motion artifact and whether those reactions push the infant out of normoxemia.

The second supervisory program, baby 2, suffers from a 30% pulmonary shunt with sporadic episodes of ductus arteriosis (S2) shunts coupled with a few periods of motion artifact. This model will illustrate the controller's performance associated with dynamic shunting.

Baby 3 has a 20% pulmonary shunt and a 10% S2 shunt with many periods of S2 shunts going to 30%. This is an unstable infant model and there is only one motion artifact which represents physiotherapy activity resulting in a right shift of the dissociation curve (condition (7)). The purpose of this model is to stress the controller's ability to regulate the FiO_2 after the dynamic response of the model has changed.

Each script was verified by adjusting the FiO_2 to ensure that a target SpO_2 of 92% could be attained during periods of non-motion artifact. See Chapter 5 for a more detailed description of the test scripts and plots of each under various modes of control.

3.10 Summary

A software based model of the neonatal oxygen transport system is developed in this chapter. The model traces oxygen levels as partial pressures of gas through the respiratory system and as concentrations bonded to hemoglobin in the circulatory system. Four compartments - mouth, trachea, bronchi and alveoli - are modelled as RC compartments connected in series to make up the respiratory system. Perfect mixing chambers, modelled as first order transfer functions, and delay compartments make up the circulatory system of pulmonary capillaries, left atrium, left ventricle, aorta and large arteries, small arteries, tissue capillaries, tissue, small veins, right atrium, right ventricle and pulmonary artery. Circulation and respiration circuits are linked by the oxygen dissociation curve.

An adult model is first constructed and tested; it is then scaled to a neonatal model using empirical parameters and mammalian scaling functions. The circulatory model was designed to accommodate the dynamic adjustment of pulmonary and cardiac shunts plus the shifting nature of the oxygen dissociation curve. Models for the actuator (air/oxygen blender) and monitor (pulse oximeter) where also designed in this chapter. The pulse oximeter model features sensor noise and software control of motion artifact. Three supervisory programs were developed to mimic the behaviour of three types of neonate: Baby 1 - stable (only two pulmonary shunt events) but active; Baby 2 - unstable (frequent pulmonary and cardiac shunts) but not active; Baby 3 - unstable (frequent cardiac and pulmonary shunting), not active and changing oxygen affinity.

4.0 FUZZY LOGIC CONTROLLER

4.1 Introduction

Even with developments in drug therapy, the incidence of oxygen therapy related illness such as ROP and bronchopulmonary dysplasia is relatively high (Gibson, 1990; Bancalari, 1979). Bancalari (1987) has shown that even with continuous monitoring and manual response, the quality of oxygen therapy was not improved in low birth weight infants. These results, possibly due to a lower mortality rate in low birth weight infants or an incorrect definition of hyperoxemia (upper limit of PaO_2 set too high), prompts the author to explore improvements in the administration of oxygen therapy.

If a patient is labile (frequently outside of normoxemia), an attendant must regulate tissue oxygenation by constantly adjusting FiO_2 levels. Automatic control systems in the medical arena are becoming more prevalent - including devices which control anesthetic gases, blood pressure, heart rate, etc. (Sheppard, 1980; Linkens, 1992; Hacisalihzade, 1992) - and the need to automate oxygen therapy has been identified by the medical community (Flynn, 1992). A few researchers have developed prototype controllers (Beddis, 1979; Taube, 1989; Morozoff, 1991) but to date, none have been commercialised; possibly due to the limited market and high risk associated with an automatic neonatal oxygenator. However, if available, this type of instrumentation could serve as an assistant to nursing staff and make minor FiO_2 adjustments in their absence.

When formulating a controller, the designer must consider the limitations associated with the controller's actuator and observer. Noise from the observer's sensors will affect the designer's choice of controller parameters, as will actuator saturation points. In most neonatal care units, a pulse oximeter is used by staff to indicate the level of tissue oxygenation. This technique is non-invasive and, when correlated to blood gas samples, reliable within the range of 85% to 95% SpO_2 (Poets, 1994). For the controller's input, the author chooses to use the SpO_2 signal from a model of a commercial pulse oximeter which includes sensor noise and motion artifact. A model of a motorised air/oxygen blender, as described in Chapter 3, will be the actuator with saturation points at 21% and 100% FiO_2.

This chapter discusses manual and automatic oxygen therapy methodologies for application to the neonatal model developed in Chapter 3. The design of two types of automatic controllers, proportional-integral-differential (PID) and fuzzy logic, will be presented.

4.2 Manual Control

Experienced nursing staff can provide stable and accurate oxygen therapy for preterm infants. They have the ability to filter (ignore) erroneous pulse oximeter signals that are the result of sensor noise or motion artifact. Another skill they possess is the ability to accommodate the non-linearity of the oxygen transport system; small FiO_2 adjustment for desaturation and large adjustment for saturation. The most important ability of nursing staff is associated with the knowledge they gain while working with a patient for a few days. They can pick up trends, accommodate changes due to drug therapy, etc. All these skills have been observed in neonatal

nursing staff by the author who has spent hundreds of hours in their environment at the Special Care Nursery of British Columbia's Children's Hospital.

The above paragraph seems to contradict previous statements by the author about the automation of oxygen therapy leading to an improvement. This contradiction is related to the fact that, in real nursery environments, staff cannot dedicate their time to continuous oxygen therapy. Nursery staff may attend to more than one infant and also must provide time for other tasks such as feeding, changing, suctioning, cleaning, parental consultation, etc.

A common method of applying O_2 therapy in the nursery is to find an FiO_2 setting which provides the infant with an SpO_2 of about 92%. Then alarm levels are set at about 88% and 96%. When an alarm occurs, the attendant checks for motion artifact by observing the infant and then compares the pulse oximeter's heart rate reading with that from an independent heart rate monitor. If the independent source is stable but the pulse oximeter's heart rate value is low or high, the staff conclude that the alarms are the result of sensor or motion artifact and no FiO_2 adjustment is made. If, however, the heart rates from the two instruments are about the same, a saturation, or desaturation has occurred. In this case, nursery staff may wait 10 to 15 seconds to see if the infant returns to normoxemia. During this period another check is made of the infant's condition - skin tone is often an indicator of tissue oxygenation. At the discretion of the nurse, an FiO_2 adjustment is made if further episodes occur or SpO_2 levels appear poor.

The above paragraph is a general description of a method for providing oxygen therapy requiring several inputs - SpO_2, pulse oximeter heart rate, skin tone, independent heart rate, patient motion, previous occurrences, etc. The essence of this type of control is to maintain normoxemia (90% to 95%) rather than a specific set point. Manual control for the three test scripts described in Chapter 3 will mimic the nursery staff. Baby 1 is a very stable infant and its FiO_2 will be set at 30% for the entire experiment; motion artifacts will be ignored as will small changes in SpO_2. Baby 2, similar to Baby 1, will require no FiO_2 adjustments from its 35% setting. The physiology of Baby 3 changes halfway through the experiment as its oxygen dissociation curve shifts right. A resulting decreased oxygen affinity requires that the FiO_2 value, which started at 32%, be slightly increased to 35% a few minutes the event.

Should the test scripts have a requirement for more manual adjustments? Perhaps, but the end result, in manual mode, would be the same. In response to the programmed manual adjustments, the neonatal model would spend most of its time in normoxemia. The automatic controllers would react to SpO_2 changes outside normoxemia in a similar fashion to SpO_2 changes within.

4.3 PID Control

Classic feedback control methodology can be applied to SaO_2 control as was done by Taube (1989). His controller is based on a first order model of the system which consists of a non-ventilated neonate in an air/oxygen filled incubator. This resulted in a simple system with, understandably, a large lag. Taube's work is biased by the fact that most non-ventilated

neonates tend to be quite stable. In other words, his controller was applied to a relatively stable system where the neonate's oxygen transport system acted in a linear fashion; i.e. their SpO_2 set points were far from the "knee" of the oxygen dissociation curve. This thesis is focused on ventilated low birth weight neonates who tend to be unstable with target SpO_2 values close to the "knee" of the dissociation curve.

The neonate model developed in Chapter 3 is non-linear as illustrated in Figure 27. This diagram presents the model's open loop step responses to 10% FiO_2 increments at time 200 and 350 seconds (steps 1 and 2) plus 10% FiO_2 decrements at 500 and 650 seconds (steps 3 and 4). In this test, the model is set up with only a 20% pulmonary (S3) shunt. Note that the first positive response is a 15% SaO_2 increase while the second is only 5%. Time constants are quite different: 40 seconds for step 1; 15 seconds for step 2; 40 seconds for step 3; 40 seconds for step 4. These differences can be explained by the effect of the PvO_2 level (partial pressure of oxygen in blood returning to the lungs). Before step 1 begins, the model has a 21% FiO_2 resulting in very low SpO_2 and SvO_2 values. When the 10% FiO_2 occurs, the PAO_2 value (alveolar oxygen partial pressure) becomes much higher than the PvO_2. This high pressure drives oxygen into the system quickly, increasing the PaO_2 and SaO_2 values and, with a total transport time of about 10 seconds, the PvO_2 and SvO_2 levels as well. The second step gives a similar initial response, but a saturation point is reached in about 20 seconds resulting in what appears to be a fast time constant. When an FiO_2 decrease is implemented at step 3, the model is fully saturated at 97% and the sudden drop in PAO_2 can only be accommodated by two mechanisms - oxygen metabolism at the tissue and via the lungs at exhale. If the new PAO_2

value is still higher than the PvO_2 then oxygen will not be exhaled and so, it appears that the rate of desaturation is controlled by the O_2 consumption rate.

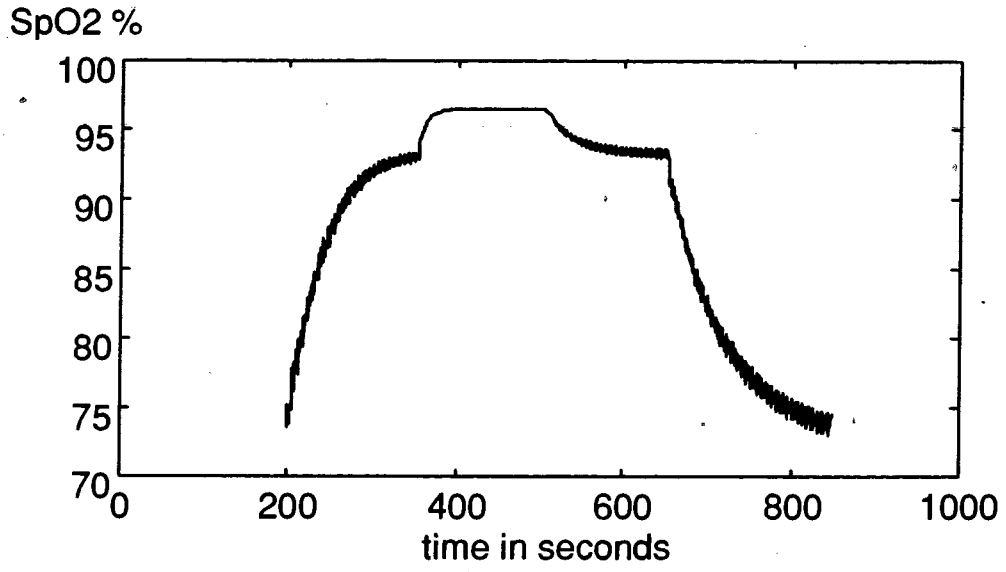

Figure 27. Open Loop Step Responses - *10% FiO_2 increments occur at 200 and 350 seconds; 10% FiO2 decrements occur at 500 and 650 seconds. This figure illustrates the non-linearity of the oxygen transport system and shows that, depending on the SaO_2 levels, similar FiO_2 increments/decrements do not result in the same response.*

Equations (4.1) and (4.2) define the feedback value, u(t), as a function of the error, e, its integral and derivative.

$$u(t) = Kp\,(e + (1/Ti) * \int\{e\}dt + Td *(de/dt)) \quad (4.1)$$

$$u(t) = Kp*e + Ki * \int\{e\}dt + Kd*(de/dt) \quad (4.2)$$

where:

$$Ki = Kp/Ti \quad (4.3)$$

$$Kd = Kp*Td \quad (4.4)$$

The step responses in Figure 27 can be used to design the PID controller. Franklin (1986) suggests a simple method where the general slope and system lag illustrated by a step response can be used to set the PID gains. Figure 28 is a simplified diagram of a generic system open loop step response. The PID gains can be calculated as follows:

$$Kp = 1.2 * R * L \tag{4.5}$$

$$Ki = Kp/2L \tag{4.6}$$

$$Kd = 0.5 * L * Kp \tag{4.7}$$

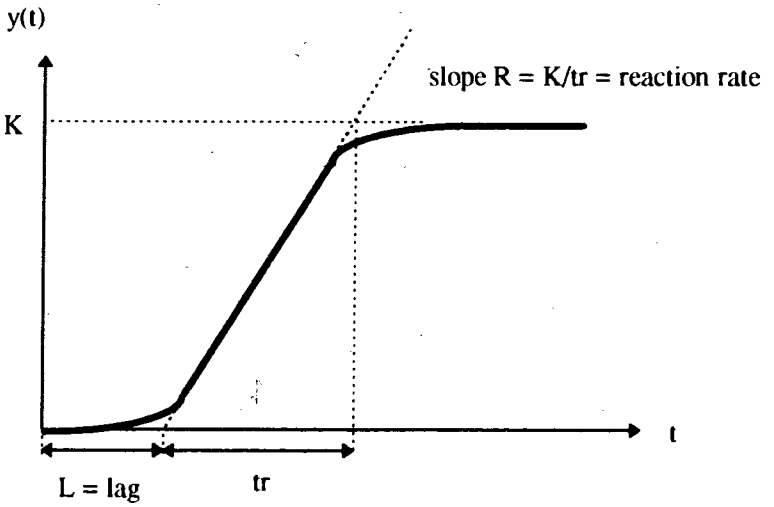

Figure 28. Generic System Response - *modified from Franklin GF. Feedback Control of Dynamic Systems. Addison-Wesley, Don Mills, Ontario, 1986, p. 104.*

From a detailed plot of Figure 27, the parameters R and L where extracted and applied to equations (4.5), (4.6) and (4.7) to produce Table V. With the exception of step 3, Table V suggests that average gains of (1.00, 0.100 and 2.5) for (Kp, Ki and Kd) would provide adequate control. This controller, however, would be slow to respond to SaO_2 drops within the 90% to 95% range since Table V suggests gains three times larger for this region. Since the

region in question is normoxemia, the proposed average values are acceptable. If we plotted a histogram representing percent of time spent by the closed loop system at SpO_2 values from 0 to 100, this controller should give a peak at the target (set to a point in normoxemia) with a slight hyperoxic skew.

Table V. PID Gains from Open Loop Step Responses

Step#	R (SpO_2/sec)	L (sec.)	Kp	Ki	Kd
1	0.30	5	0.800	0.080	2.000
2	0.20	5	1.200	0.120	3.000
3	0.08	5	3.000	0.300	7.500
4	0.22	5	1.091	0.109	2.727

In 1993 the author used various PID gains in clinical trials for his prototype controller (Morozoff, 1994). A review of the data suggested that, empirically, the best gains were (1.750, 0.164, 0.1094) for (Kp, Ki, Kd). These values agree with those suggested by Franklin's method (see Table V) with the exception of the differential gain, Kd. The author found that this gain must be dropped an order of magnitude to reduce the effect of motion artifact.

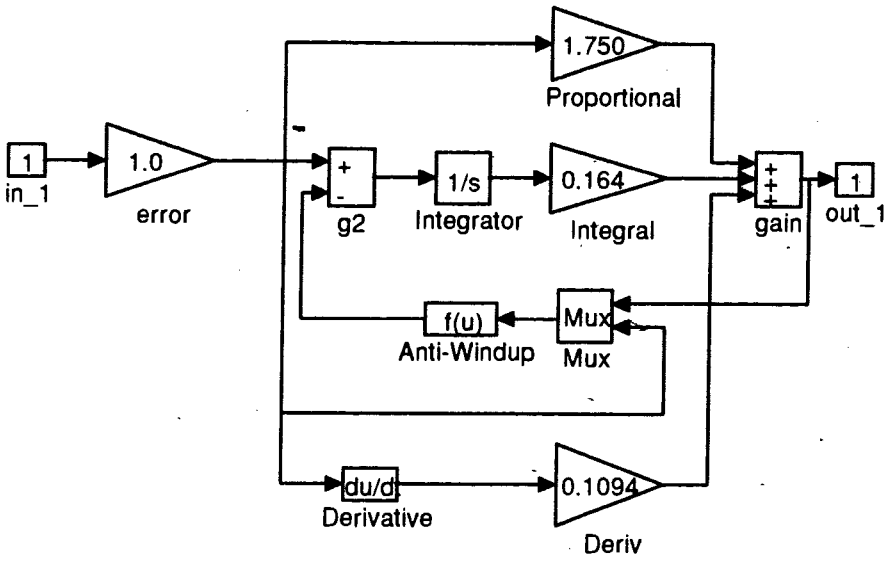

Figure 29. PID Controller SIMULINK Implementation

A PID controller was designed using the empirical gains (Kp = 1.750, Ki = 0.164, Kd = 0.1094) and is illustrated in Figure 29. Included in this diagram is the integrator anti-windup mechanism which was implemented in the prototype PID controller. Since the air/oxygen blender has a limited range of 0.21 to 1.00 it saturates often. When this occurs, the anti-windup circuit turns the integration off. The input to the controller, as with the prototype, is filtered using a low pass first order filter with a 3.2 second time constant. Figure 30 represents the system's filtered SpO_2 response (with the PID controller) to a 2% target increase at 250 seconds and a 2% decrease at 300 seconds. It shows a reasonable response with a 25% overshoot (M_{pt}), 15 second rise time (t_r) and 75 second settling time (t_s). The associated FiO_2 output is relatively smooth. Overshoot is the maximum percentage of a step change the system transient by-passes its final value. The rise time is defined as the time that the system takes to cover the 10% to 90% range of a step change. Settling time will be defined as the time a system takes to settle to within +/- 5% of its final value after a step change.

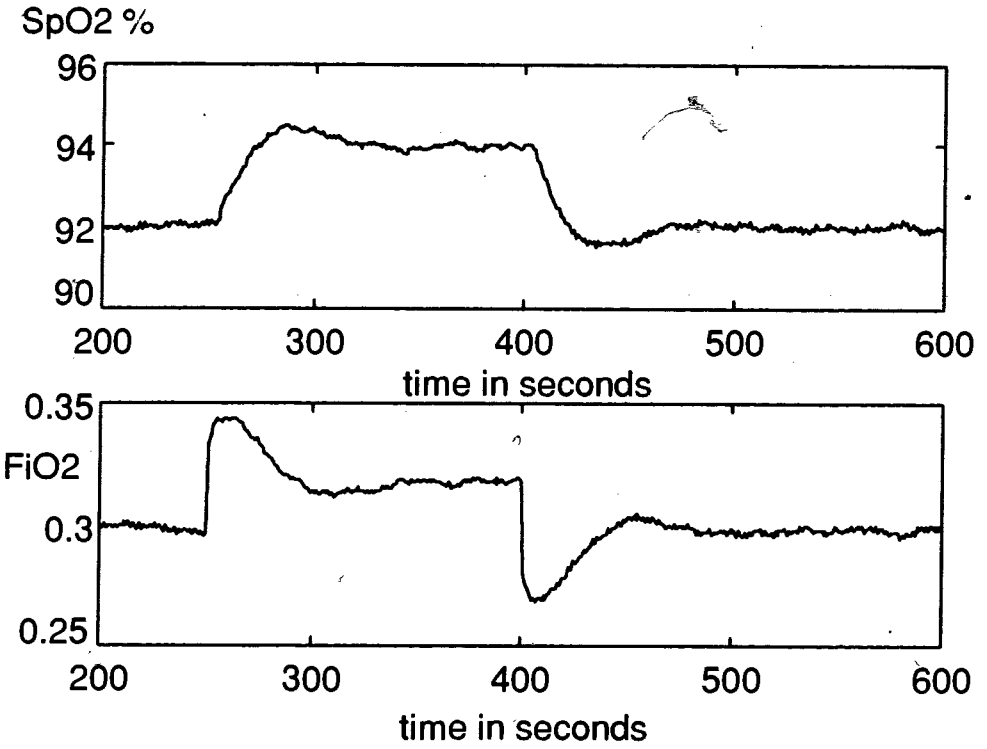

Figure 30. PID Controller Step Response - *2% target increment at 250 seconds and 2% target decrement at 400 seconds. Top graph is filtered SpO_2% and lower is FiO_2.*

4.4 Fuzzy Logic Control

4.4.1 Introduction

Fuzzy logic theory uses multi-valued logic and probability theory as a means of quantifying statements which have a qualifying nature. It was first developed by Zadeh (1965; 1973; 1975) who proposed a degree of membership in sets, rather than a strict (true/false) membership. Using his methods, the qualifying statement "error is large" can be quantified by a membership function, U_{large}(error), which returns a value from 0 to 1 for the linguistic variable "error". This is in contrast with classic binary logic membership which would return a value of 0 or 1 (false or true respectively). A crisp set is strictly defined - members of a population are either in the

set or not in the set. A fuzzy set, however, is not as strictly defined; members of a population belong to the fuzzy set to a degree and that degree is defined by a membership function which returns a value between 0.0 and 1.0.

Combinatory fuzzy logic can be implemented using maximum and minimum functions as "AND" and "OR" operators. For example, if we have two linguistic variables, error and error_rate, then the statement

"(error is large) AND (error_rate is positive)"

is equivalent to:

$$\text{minimum}(U_{large}(\text{error}), U_{positive}(\text{error\_rate}))$$

where U_{large}(error) and $U_{positive}$(error_rate) are membership functions that each return the degree of membership (0 to 1) of its given variable.

Conditional statements, or rules, of the "IF (error is large) THEN (output is small)" format can be implemented in two parts. The first part, "IF (error is large)", is defined as the antecedent and is the output from the membership functions and any associated combinatory logic. The second part, "THEN (output is small)" is known as the consequence and appears to be a membership function. The membership function of the antecedent is tied to the consequence by an implication function. In binary logic, the implication function is "p => q" where p and q are either true or false. In fuzzy logic, the linear implication function is of the form "0.5p => 0.5q"; this means that partial antecedents imply partially.

The consequence specifies a fuzzy set to be assigned to the output and the implication function then modifies that fuzzy set to the degree specified by the antecedent. A common implication function is the "minimum(x, A)" function where x is the antecedent's value (0 to 1) and A is a fuzzy set to be assigned in the consequence. The fuzzy set A can be defined as a distribution and the fuzzy implication operator, minimum(x, A), returns A truncated at x. In order to implement a series of rules, one can aggregate the rule output sets into a single fuzzy set. Deffuzification is the process of quantifying this aggregate and the centroid location of the aggregate fuzzy set is commonly used by software.

Mamdani (1975) devised a fuzzy logic controller to mimic human operator behaviour for a steam engine plant. His work demonstrates the first application of fuzzy logic towards implementing a heuristic control algorithm. Sugeno (1985) further explored industrial fuzzy control applications but fuzzy controllers for closed loop drug delivery where not closely studied until Ying and Sheppard's work on controlling arterial blood pressure by drug infusion (1988; 1992; 1994) and Linken's work on anesthetic gases (1988; 1992; Mason and Linkens 1994). These two areas of fuzzy control have been explored by other researchers (Meier, 1992; Oshito, 1994) but to date, no researchers have published any material about their work on the application of a fuzzy logic controller towards oxygen therapy - closed loop oxygen delivery.

What can a fuzzy logic based controller offer to neonatal SaO_2 control that a PID controller cannot? There are three areas that adversely affect the PID controller's performance (time spent near target SpO_2 in normoxemia): the non-linearity of the oxygen transport system; its failure

to ignore sensor and motion artifact; the dynamic nature of the patient's physiology due to drug therapy, increased severity of BPD, oxygen affinity change, etc. The last item causes the controller to go out of tune and is a problem that may be solved by intelligent control but is beyond the scope of this thesis. This section, describes the design of a fuzzy logic controller that will attempt to provide improved performance over the PID controller by considering the non-linearity of the system and insensitivity to artifact.

4.4.2 Non-Linear Controller

A common method of implementing a fuzzy controller is to use the error and error rate as inputs (Driankov, pp. 103-144, 1996) which are used to implement a proportional-derivative (PD) controller. Error inputs have memberships associated with the fuzzy sets: positive big (PB); positive medium (PM); positive small (PS); zero (ZO); negative small (NS); negative medium (NM); negative big (NB). On first trial, the error rate input had memberships with three fuzzy sets - "positive", "zero" and "negative" - but produced an oscillatory unit step response so another two sets, "very_positive" and "very_negative" where added by the author.

The output is an FiO_2 increment/decrement which is integrated over time to produce the control. Seven fuzzy sets make up the universe to which "FiO2_increment" can have membership and include: positive big (PB); positive medium (PM); positive small (PS); zero (ZO); negative small (NS); negative medium (NM); negative big (NB). A single rule has the form:

"if (error is PB) and (error_rate is very_positve) then (FiO2_increment is NB)"

Table VI is a summary of the 35 rules which make up the control law. The first row and column represents the "error_rate" and "error" fuzzy sets respectively; the remaining table entries represent the resultant "FiO2_increment" sets. The membership functions for the fuzzy sets associated with the inputs are illustrated in Figure 31. Triangular and trapezoidal error functions have been used in an effort to reduce computational time. The "error" values greater than +10% are all PB and less than -10% are NB. Since the physiologically significant SaO_2 values are within this range, by setting these saturation points, the designer de-emphasises large errors by setting a constant gain. This is one method of ignoring artifact which tends to be outside this region. In other words, error values outside +/- 10% SpO_2 are suspected as artifact.

The "error_rate" input is sensitized near zero by placing the "positive" and "negative" membership functions within +/- 0.5 which is half the total +/- 0.1. The total range of the "error_rate" input has been given saturation points since the open loop response of the filtered SpO_2 tends to very slow.

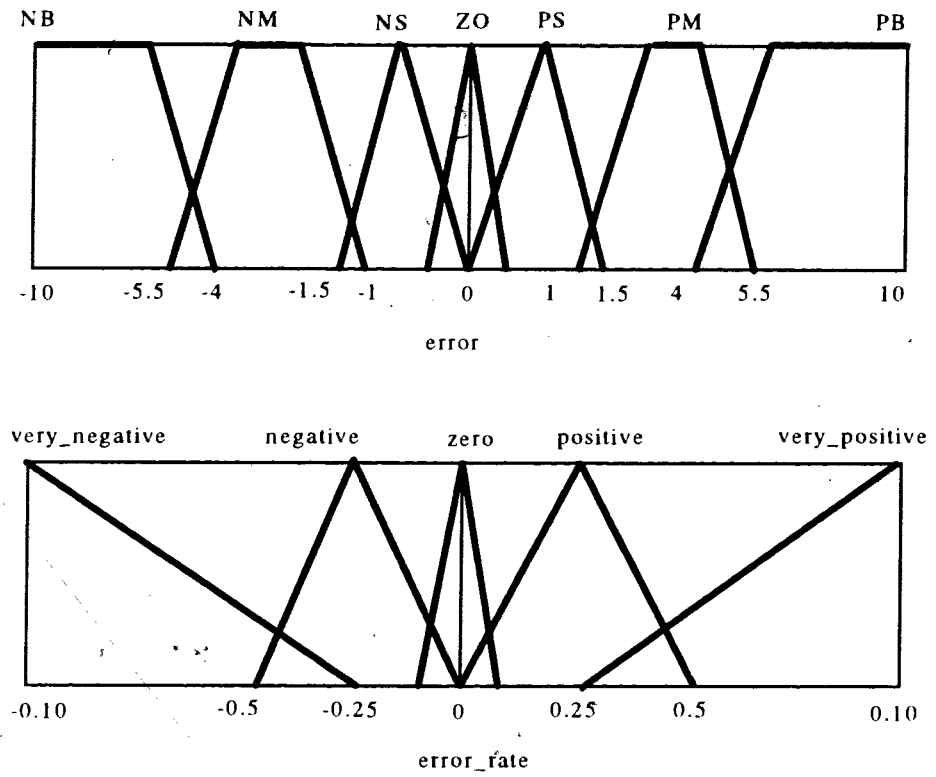

Figure 31. Input Fuzzy Set Membership Functions

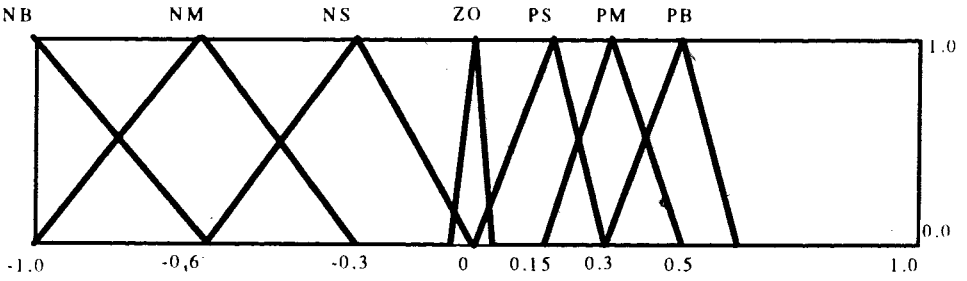

Figure 32. Output Fuzzy Set Membership Function.

The range of the output linguistic variable "FiO2_increment", as shown in Figure 32, has been normalised so that the overall gain can be set external to the fuzzy controller - a convenient means of tuning it. Also, note that the positive membership functions cover half the range as those of the negative. This a method of implementing the non-linearity of the oxygen

transport system. The slope of the oxygen dissociation curve tends to very small above normoxemia but large below implying that negative increments, due to hyperoxemia should be large to effect a small SaO_2 decrease. Conversely, positive increment to counter-act hypoxia should not have to be as large since, due to the steep portion of the curve, small FiO_2 increments will realise large SaO_2 increments.

Table VI. FiO2_increment look-up table for error and error_rate.

	error_rate				
error	very_positive	positive	zero	negative	very_negative
PB	NB	NB	NM	NS	ZO
PM	NB	NM	NM	NS	ZO
PS	NM	NS	NS	ZO	PS
ZO	NM	NS	ZO	PS	PM
NS	NS	ZO	PS	PS	PM
NM	ZO	PS	PM	PM	PB
NB	ZO	PS	PM	PB	PB

A non-linear fuzzy controller was implemented for the SIMULINK neonatal model developed in the previous chapter using MATLAB's Fuzzy Toolbox and is presented in Figure 33. An anti-windup mechanism was placed around the integrator to account for the blender's 21% and 100% saturation limits. The gain was set to 1.75 which is the same as used for the

PID controller. Figure 34 presents the controller's response to a target SpO_2 step increase from 92% to 94% at 250 seconds and a step decrease back to 92% at 400 seconds.

Table VII compares the transient responses of the PID and FL controllers with respect to the responses plotted in Figures 30 and 34. For a positive response, the FL controller is over-damped with no overshoot. This is an attempt to get the controller to respond quickly to hypoxemia, with limited oscillation. The FL controller's negative response shows a larger overshoot and settling time than the PID controller. This feature was designed to bring the neonate out of hyperoxemia quickly; especially when the FiO_2 levels are falsely saturated at 100% due to negative artifact.

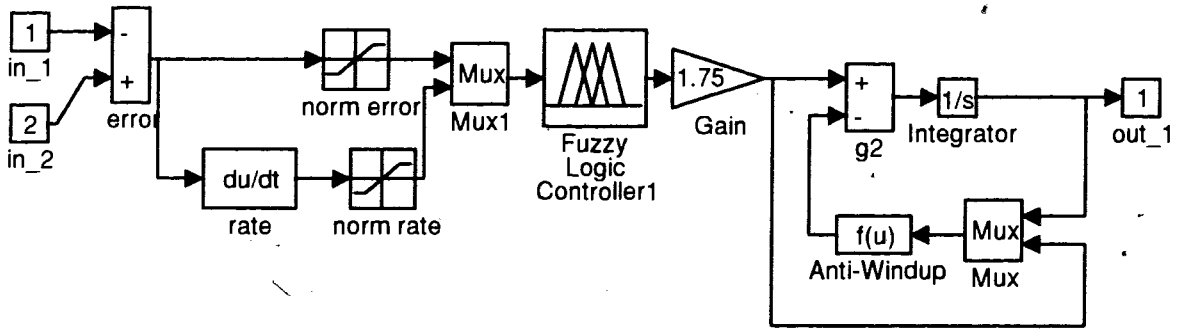

Figure 33. Non-Linear Fuzzy Controller Implementation - *input 1 (in_1) is the target SpO_2 and input 2 (in_2) is the filtered SpO_2.*

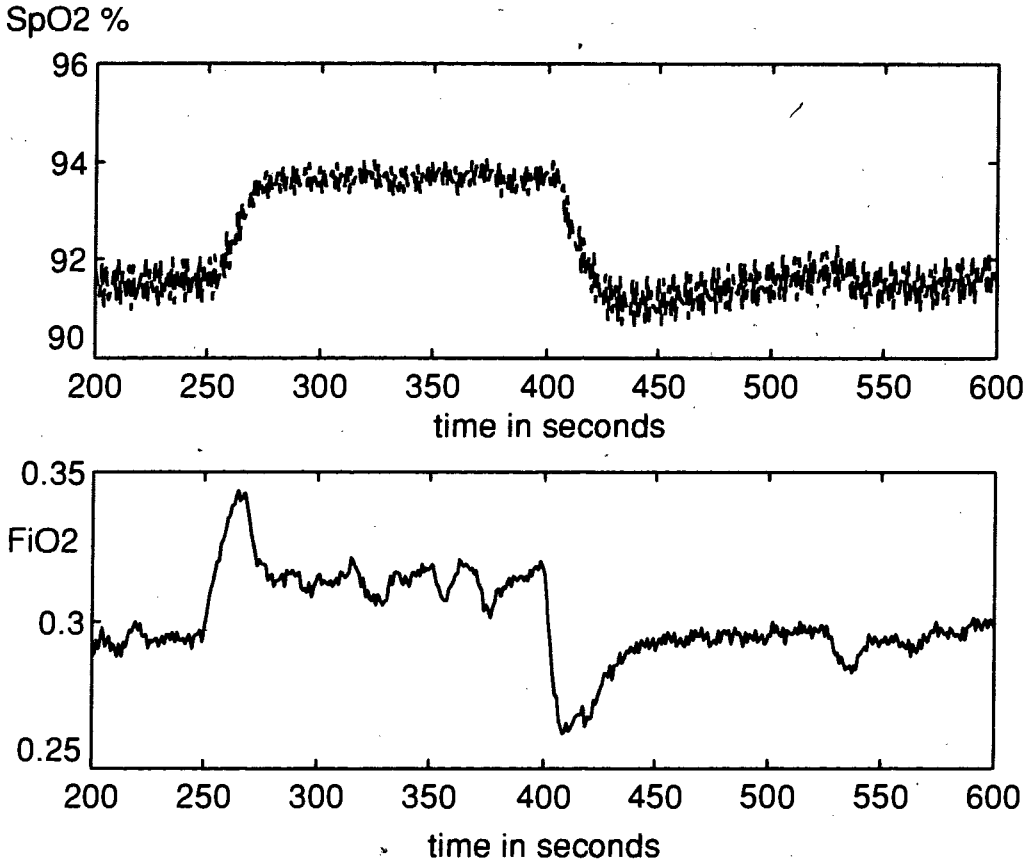

Figure 34. Fuzzy Controller Response to Step Target Change - *2% change increase in target at 250 seconds and a 2% drop at 400 seconds. SpO_2 is not filtered.*

Table VII - Comparison of PID and FL Step Responses

	Positive Response			Negative Response		
Algorithm	M_{pt} (%)	t_r (sec.)	t_s (sec.)	M_{pt} (%)	t_r (sec.)	t_s (sec.)
PID	25	15.	75	25	15	75
FL	0	30.	>150	50	15	>200

4.4.3 Artifact Detection

Artifact is an erroneous SpO_2 signal and can cause an automatic controller to react and, in turn, drive the patient out of normoxemia. If a controller can correctly detect artifact, it can then be programmed to ignore the inputs for the artifact duration. One method of detecting artifact is to use the raw (un-filtered) SpO_2 signal from the pulse oximeter and compare it to the filtered SpO_2 value. Figure 35 shows a positive artifact as the raw SpO_2 line; the filtered SpO_2 line is also shown.

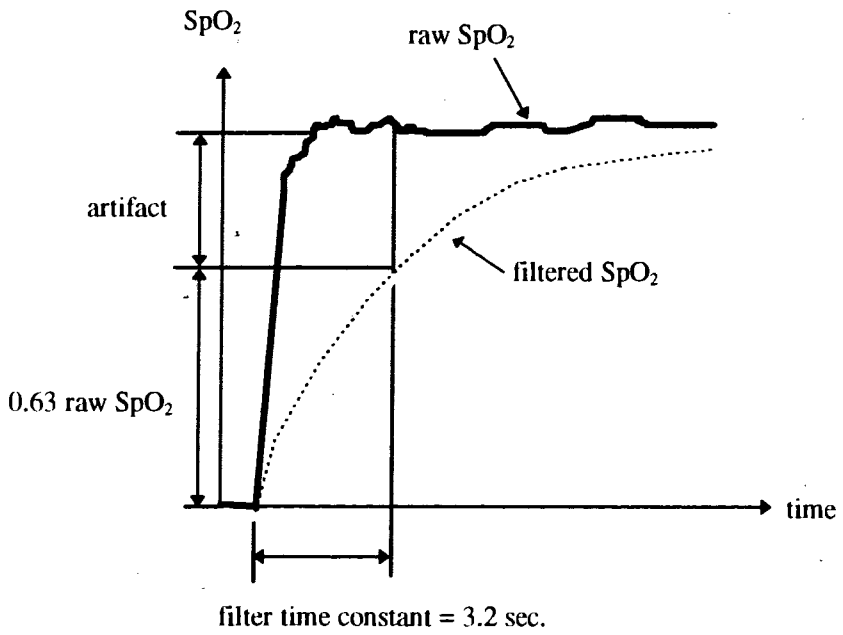

Figure 35. Definition of artifact

The filter's time constant is 3.2 seconds and will be used as the minimum amount of time that the controller will ignore a saturation/desaturation. Since the time constant of the open loop response to a step input has a range of 15 to 55 seconds (Section 4.3), most "true" SpO_2

adjustments will be tracked by the filter. An artifact, however, has a small time constant (< 0.1 seconds) and the filter will prevent an immediate jump in SpO_2.

$$\text{artifact} = \text{raw } SpO_2 - \text{filtered } SpO_2 \tag{4.8}$$

Artifact, as defined by equation (4.8) will decay exponentially to about 1/3 of the total raw SpO_2 value in one time constant. If we define a linguistic input variable , "artifact", we can give it three possible fuzzy sets - "positive_evident", "not_evident" and "negative_evident" - with membership functions shown in Figure 36.

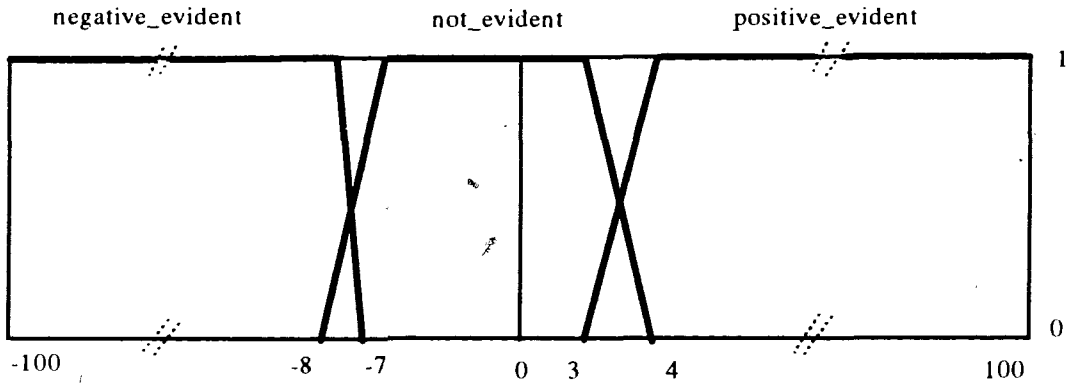

Figure 36. Artifact Fuzzy Set Membership Functions

With target SpO_2 values set in the range of 90-95% (normoxemia), the maximum positive artifact would be 10% SpO_2. After one time constant the artifact would be about 3-4%; the boundary between "not_evident" and "positive_evident" has been set at this range. The author has chosen -20% SpO_2 as a minimum negative artifact since 70% SpO_2 (20% below normoxemia) is about the limit of a "true" desaturation. After 3.2 seconds, the negative artifact

would be about -7% to -8% SpO_2 and these values have been used to set the boundary between "negative_evident" and "not_evident".

All previous rules developed in Section 4.4.2 have been augmented by "and"ing "(artifact is not_evident)" into the combinatory logic of the antecedent. For example,

"if (error is PB) and (error_rate is very_positive) then (FiO2_increment is NB)"

becomes

"if (artifact is not_evident) and (error is PB) and ... then (FiO2_increment is NB)".

Also, for completeness, the following rules were added:

"if (artifact is positive_evident) then (FiO2_increment is ZO)"

"if (artifact is negative_evident) then (FiO2_increment is ZO)"

Artifact, as a third input, was added to the fuzzy logic controller shown in Figure 37. A test script with positive and negative artifact was run on this controller and the resulting SpO_2 and FiO_2 plots are illustrated in Figure 38. Artifact has been defined as a four second square pulse occurring every ten seconds. Note that the negative artifact is completely ignored (no FiO_2 adjustment) since its magnitude is quite large (-40%). The positive artifact are not completely ignored and the controller eventually falsely drops the FiO_2 to its 21% lower limit which desaturates the neonatal model. The rate and depth of desaturation are much less than those from the controller without artifact detection where the controller would have driven the FiO_2 setting to 21% by the end of the second artifact pulse.

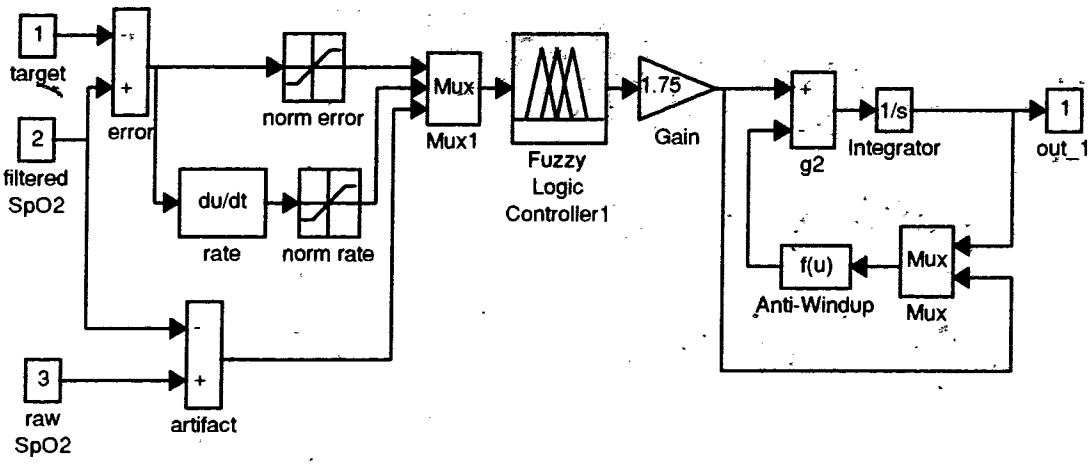

Figure 37. Fuzzy Logic Controller with Artifact Detection

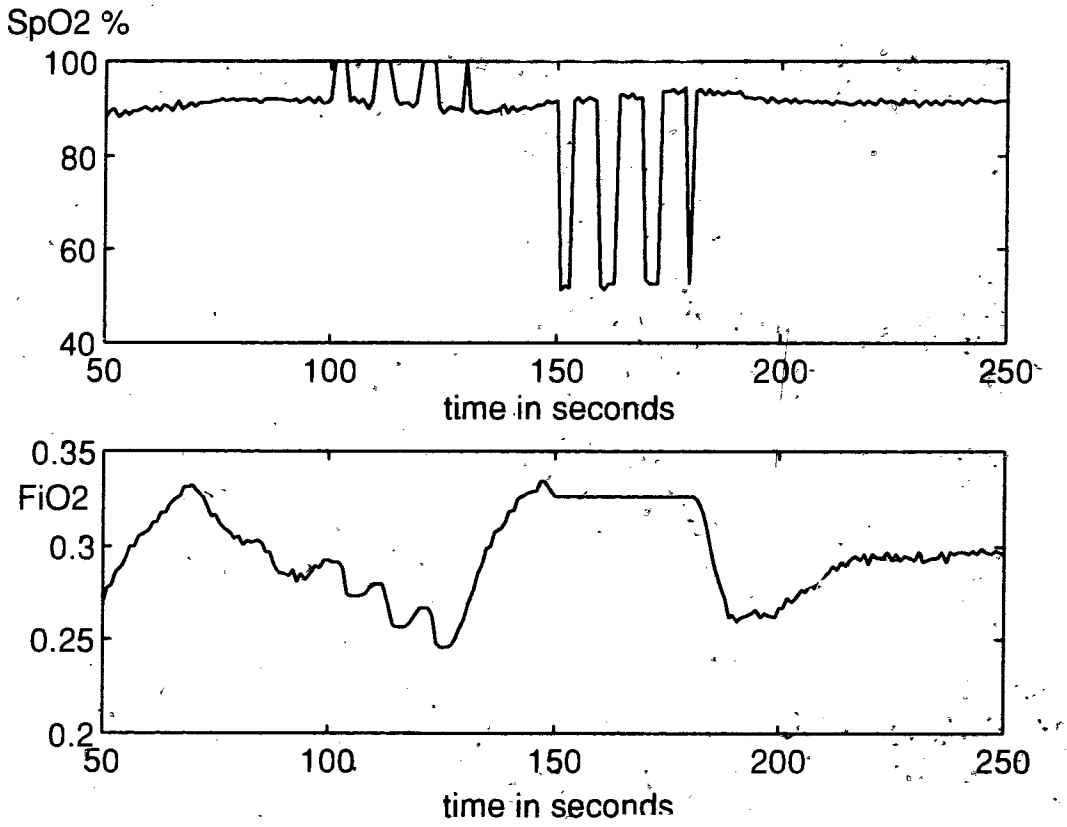

Figure 38. FLA Controller Response to Artifact

A final note of caution; this artifact detection mechanism was designed and tested using a repeating 4 second pulse. In reality motion artifact may be longer and more erratic. Also, negative motion artifact can be coupled with actual desaturation. If a neonate's heart rate is actually erratic and showing signs of instability or slowing down, the SaO_2 values will also begin to quickly drop. Since the pulse oximeter triggers on the heart rate, an erratic heart signal will result in the pulse oximeter reporting artifact-like SpO_2 values. These SpO_2 values, though lower than actual SaO_2 values do, however, report the trend of a desaturation and, in this case, should not be ignored. The purpose of designing this artifact detection algorithm was to demonstrate the potential of such a mechanism using fuzzy logic.

4.5 Summary

This chapter describes the design of four control algorithms - manual, PID, fuzzy logic and fuzzy logic with artifact detection - each of which will be tested in Chapter 5 using the three neonatal model test scripts developed in Chapter 3. Manual control is characteristic of oxygen therapy as observed by the author in the neonatal nursery; minimal to no FiO_2 adjustment if the infant stays within normoxemia. A PID controller was designed using gains empirically defined in the nursery with a prototype controller built by the author in previous years. These gains were also verified by using the open loop response to step FiO_2 increments. Fuzzy logic was used to implement a non-linear controller that gave good response to a step target change. The non-linearity of the neonatal oxygen transport system was accommodated by setting the output's possible positive fuzzy sets to cover half the range of the negative fuzzy sets. This

resulted in positive gains lower than negative ones as are implied by the oxygen dissociation curve. A method of detecting false readings, artifact, was added to the non-linear controller to produce the fourth algorithm. Artifact is defined as the difference between non-filtered and filtered SpO_2 values and is used as a third input into the fuzzy controller. As long as artifact is greater than 4% or less than -8% SpO_2, the controller will ignore the error and error rate. On test data, the controller completely ignored negative artifact and reacted slowly to positive artifact.

5.0 RESULTS AND DISCUSSION

5.1 Introduction

Four oxygen therapy controllers developed in the previous chapter are applied to three neonatal models designed in Chapter 3. Each neonatal model represents one hour of behaviour for a specific type of infant and each is characterised by motion artifact, shunting and, in one model, an O_2 dissociation curve shift. The timing and magnitude of these events are identical for the four tests performed on each model. Figure 39 presents the closed loop test environment. Three controllers, PID, fuzzy logic (FL) and fuzzy logic with motion artifact (FLA) are shown and along the bottom is the data harvesting mechanism. In the lower right of Figure 39 the event control functions for each neonate type are presented. An initialisation routine, "initepm1.m", (see Appendix C) must be run before the simulation is started. Minimum step size is set to 0.005 and the Adams/Gear method is selected for numerical integration.

A target value of 92% SpO_2 was chosen by the author for all 12 experiments. Normoxemia, for this discussion, will be defined as SpO_2 between 90% and 95%. The target is just below the mean of normoxemia, representative of a clinical target value.

For each experiment, with the exception of manual mode, SpO_2 and FiO_2 values, sampled at 1 Hz. are plotted. The first 200 seconds of each experiment is ignored since it contains the start-up transient. A histogram representing the percentages of experiment duration spent at SpO_2 values is also used as a graphical representation of the controller's performance. Qualitatively speaking, good performance is represented by a tight distribution on the

histogram with a large peak at the 92% SpO_2 target. A method of quantifying the target performance and comparing controllers is to look at the percentages of time spent by each at +/- 0.5% SpO_2 of target (defined as "at target") and +/- 1.5% of target (defined as "close to target"). Higher values of each generally imply higher target performance.

The purpose of manual mode is to model oxygen therapy as it would be applied in the clinical setting where the purpose is to maintain normoxemia rather than a specific target SpO_2. A comparison between manual mode and the automatic controllers, with respect to at target, close to target, or normoxemia, may not be completely valid for this reason.

In some sense, for the Baby 1 and 2 models, manual mode is representative of an open loop or fixed input system since no FiO_2 adjustments are made during their respective experiments. The author has chosen to list the manual mode "at target" and "close to target" percentages in the results table for completeness and as a mechanism for limited comparison. Along this theme, the percentages of experiment duration hypoxemic ($\leq$ 90% SpO_2), normoxemic (90% to 95% SpO_2) and hyperoxemic ($>$ 95% SpO_2) are tabulated even though the automatic controllers were not directly designed to maintain normoxemia. The general point of comparison will be how one control algorithm effects another's standard.

This chapter presents and discusses the results from each controller's application to each neonatal model - Baby 1, Baby 2 and Baby 3. The overall performance of the controllers is then presented and discussed.

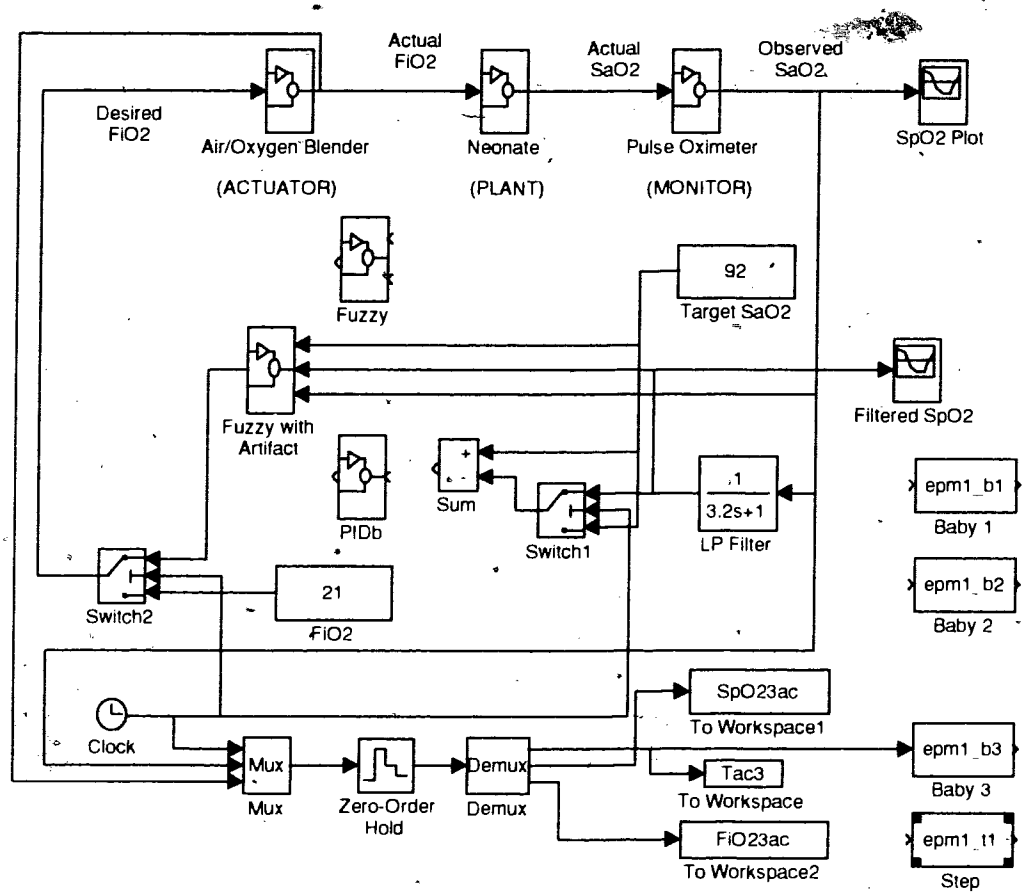

Figure 39. Oxygen Therapy Development Environment

5.2 Baby 1 Model

Baby 1 model represents a relatively stable neonate, starting out with a 20% pulmonary shunt (S3) which increases 10% every 20 minutes as shown in Figure 40. This model, however, represents an active infant; positive and negative motion artifact are frequent but their pattern is repeated every 20 minutes as shown in the SpO_2 plot for manual mode (Figure 41). This is unrealistic but provides us with feedback on the controller and model response to artifact at three separate levels of pulmonary shunt. In this diagram one can also see the step SpO_2 drops at 1200 and 2400 seconds in response to the 10% S3 shunt step increases. FiO_2 is maintained

at 30% and the resulting SpO_2 histogram is presented in Figure 42. The histogram distribution is broad but shows an infant model that spends almost 90% of its time in normoxemia (assuming that the infant is Normoxemic during artifact).

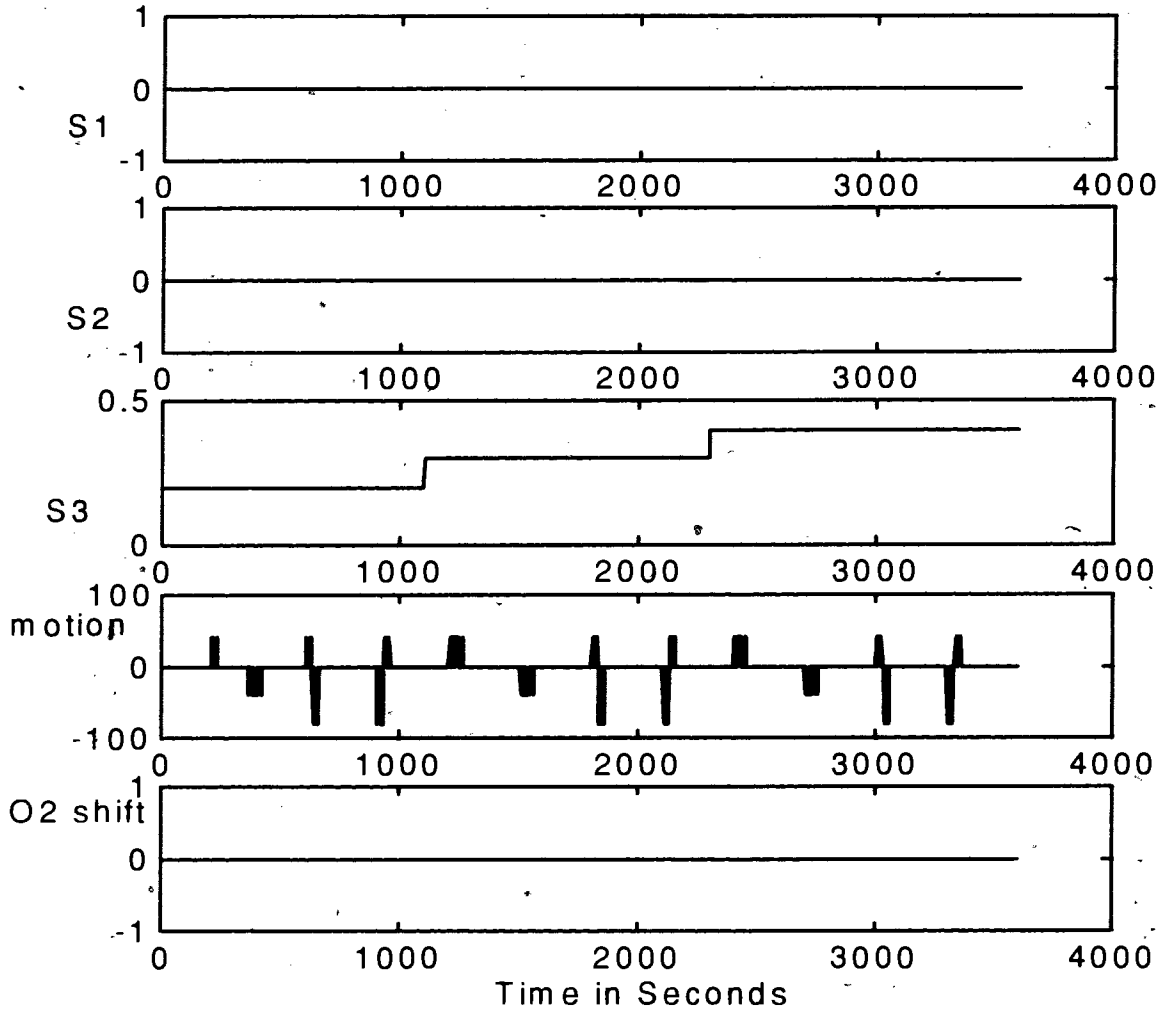

Figure 40. Baby 1 Model Disturbances

Figures 43, 44 and 45 represent the PID controllers SpO_2 plot, FiO_2 plot and SpO_2 histogram for Baby 1. The FiO_2 plot shows the controller's false reaction to artifact by driving the blender

to its saturation points. This results in the saturation and desaturations shown after the artifact events in the SpO_2 plot. The distribution in the SpO_2 histogram has a large peak at target but also some time is spent in hyperoxemia. Note, from the SpO_2 plot, that as the S3 shunt increases, the overshoot decreases since the maximum SpO_2 value drops. Unfortunately, a reduction in overshoot does not improve the situation because coupled with this behaviour is an increase in the time constant (see section 4.3 for a discussion of this feature).

SpO_2 plot, FiO_2 plot and SpO_2 histogram for the fuzzy logic (FL) controller are shown in Figures 46, 47 and 48 respectively. The FiO_2 plot, like that of the PID controller shows the false reaction to artifact but, in the case of the FL controller, it does not reach the blender's upper limit. This is due to the non-linear mechanism in this controller which produces positive increments at almost half the value of negative ones (see Section 4.4.2). The SpO_2 histogram illustrates a very good distribution.

Data from the fuzzy logic controller with artifact detection (FLA) is presented in Figures 49, 50 and 51. The SpO_2 plot shows a very well regulated system with minor desaturations due to graduated false responses to positive motion artifact. The FiO_2 plot, Figure 50, shows a small FiO_2 bandwidth with the average stepping from 28% to 30% to 32% in response to the 10% S3 shunt increases at 1200 and 2400 seconds. These averages confirm that 30% for manual mode is a realistic value. A large peak, about 45% of experiment duration, is defined in Figure 51, the SpO_2 histogram. Ignoring the artifact time (at 80% and 100%) no time is spent in hyperoxemia and only about 5% of the experiment duration is spent in hypoxemia.

Table VIII summarises the controllers' target performance by listing the percentages of experiment time spent at +/- 0.5% SpO_2 of target and +/- 1.5% SpO_2 of target. From this table, in terms of at target, the FL and FLA controllers provide a the best improvement of performance over PID and manual modes. In the wider error band, +/- 1.5% SpO_2 of target, the FLA controller provides a 20% experiment duration improvement in target performance over PID control. For Baby 1, the FLA controller provides the best target performance. Table IX lists the normoxemic performance of the controllers. The PID controller has the largest percent of experiment duration hyperoxemic as a result of its slow return from artifact invoked saturation. The FLA controller has the best normoxemic performance.

Table VIII. Target Performance of Controllers on Baby 1 - *model is relatively stable but has many varied motion artifacts. Initial 20% S3 shunt degrades 10% every 20 minutes.*

Controller	% of experiment duration	
	+/- 0.5% SpO_2	+/- 1.5% SpO_2
Manual	22.44	54.47
PID	39.50	63.03
FL	45.44	76.26
FLA	46.59	82.74

Table IX. Normoxemic Performance of Controllers on Baby 1

Controller	% of experiment duration		
	Hypoxemic	Normoxemic	Hyperoxemic
Manual	12.88	87.12	0
PID	3.35	86.00	10.65
FL	7.52	90.78	1.70
FLA	5.18	94.82	0

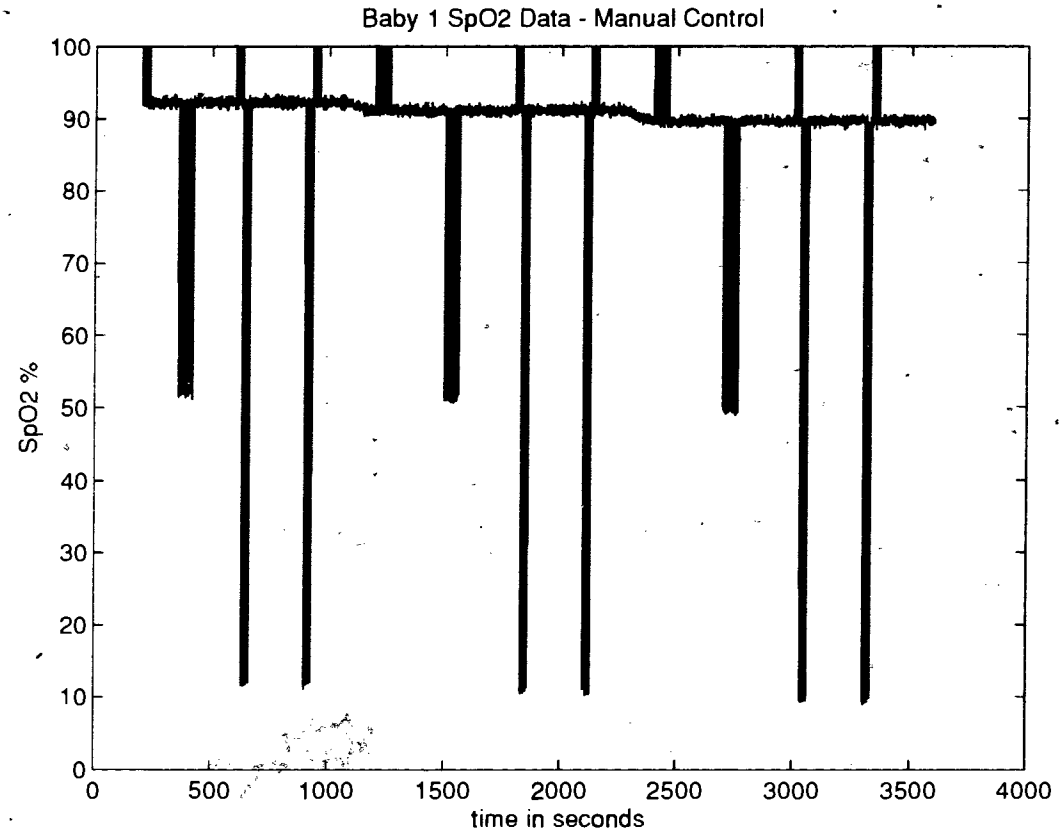

Figure 41. Baby 1 SpO_2 Plot - Manual Control

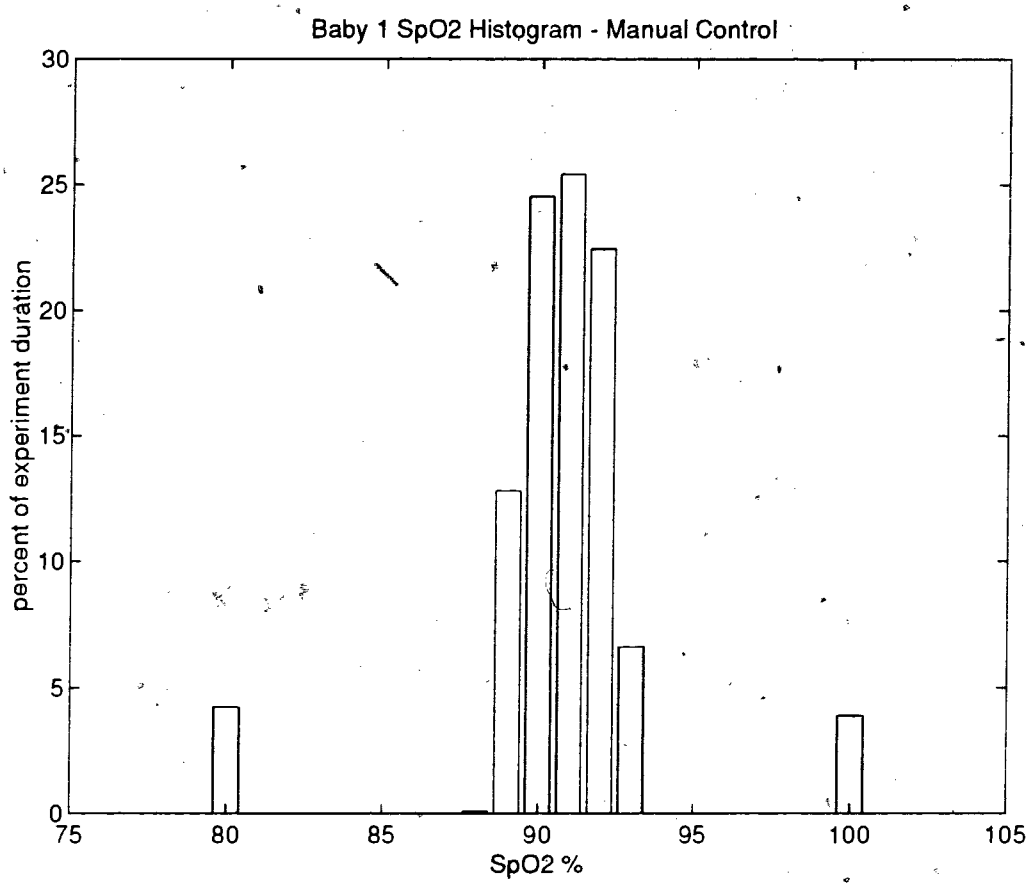

Figure 42. Baby 1 SpO_2 Histogram - Manual Control - *mean = 90.48% SpO_2; standard deviation = 1.13% SpO_2.*

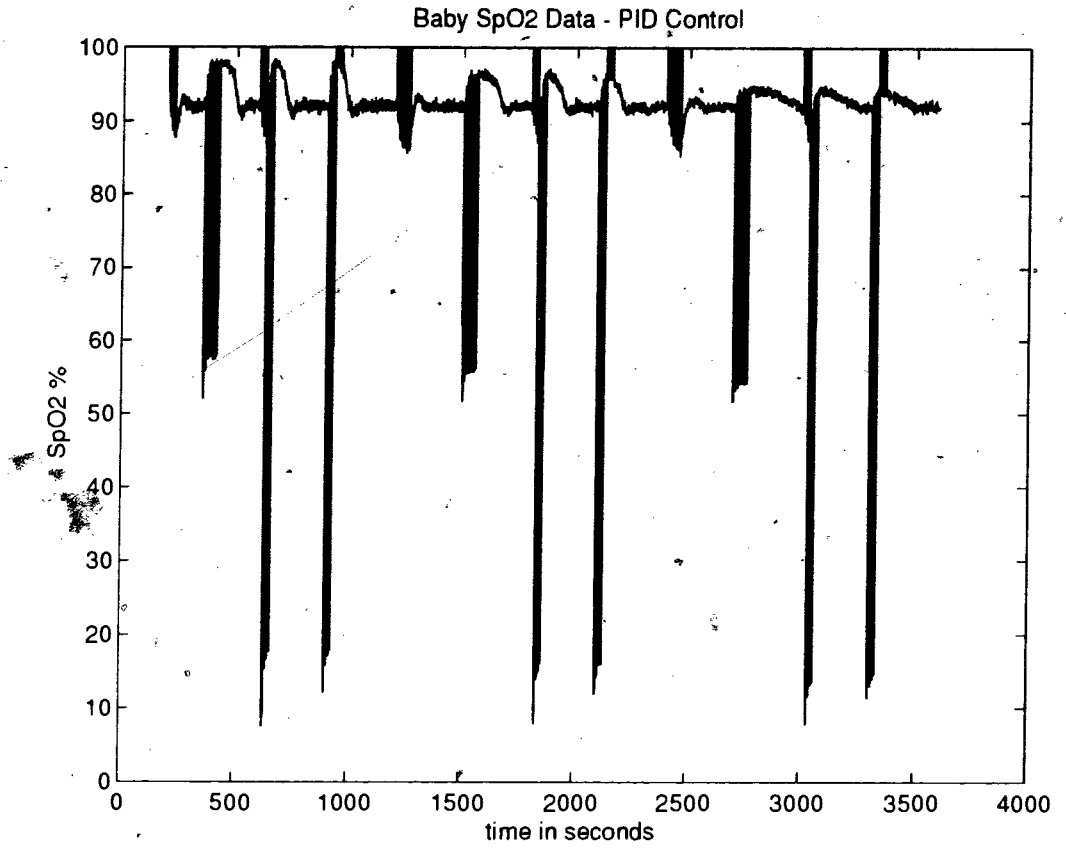

Figure 43. Baby 1 SpO_2 Plot - PID Control

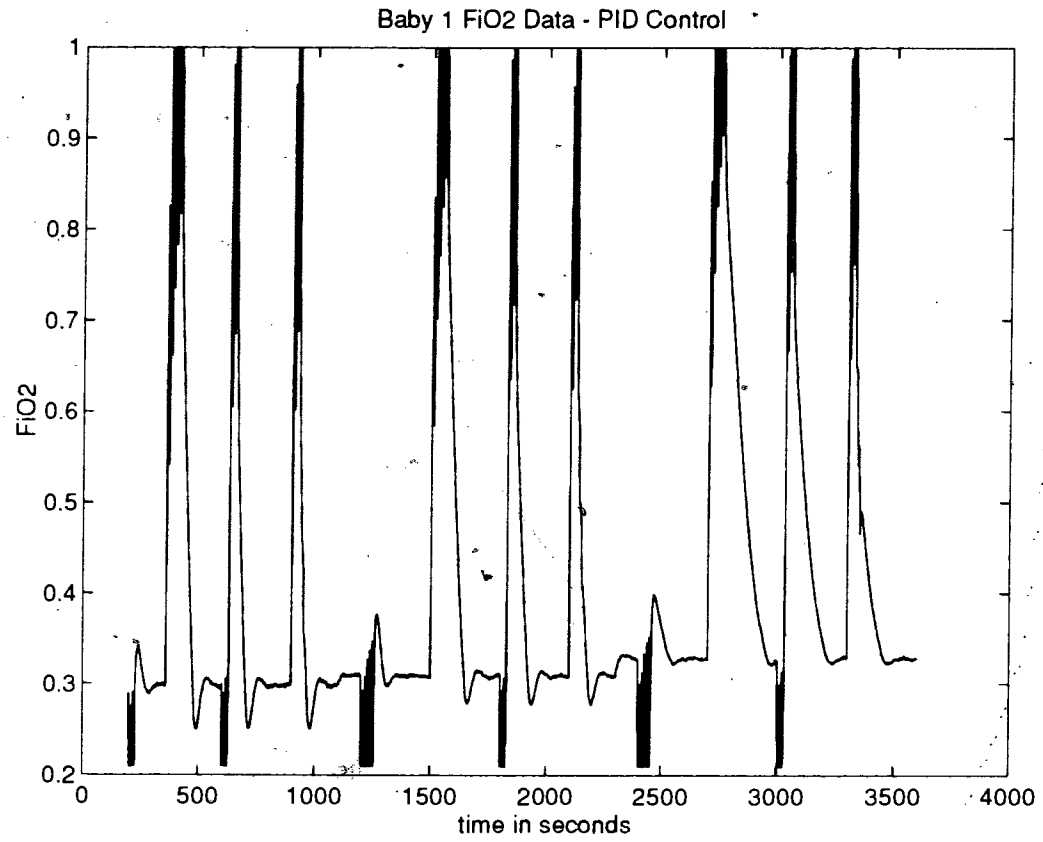

Figure 44. Baby 1 FiO_2 Plot - PID Control

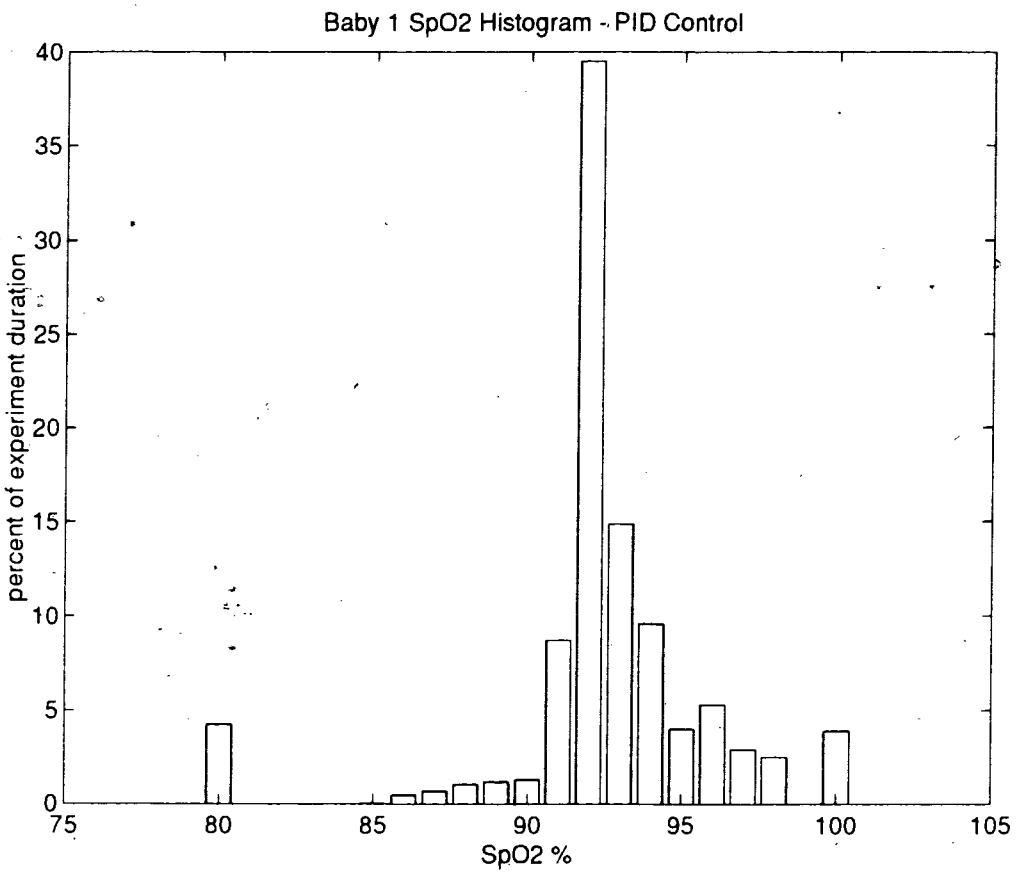

Figure 45. Baby 1 SpO_2 Histogram - PID Control - *mean = 92.77% SpO_2; standard deviation = 1.95% SpO_2.*

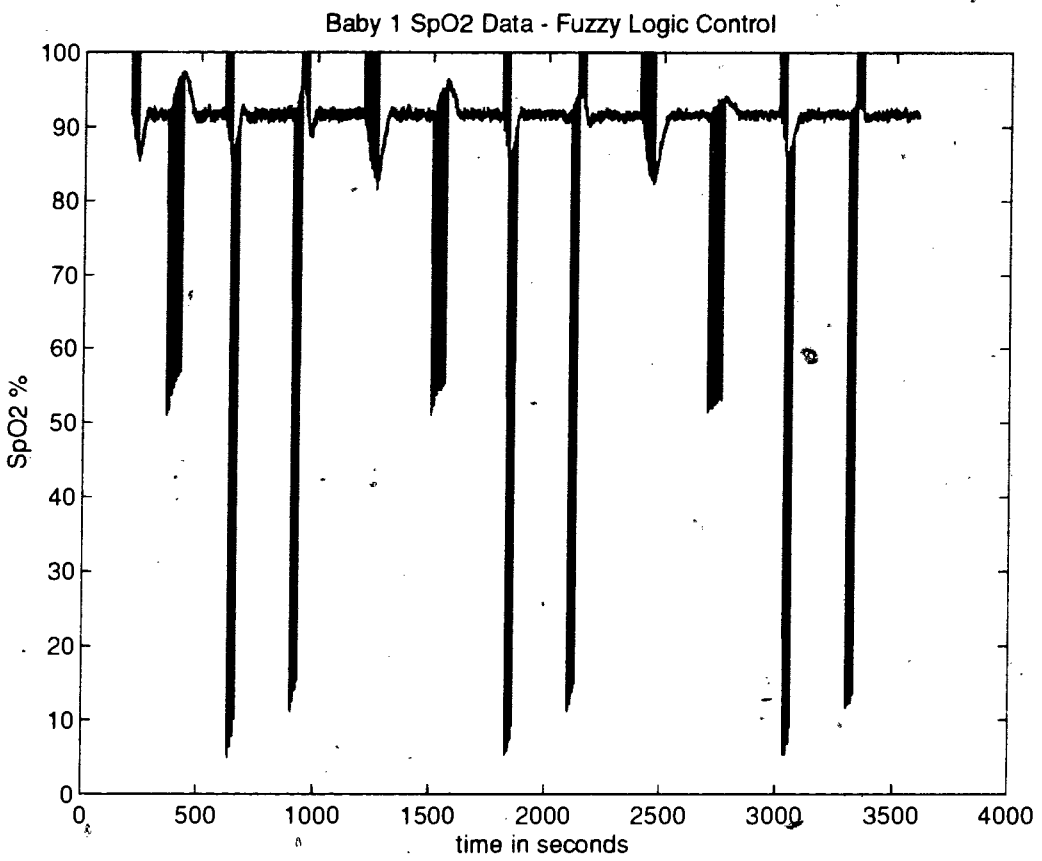

Figure 46. Baby 1 SpO_2 Plot - FL Control

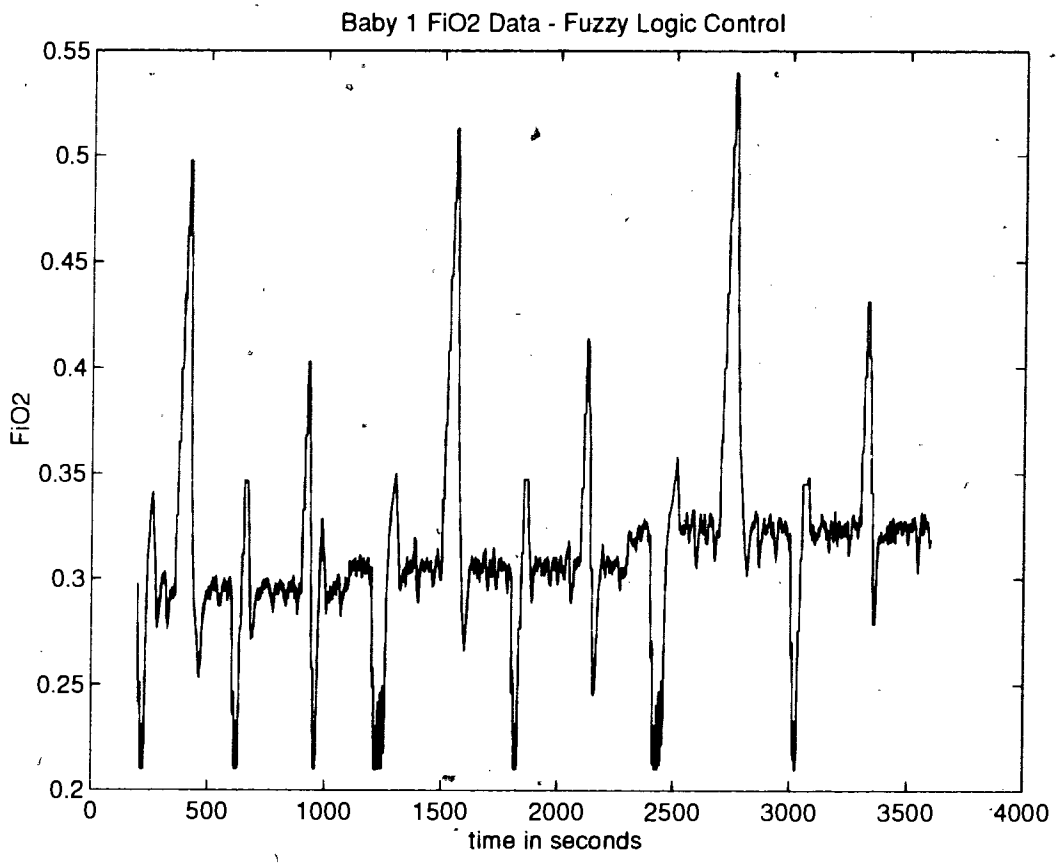

Figure 47. Baby 1 FiO_2 Plot - FL Control

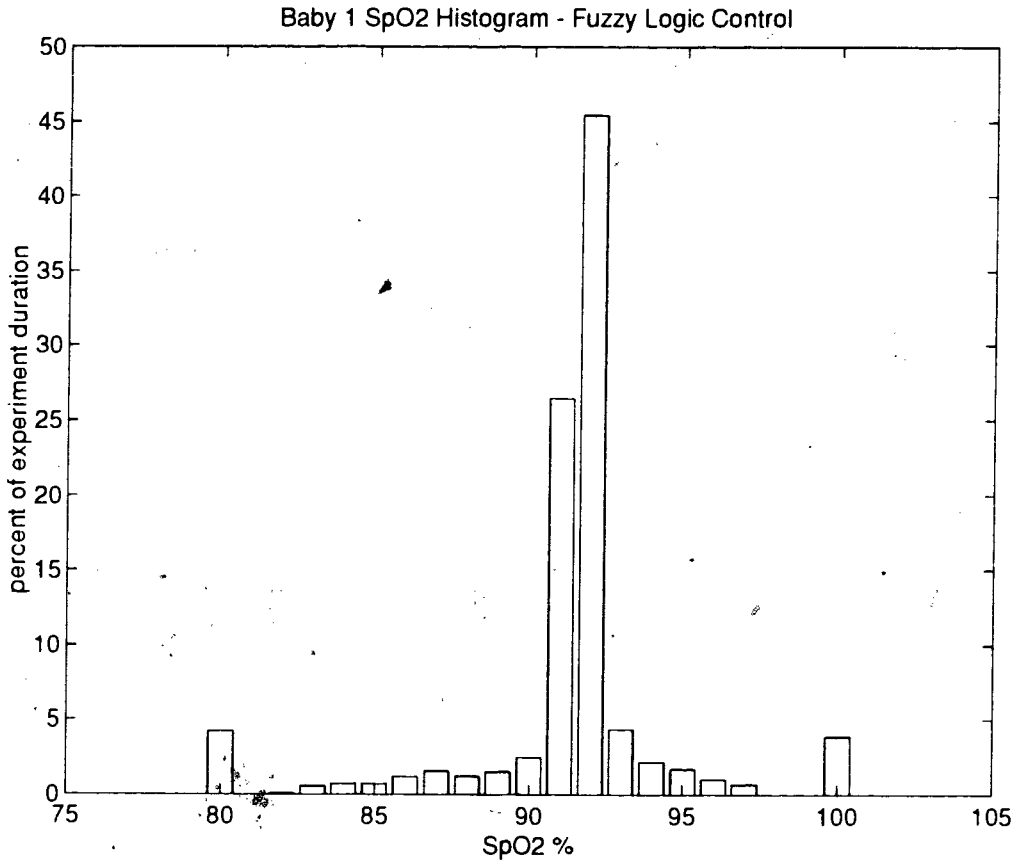

Figure 48. Baby 1 SpO_2 Histogram - FL Control - *mean = 91.44% SpO_2; standard deviation = 1.83% SpO_2.*

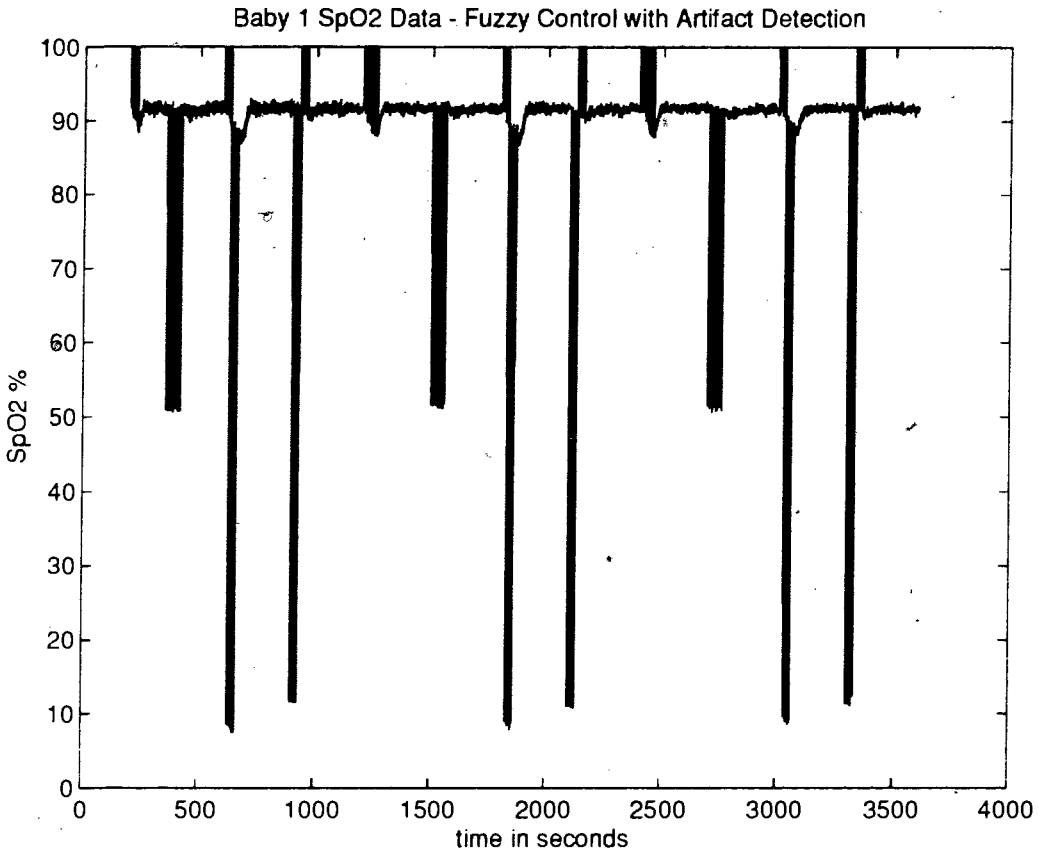

Figure 49. Baby 1 SpO_2 Plot - FLA Control

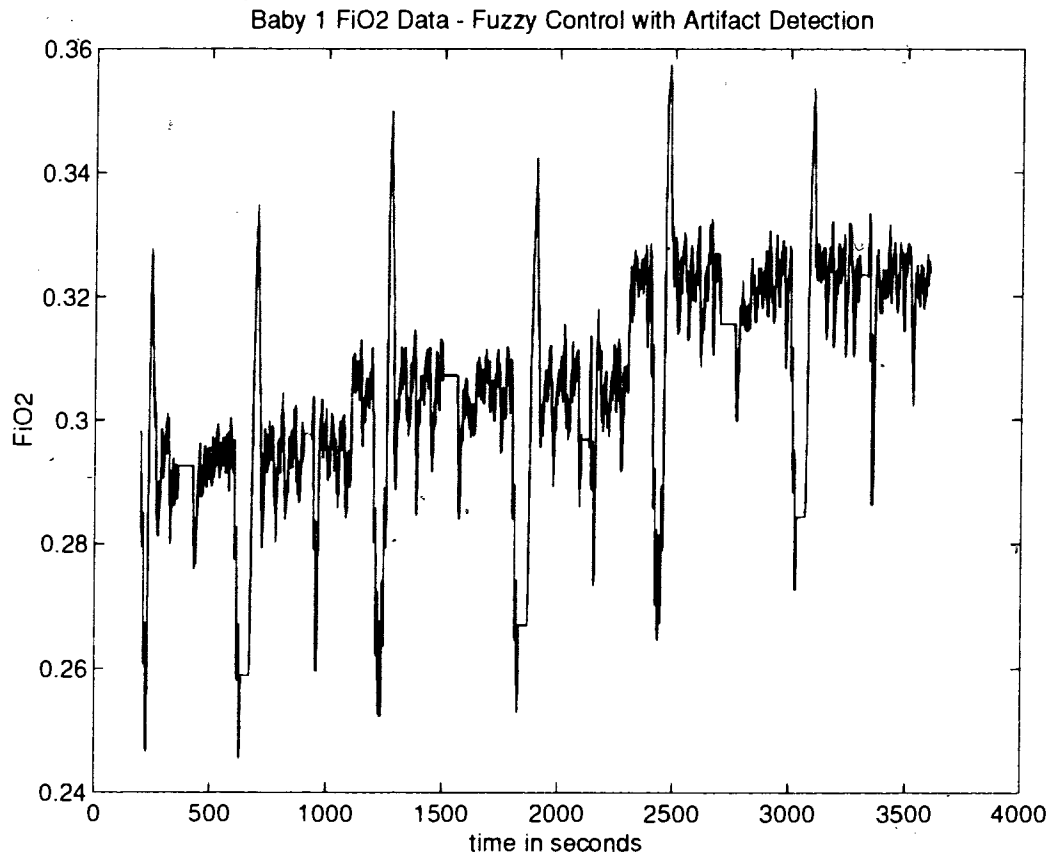

Figure 50. Baby 1 FiO_2 Plot - FLA Control

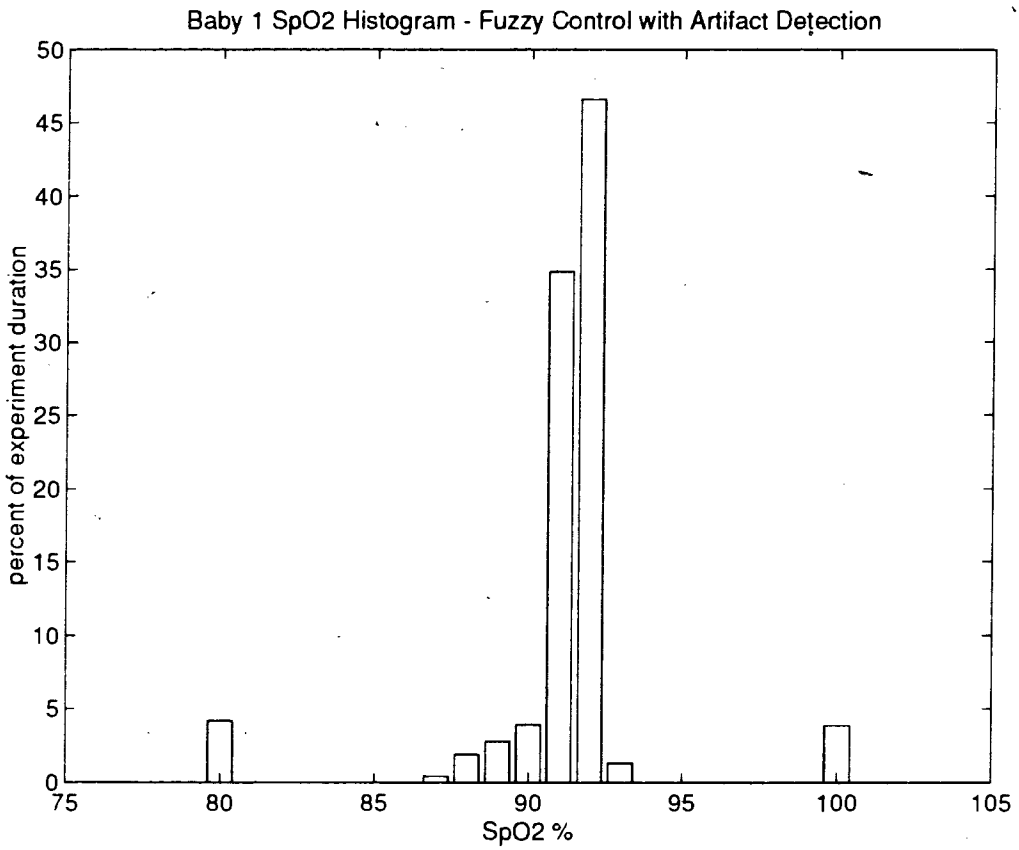

Figure 51. Baby 1 SpO_2 Histogram - FLA Control - *mean = 91.35% SpO_2; standard deviation = 0.88% SpO_2.*

5.3 Baby 2 Model

This model represents a neonate with varying pulmonary (S3) and cardiac (S2) shunts which are summarised in Figure 52. After the first 260 seconds of transient activity, the S3 shunt is held at 30% while an S2 shunt is varied from 5% to 20% in 60 second bursts. A few motion artifacts are enabled/disabled for the period of 1000 to 2000 seconds. Between the times of 2000 and 3500 seconds various combinations of shunting and motion artifact are produced; notably at 2150 seconds, the S3 shunt is increased from 20% to 30% (with S2 shunt held at 20%) while a positive artifact is produced. This event should cause the automatic controllers to drop the FiO_2 while the model's SaO_2 is actually dropping, amplifying the severity of the desaturation. At 2540 seconds, the S3 shunt is reduced to 10% from 30% (with the S2 shunt held at 5%) while a negative artifact is produced. This event should cause the automatic controllers to falsely increase the FiO_2 while SaO_2 levels are increasing - amplifying hyperoxemia. The final 210 seconds of the test represent 30 second periods of S2 shunting between 5% and 20% with an S3 shunt of 30%. In summary, this model represents an unstable neonate that is relatively inactive.

Figures 53 and 54 represent the manual mode SpO_2 plot and histogram respectively. The FiO_2 was held at 35% for the duration of the experiment and the SpO_2 histogram shows a two peaked SpO_2 distribution. The largest peak is at the target and only a slight amount of time is spent hyperoxemic. Generally, this infant stayed in normoxemia for at least 95% of the test.

PID controller output is illustrated in Figures 55, 56 and 57. The SpO_2 plot shows a high overshoot in reaction to the artifact. It also shows that the frequent shunting between 300 and 1000 seconds and at the end of the experiment cannot be regulated well by the PID controller. The FiO_2 plot in Figure 56 shows the controller pushing the blender to its limits in response to motion artifact. The SpO_2 distribution shown in Figure 57, however, is quite good with a large peak at target and tight distribution.

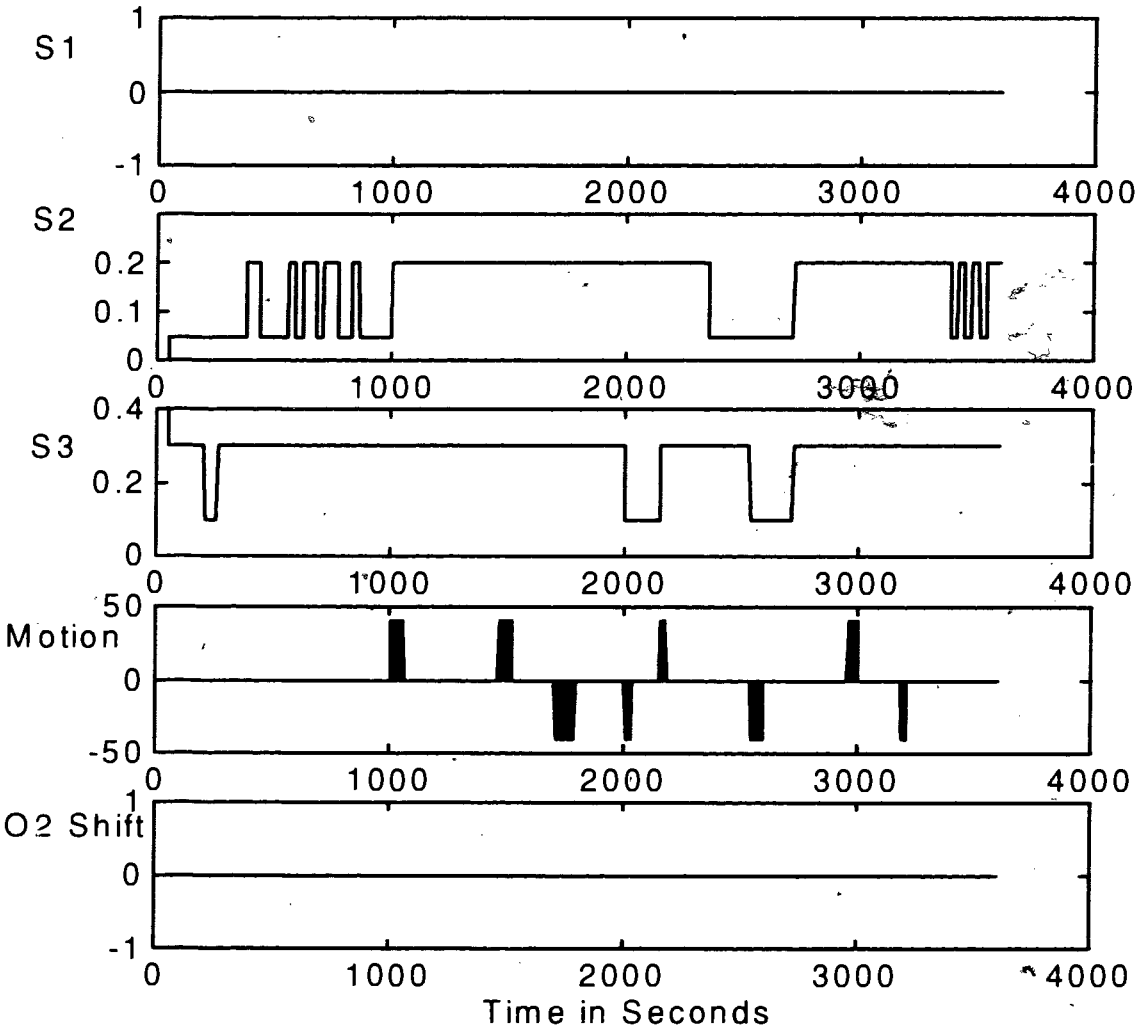

Figure 52. Baby 2 Model Disturbances

The fuzzy logic controller SpO_2 plot in Figure 58 is much better than the PID's SpO_2 plot. It appears to the author that the FL controller tracked the frequent shunting and did not drive the blender to its upper limit as a result of negative artifact. Also note, from Figure 59, the FiO_2 plot, that the FL controller is quicker to return from a high FiO_2 setting than the PID controller. An 88% FiO_2 peak occurs at 1800 seconds as a result of the negative artifact. The FL histogram presented in Figure 60 is very tight with over 80% of the experiment duration spent within +/- 1.5% SpO_2 of target.

SpO_2 plot, FiO_2 plot and SpO_2 histogram for the fuzzy logic controller with artifact detection are presented in Figures 61, 62 and 63 respectively. This controller ignored all negative artifact and so it did not amplify the severity of the shunting condition at 2540 seconds. Also, as shown in the FiO_2 plot, the FLA controller did not drive the blender to 21% as the PID and FL controllers did. This implies that the reaction to the positive artifact was not as severe. The SpO_2 histogram shows the best performance of the four controllers with a large peak of 50% experiment duration spent within +/- 0.5% SpO_2 of target. The distribution is very good with 87% of the experiment duration spent within +/- 1.5% SpO_2 of target.

Table X summarises each controller's target performance by listing the percent of its experiment duration within +/- 0.5% SpO_2 and +/- 1.5% SpO_2 of the 92% target. The PID controller offered improved target performance over manual mode by increasing the time within +/- 0.5% SpO_2 of target by 1% and providing an 11% experiment duration

improvement within +/- 1.5% SpO_2 of target. The FL controller spent 4% less time than PID mode within +/- 0.5% SpO_2 of target but a 2% improvement with regards to time spent within +/- 1.5% SpO_2 of target.

In terms of the data in Table X, and with respect to PID control, the FLA controller provided the best target performance with a 1% increase in time spent at target and a 9% increase in time spent close to target. The results of normoxemic performance are summarised in Table XI. The PID and FL controllers spent less time normoxemic than manual mode. However, the FLA controller provided the best normoxemic and target performance.

Table X. Target Performance of Controllers on Baby 2 - *model is relatively unstable and has less motion artifact events than Baby 1. S3 and S2 shunt percentages are varied.*

Controller	% of experiment duration	
	+/- 0.5% SpO_2	+/- 1.5% SpO_2
Manual	48.32	68.50
PID	49.88	80.03
FL	45.62	82.29
FLA	51.41	89.29

Table XI. Normoxemic Performance of Controllers on Baby 2

Controller	% of experiment duration		
	Hypoxemic	Normoxemic	Hyperoxemic
Manual	0	94.18	5.82
PID	3.41	91.91	4.68
FL	7.38	91.14	1.48
FLA	1.94	98.06	0

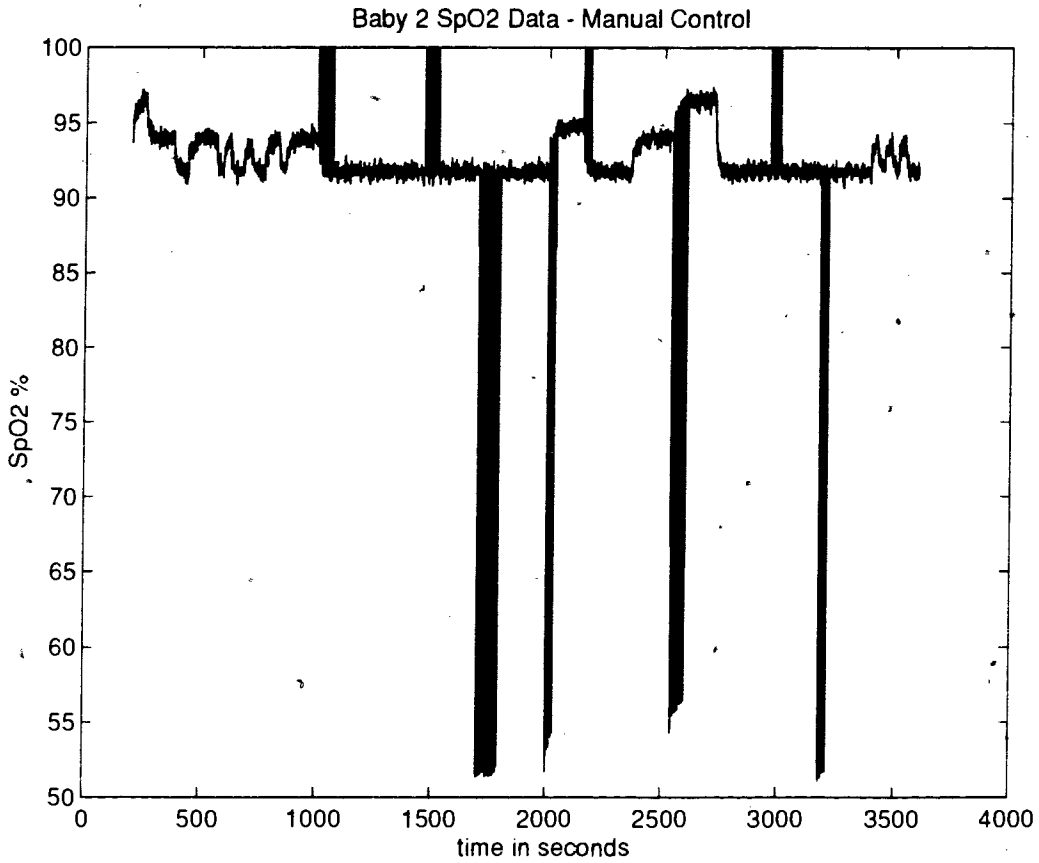

Figure 53. Baby 2 SpO_2 Plot - Manual Control

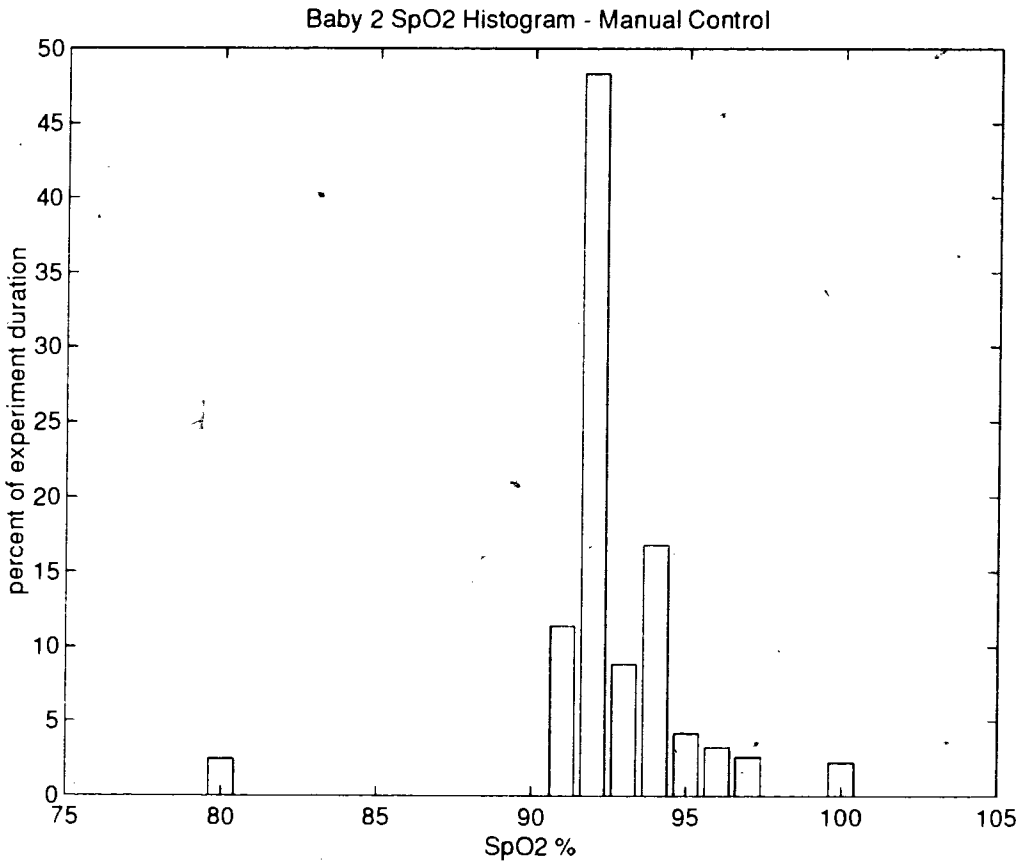

Figure 54. Baby 2 SpO_2 Histogram - Manual Control - *mean = 92.70 % Sp_{O2}; standard deviation = 1.40 % SpO_2.*

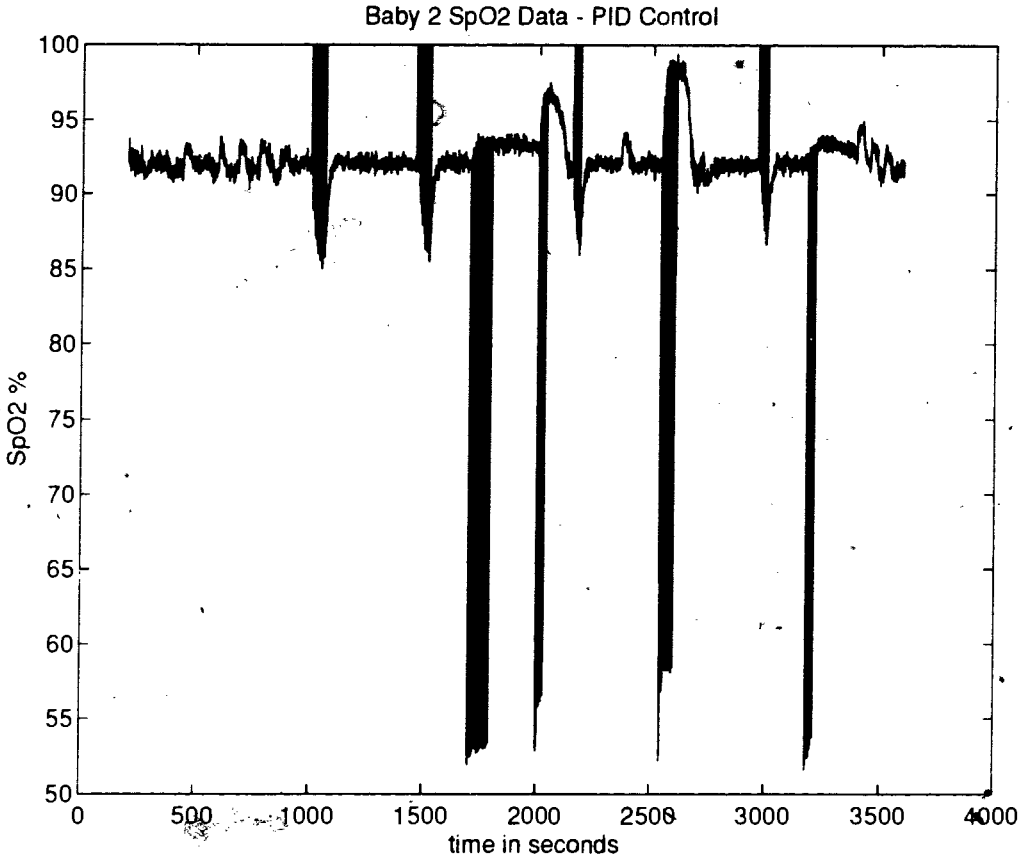

Figure 55. Baby 2 SpO_2 Plot - PID Control

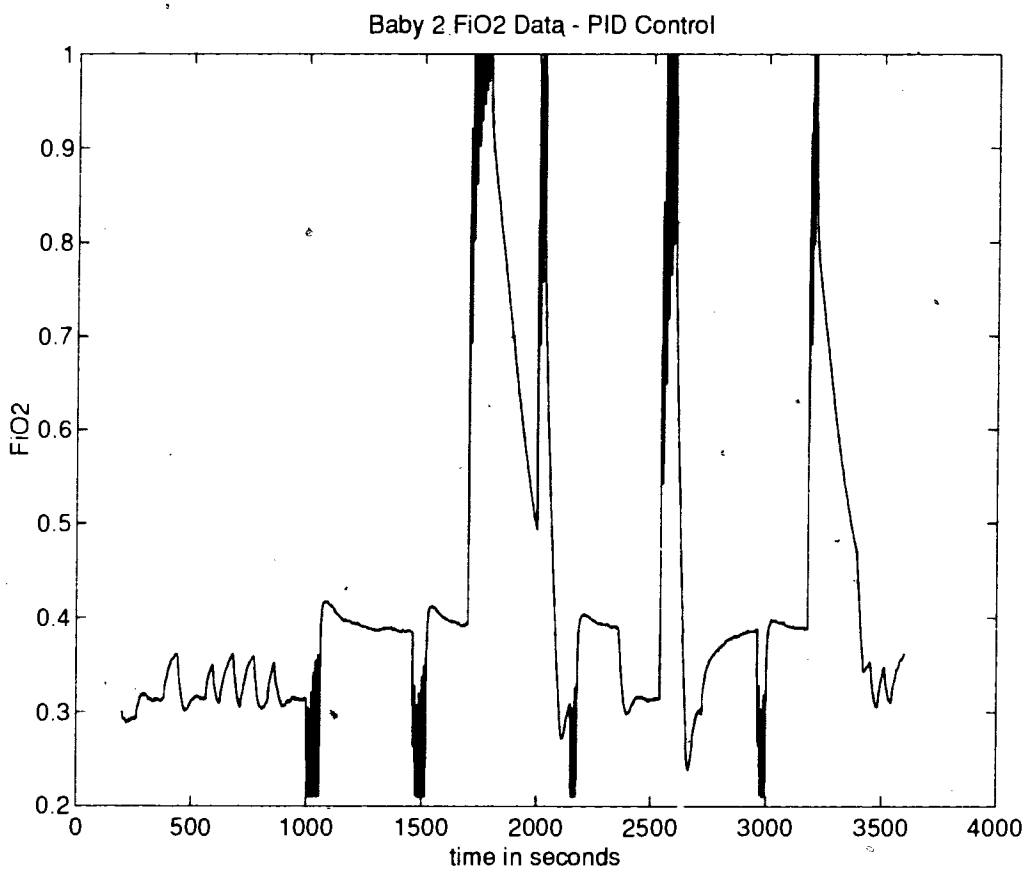

Figure 56. Baby 2 FiO_2 Plot - PID Control

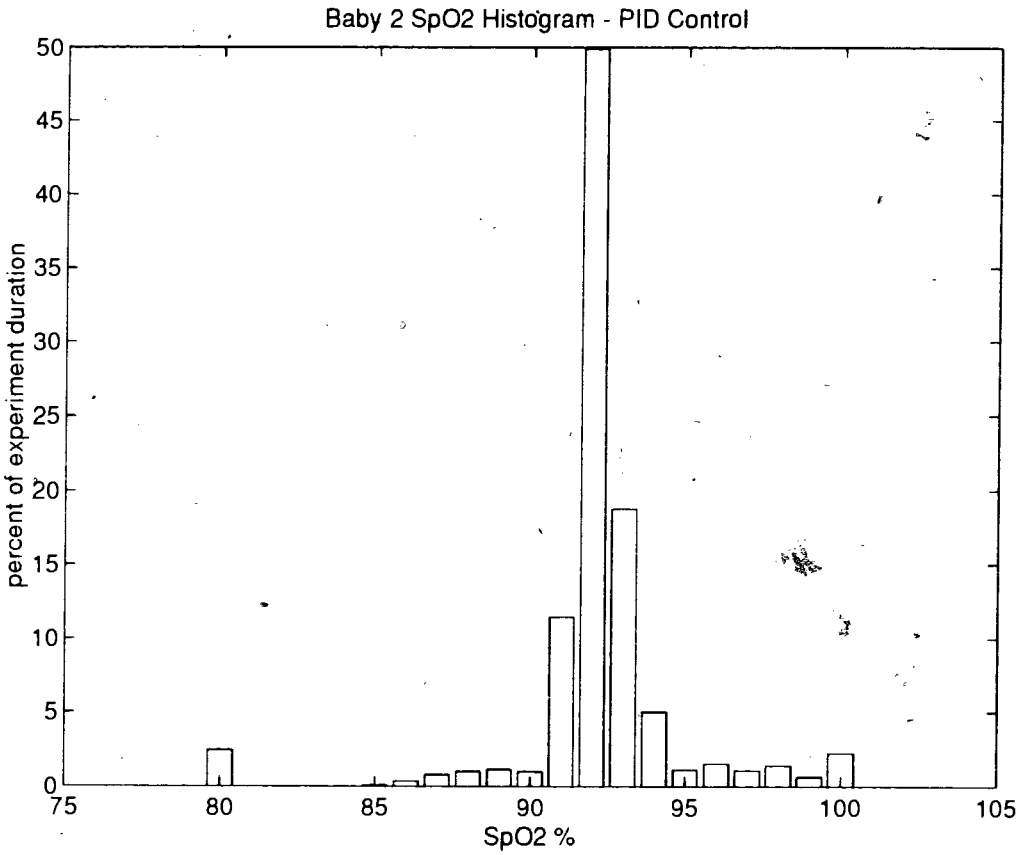

Figure 57. Baby 2 SpO_2 Histogram - PID Control - *mean = 92.30% SpO_2; standard deviation = 1.61% SpO_2.*

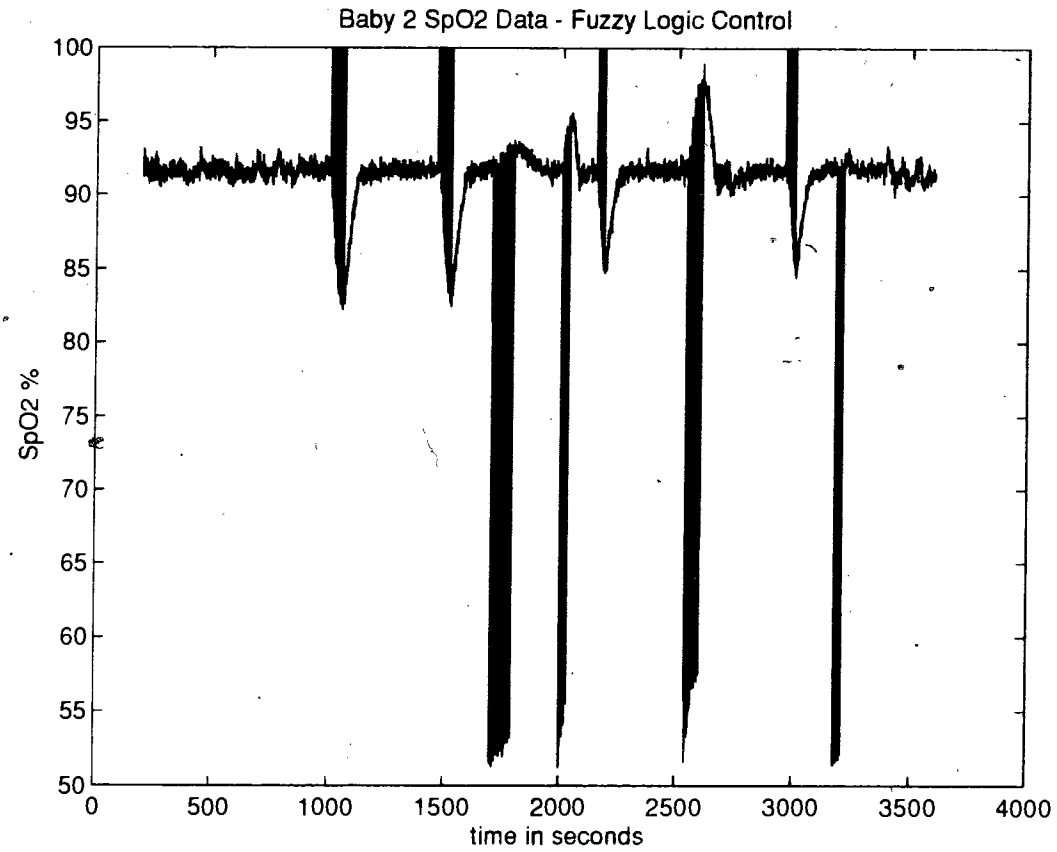

Figure 58. Baby 2 SpO_2 Plot - FL Control

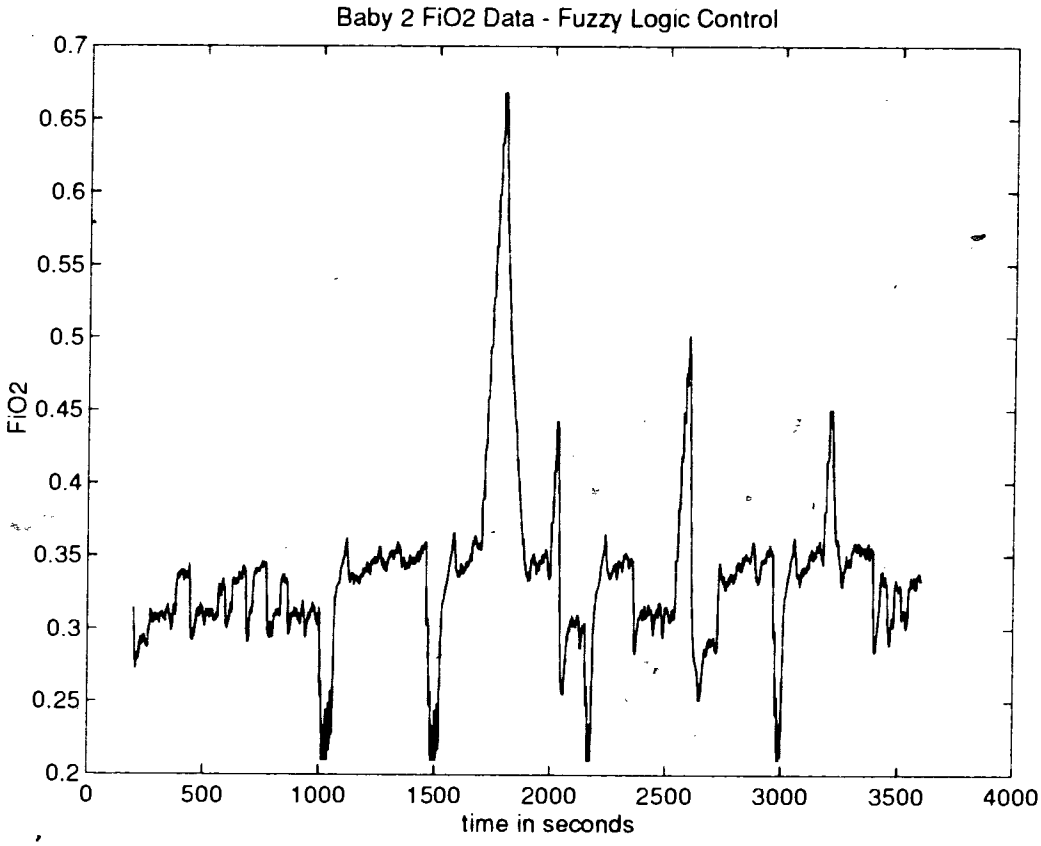

Figure 59. Baby 2 FiO_2 Plot - FL Control

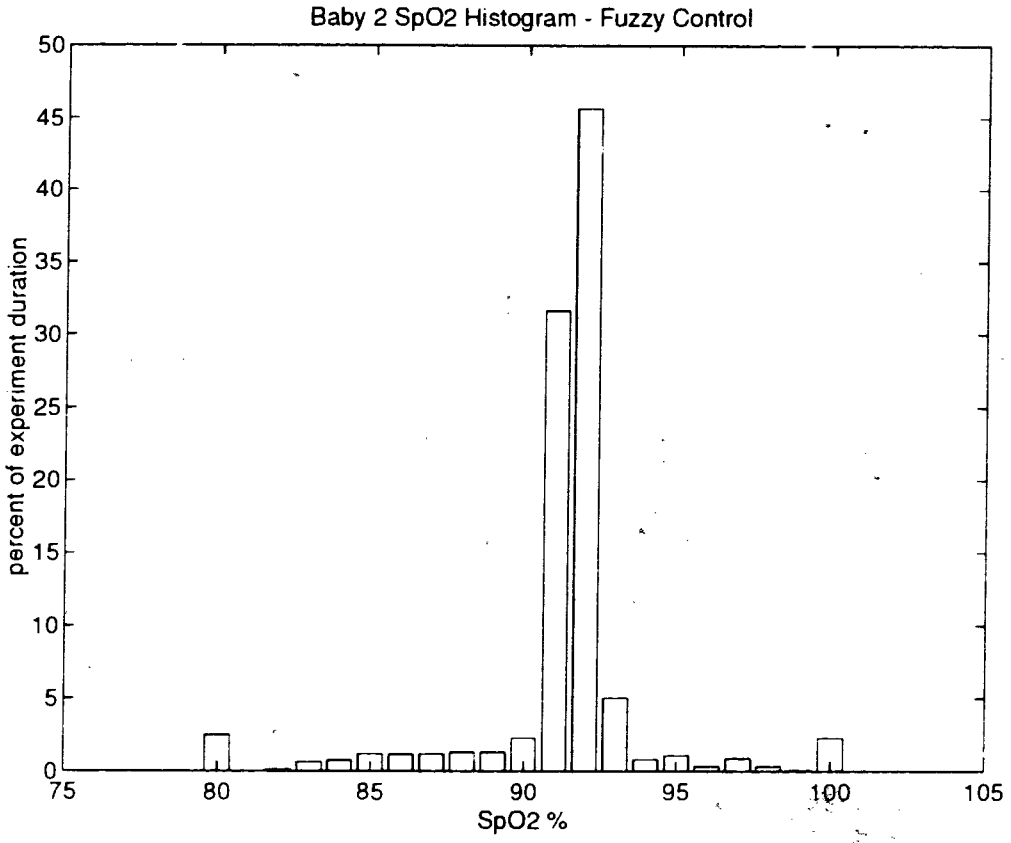

Figure 60. Baby 2 SpO_2 Histogram - FL Control - *mean = 91.36% SpO_2; standard deviation = 1.81% SpO_2.*

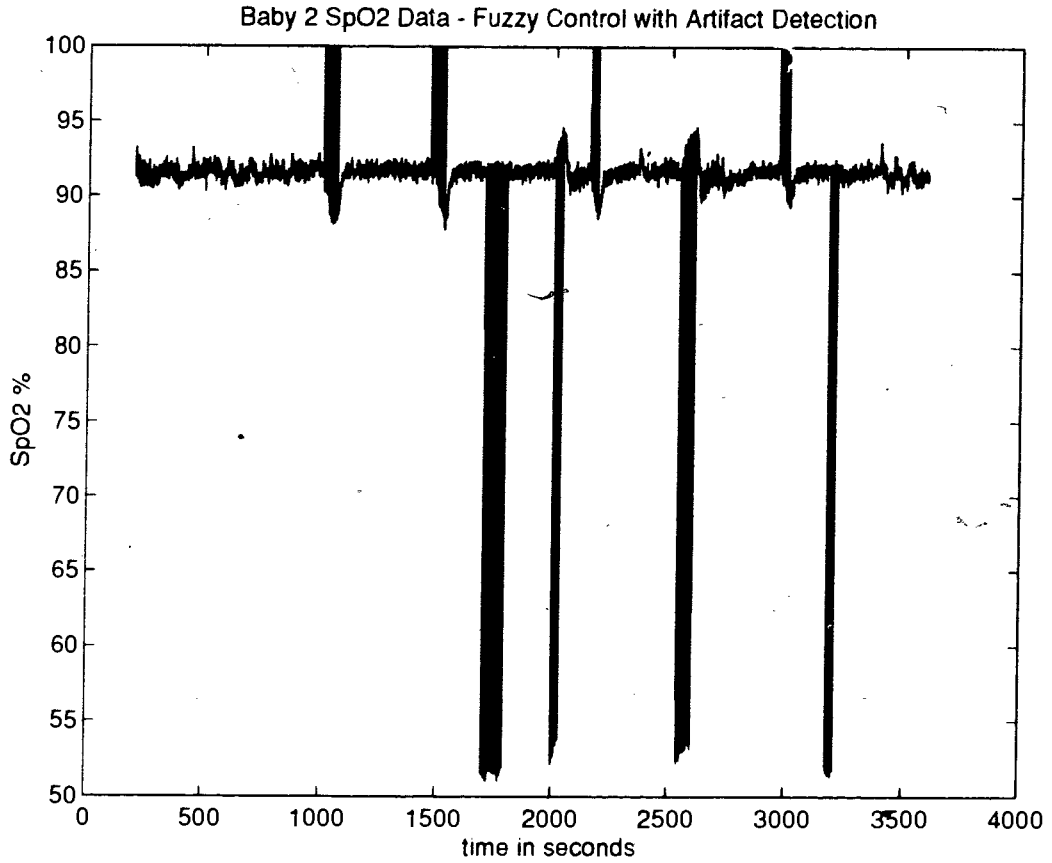

Figure 61. Baby 2 SpO_2 Plot - FLA Control

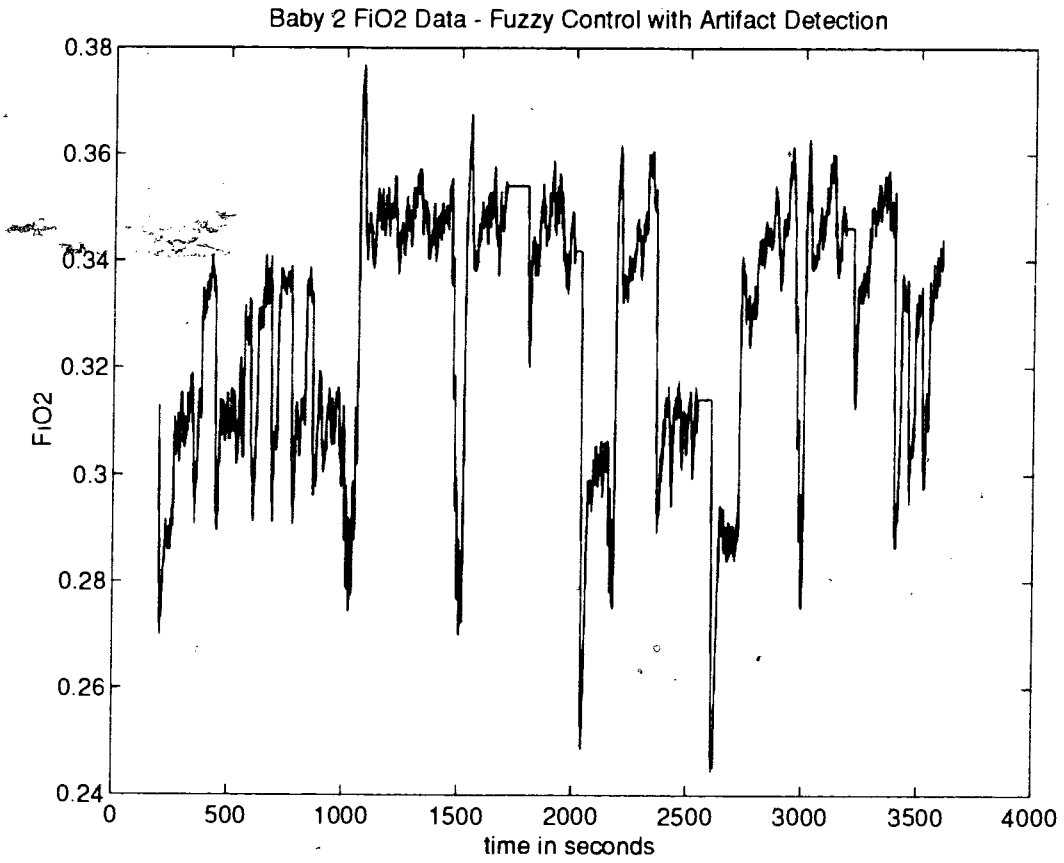

Figure 62. Baby 2 FiO_2 Plot - FLA Control

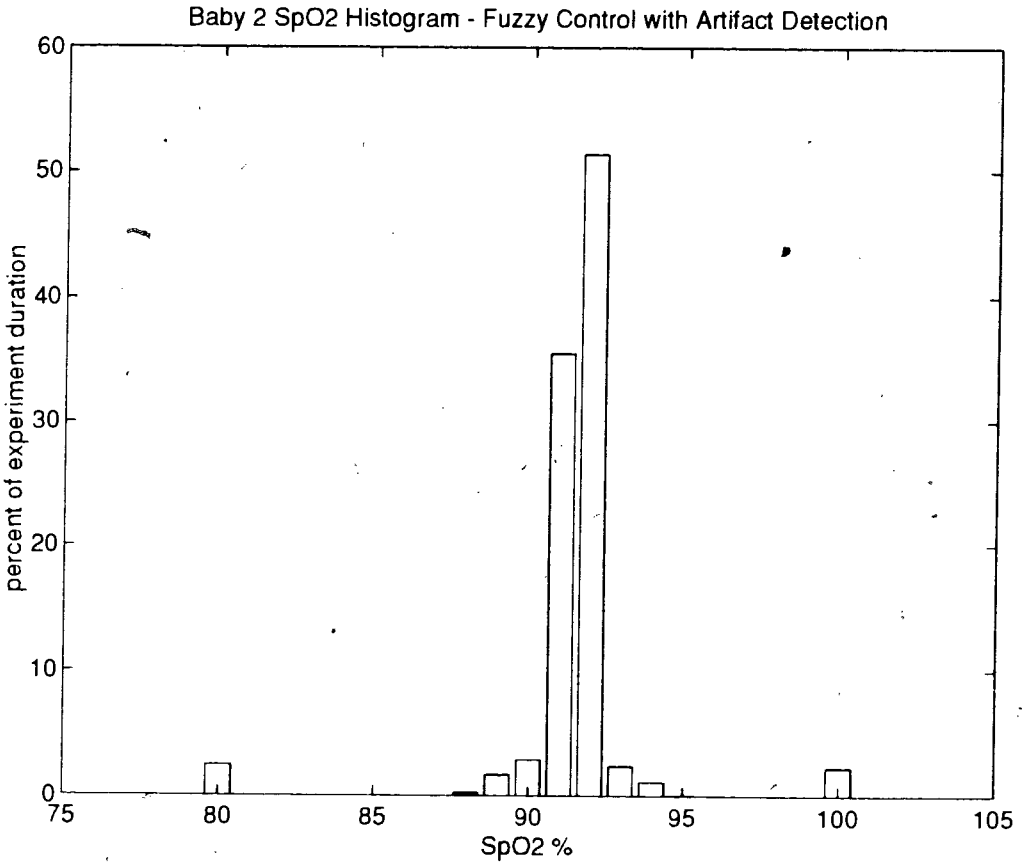

Figure 63. Baby 2 SpO_2 Histogram - FLA Control - *mean = 91.54% SpO_2; standard deviation = 0.68% SpO_2.*

5.4 Baby 3 Model

The main feature of this experiment is that the oxygen affinity decreases at 1800 seconds by a right shift of the oxygen dissociation curve. The shunting patterns during the first half of the 3600 second experiment are repeated in the second. These patterns represent an unstable infant, starting at 200 seconds, with the S3 shunt held at 20%, the S2 shunt is toggled between 10% and 30% at 30 second intervals. At time 460 seconds, the intervals are increased to 60 seconds until a time of 1000 seconds. The period is then reduced to 15 seconds from time 1075 to 1300 seconds. For the next 300 seconds, various S3 and S2 shunting combinations are implemented. At 1600 seconds, motion artifact is produced to mimic physiotherapy, drug therapy, blood transfusion, etc., and at 1800 seconds the O_2 dissociation curve is right shifted to a shape similar to a healthy infant with mostly adult hemoglobin in its bloodstream. Figure 64 summarises the baby 3 model disturbances.

Figures 65 and 66 are the SpO_2 manual mode raw data plot and its associated histogram respectively. The histogram shows that even though the model spent 25% of its time within +/- 0.5% SpO_2 of target, the model was in normoxemia for at least 95% of the experiment duration.

PID control data from the Baby 3 experiment is presented in Figures 67, 68 and 69 - SpO_2 plot, FiO_2 plot and SpO_2 histogram respectively. The SpO_2 plot shows the controller's inability to regulate the pulsed shunt conditions characteristic of this model. The motion artifact also drives the controller's output to both saturation points as shown in the FiO_2 plot. Also, note

that the outputs are lower before the O_2 dissociation curve shift. This makes sense since at a higher O_2 affinity, oxygen bonds more readily to hemoglobin (i.e. at lower PaO_2 levels). PID control resulted in a defined peak but a slight hyperoxic skew as shown in the histogram plot.

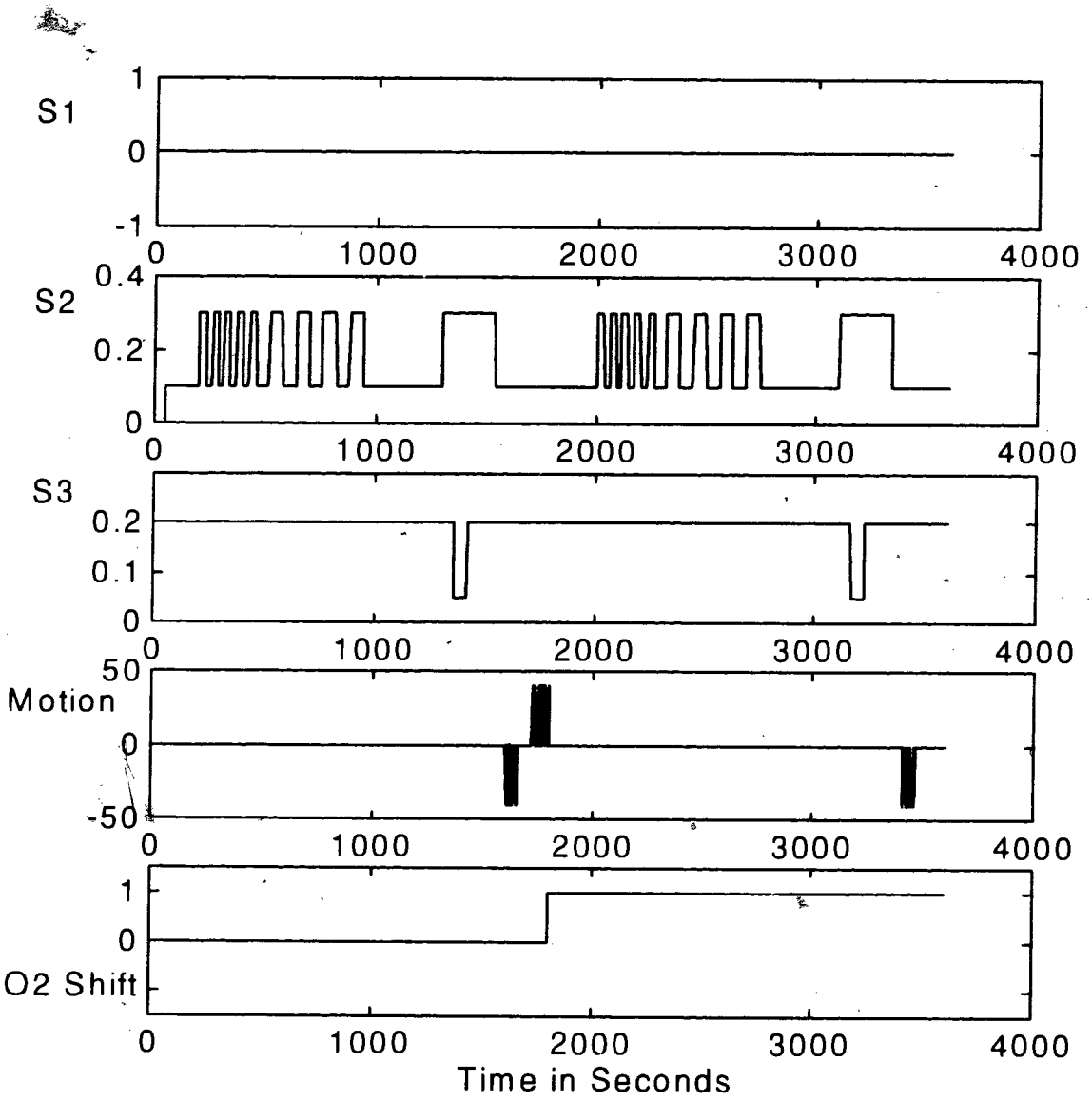

Figure 64. Baby 3 Model Disturbances - *O2 shift of 1.0 represents an increase in O2 affinity.*

The non-linear fuzzy logic SpO_2 plot, Figure 70, shows the pulsed shunt disturbances but they are not as large as those for manual or PID control. Reviewing the FL controller plot, Figure 71, shows a very fast response to the SpO_2 fluctuations as compared to the exponential shaped responses for the PID controller shown in Figure 68. The FL histogram in Figure 72 is very tight but slightly skewed below target. This behaviour is discussed in the previous chapter - the FL controller is fast to get close to target but slow to reduce small errors to zero.

Since the fuzzy logic controller with artifact detection is a super-set of the FL controller, its response to a model with minimal artifact, like Baby 3, should be similar. The FLA SpO_2 plot in Figure 73 is very similar to the FL SpO_2 plot in Figure 70; the only difference occurs at the three motion artifacts. Two negative artifacts are completely ignored by the FLA controller and it drives the model slightly hypoxemic as a result of the single positive motion artifact event. This behaviour is also illustrated in the FLA FiO_2 plot in Figure 74 where the FiO_2 is held constant for the negative motion artifact and slowly graduated downwards for positive. Like the FL controller, the SpO_2 histogram in Figure 75 has a large peak slightly below target.

Table XII summarises each controller's target performance. In terms of percent of experiment duration within +/- 0.5% SpO_2 of target, the FL and FLA controllers were better than PID and manual modes. Also, within +/- 1.5% SpO_2 of target, the FL controller showed a 3% (experiment duration) improvement over PID control and the FLA controller improved upon PID control by 8%. Table XIII lists the controllers' normoxemic performance and the FLA controller provided the best with a 2% experiment duration increase over manual mode.

Table XII. Target Performance of Controllers on Baby 3 - *model is unstable, has three motion artifacts. Oxygen affinity decreases at 30 minutes.*

Controller	% of experiment duration	
	+/- 0.5% SpO_2	+/- 1.5% SpO_2
Manual	25.65	83.12
PID	38.12	83.85
FL	39.79	86.88
FLA	40.26	91.15

Table XIII. Normoxemic Performance of Controllers on Baby 3

Controller	% of experiment duration		
	Hypoxemic	Normoxemic	Hyperoxemic
Manual	3.02	96.98	0
PID	1.03	93.50	5.47
FL	2.24	96.55	1.21
FLA	0.87	99.13	0

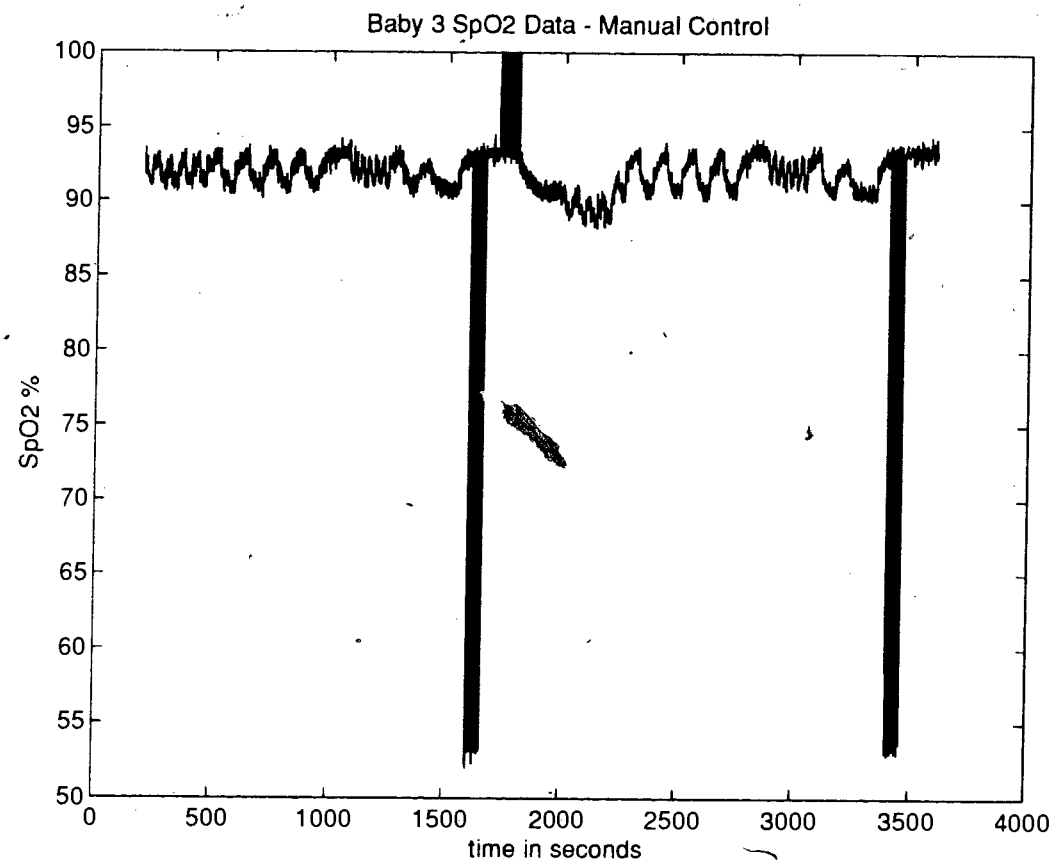

Figure 65. Baby 3 SpO_2 Plot - Manual Control

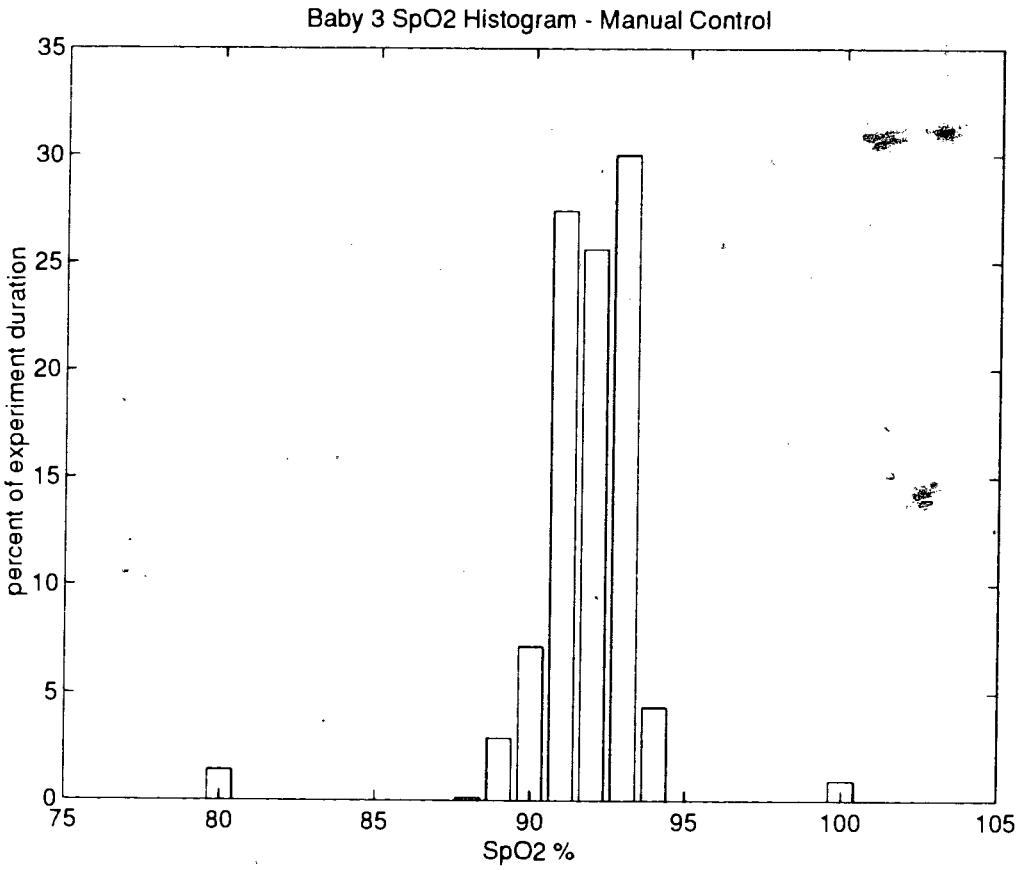

Figure 66. Baby 3 SpO_2 Histogram - Manual Control - *mean = 91.88% SpO_2; standard deviation = 1.13% SpO_2.*

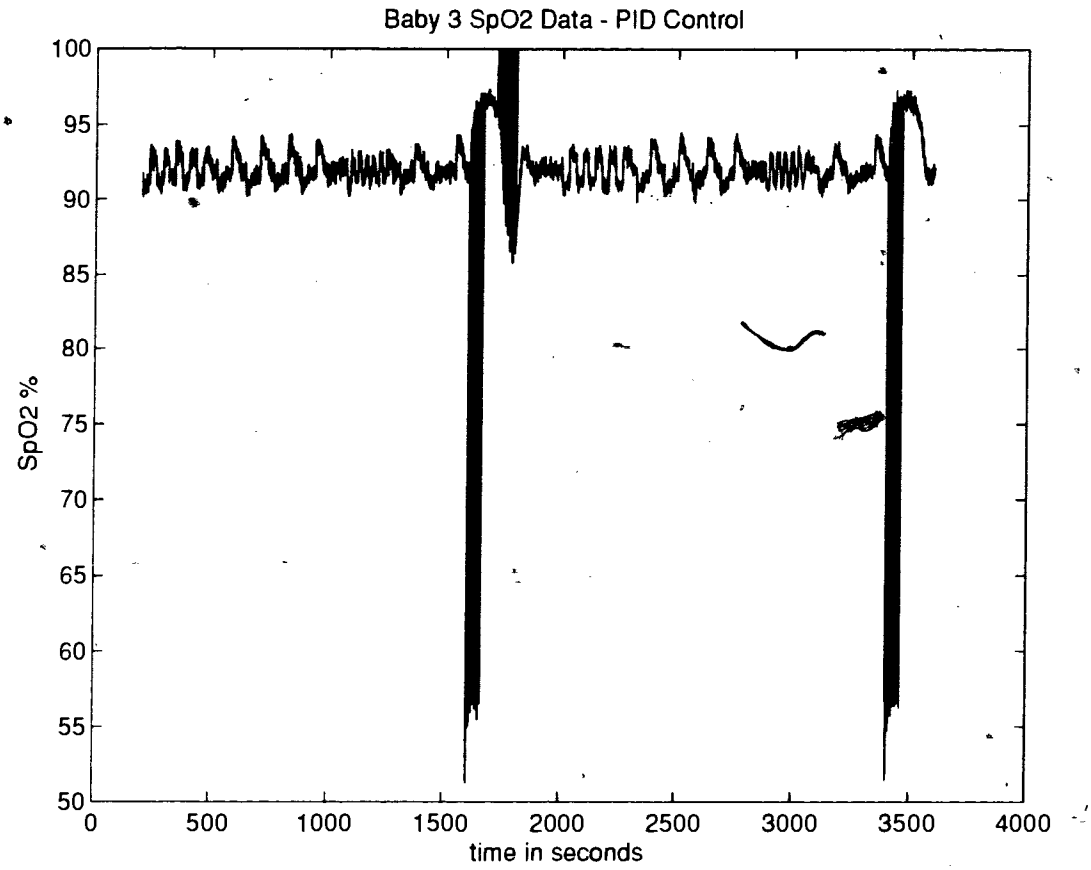

Figure 67. Baby 3 SpO_2 Plot - PID Control

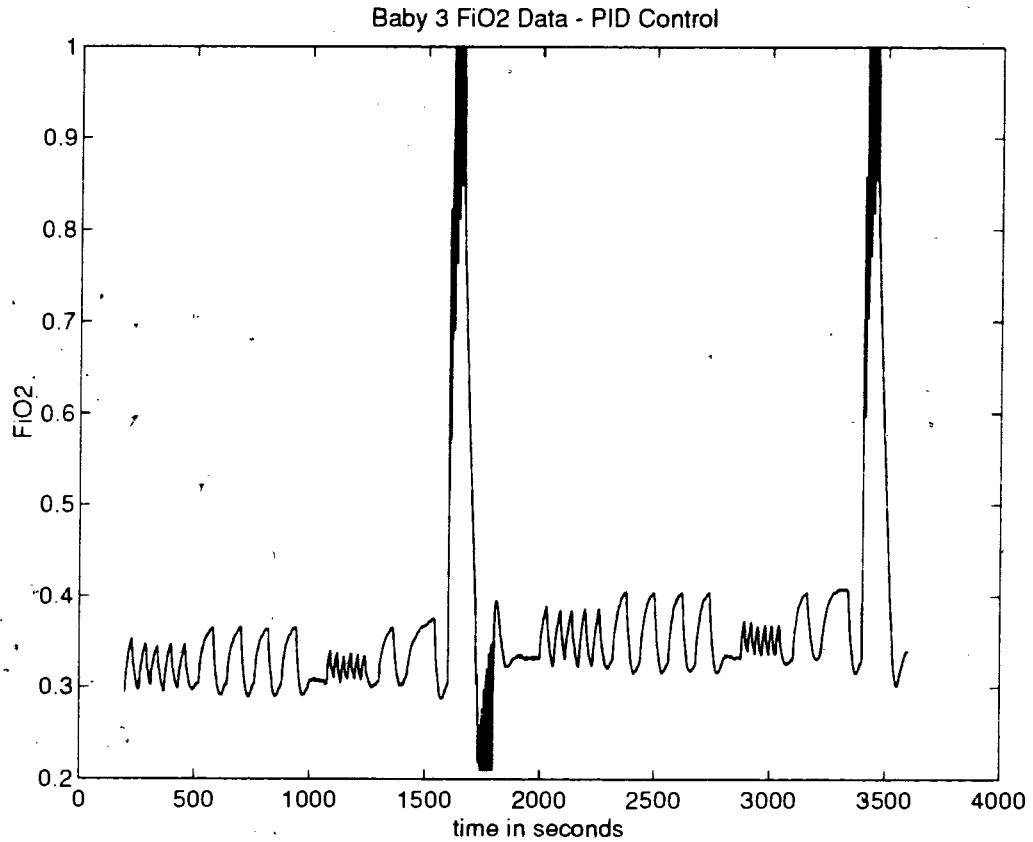

Figure 68. Baby 3 FiO_2 Plot - PID Control

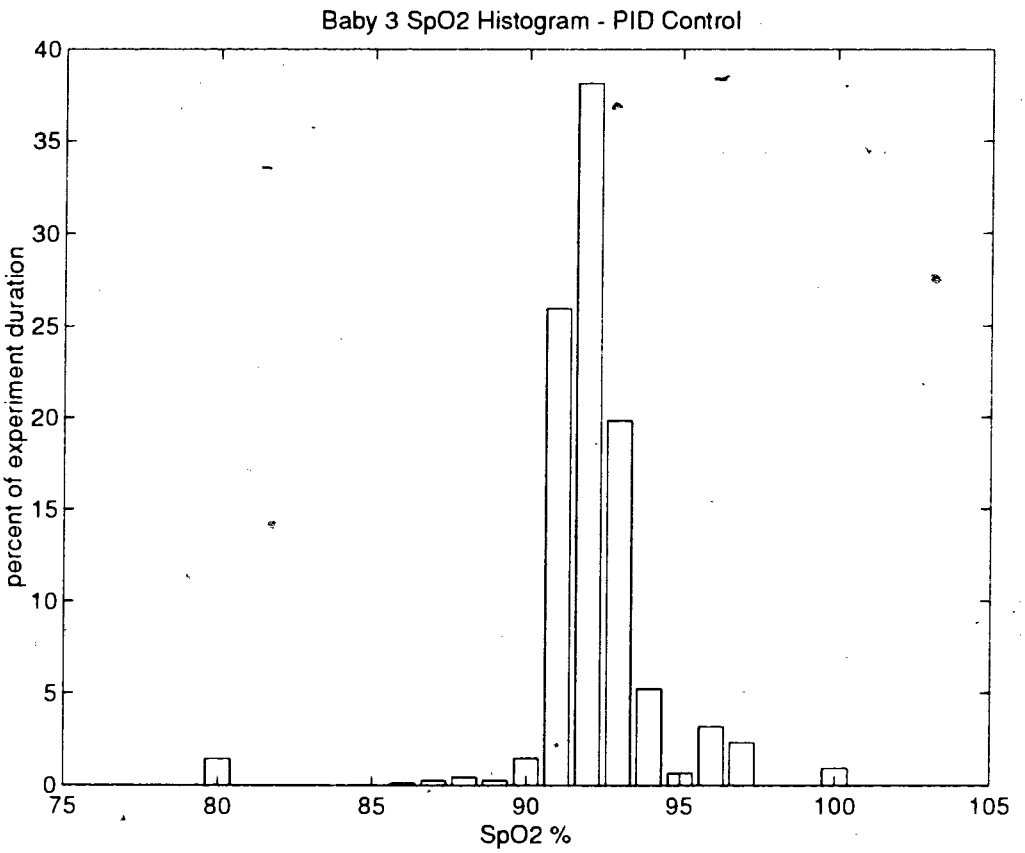

Figure 69. Baby 3 SpO_2 Histogram - PID Control - *mean = 92.24% SpO_2; standard deviation = 1.40% SpO_2.*

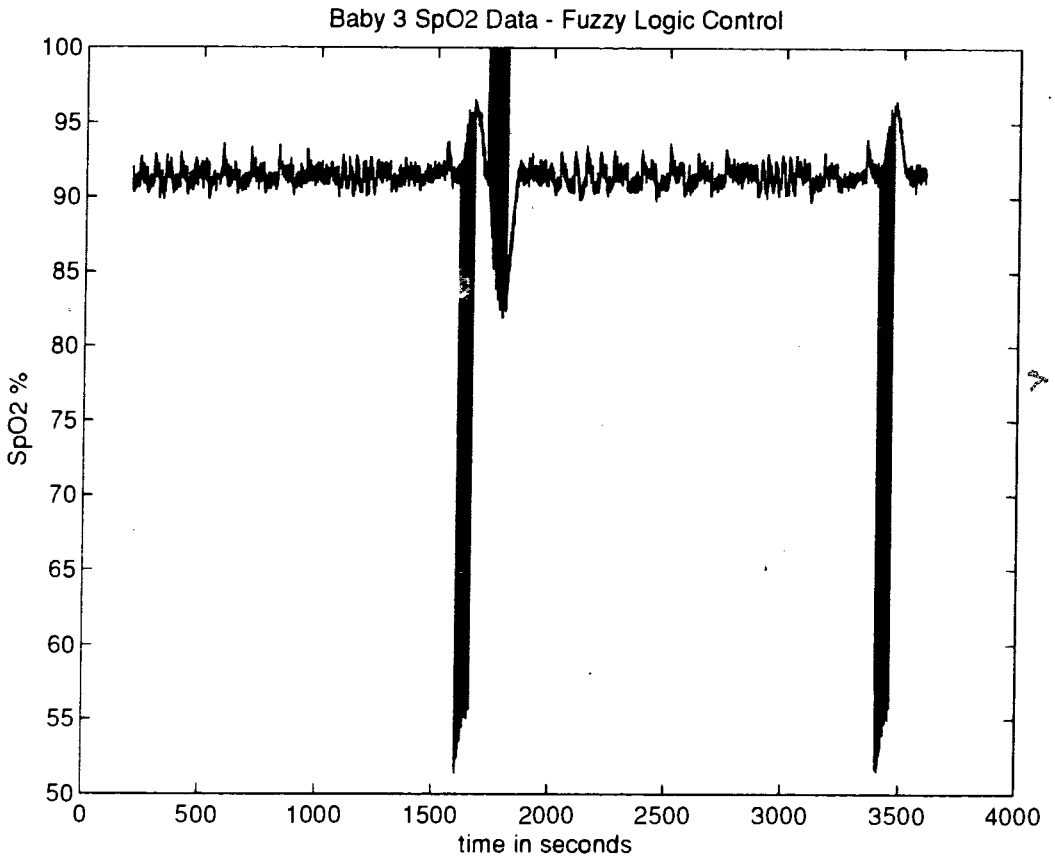

Figure 70. Baby 3 SpO_2 Plot - FL Control

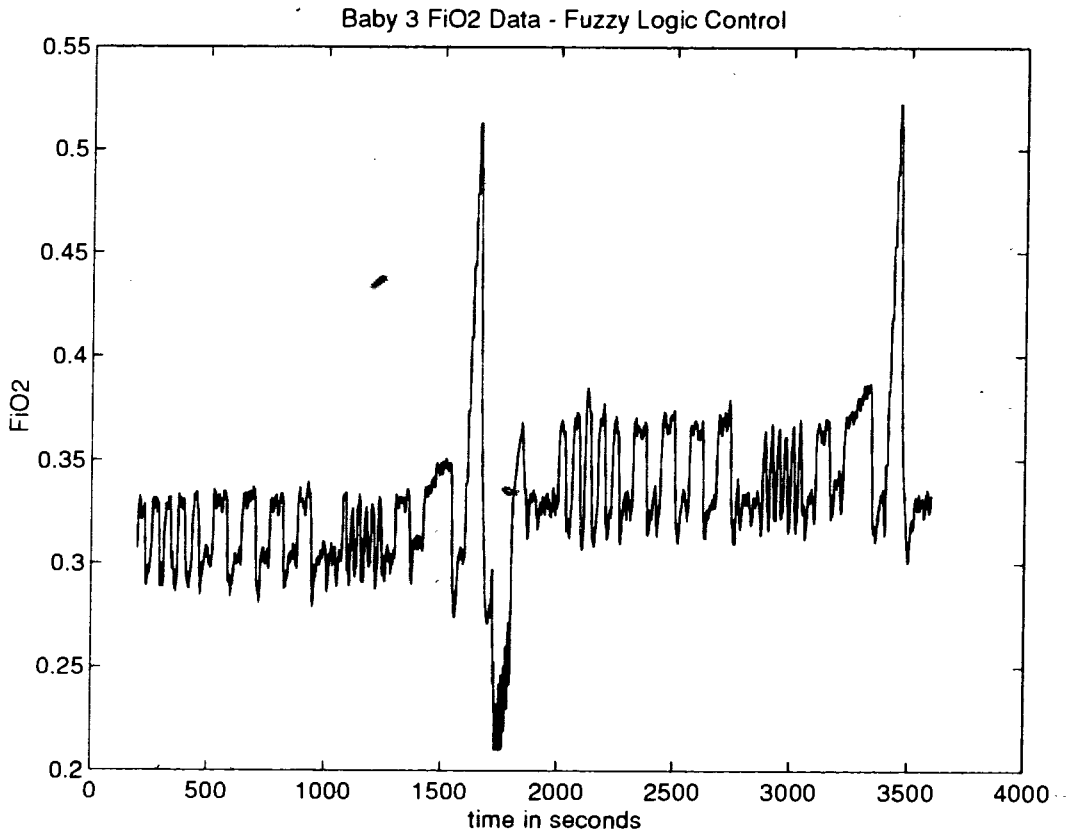

Figure 71. Baby 3 FiO_2 Plot - FL Control

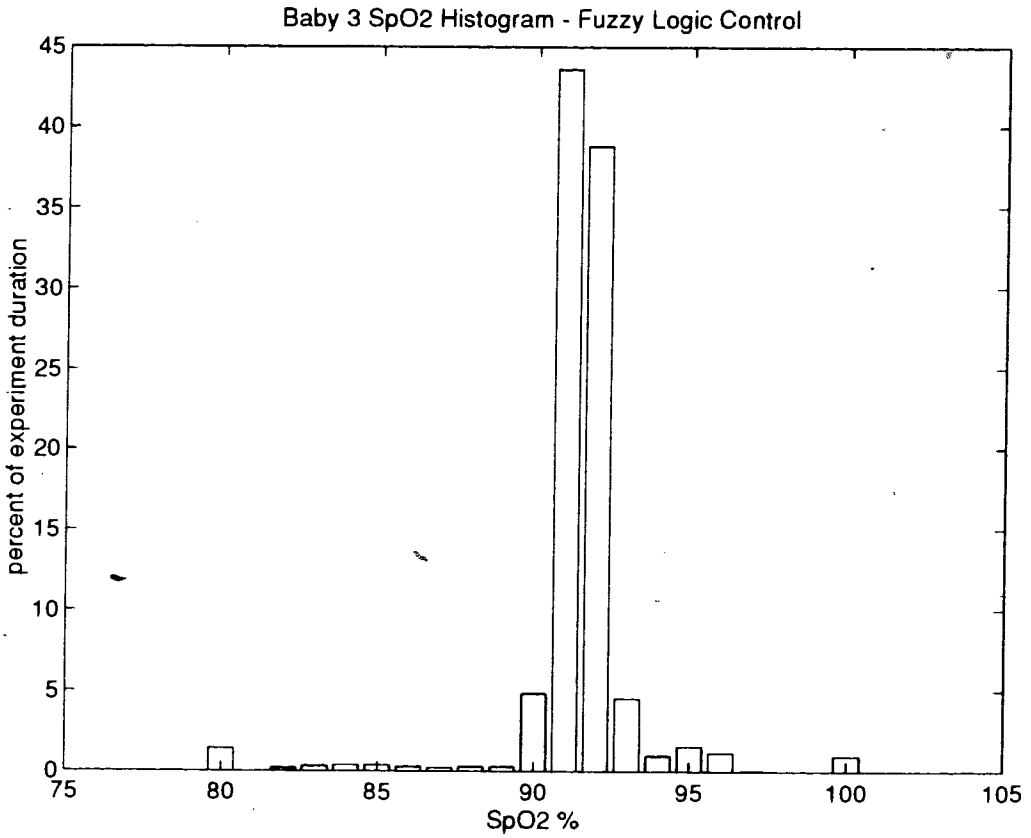

Figure 72. Baby 3 SpO_2 Histogram - FL Control - *mean = 91.46% SpO_2; standard deviation = 1.33% SpO_2.*

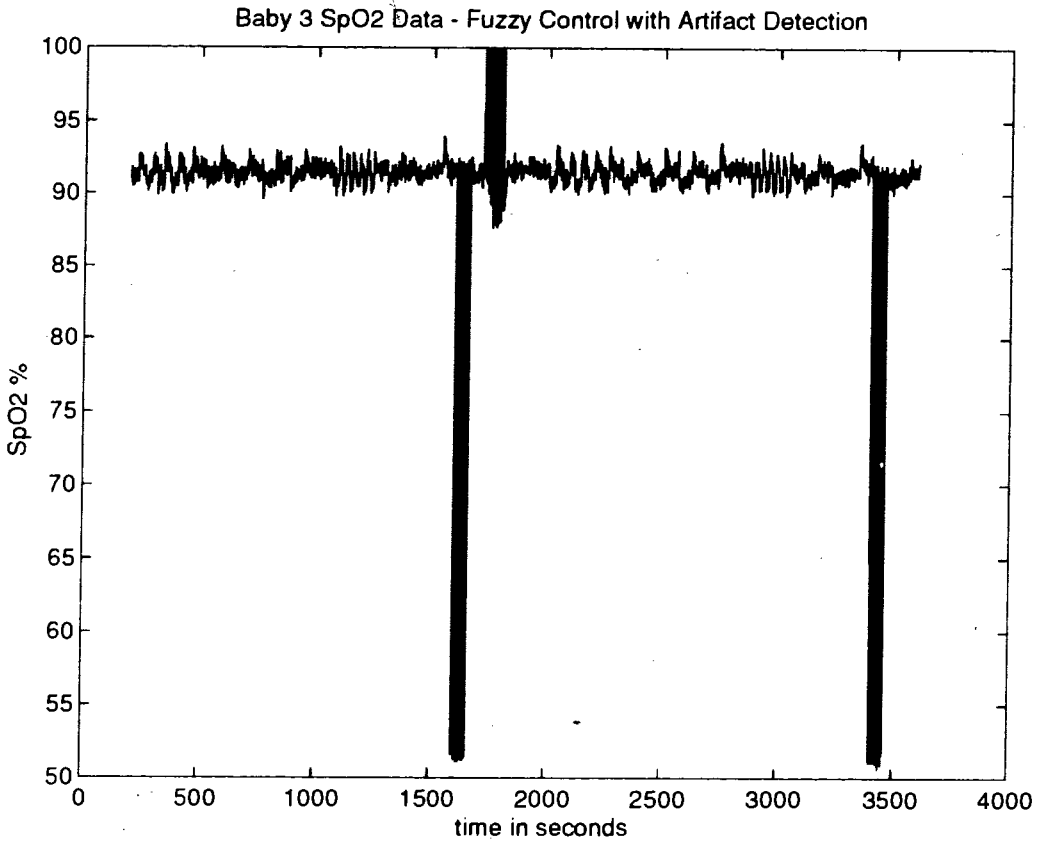

Figure 73. Baby 3 SpO_2 Plot - FLA Control

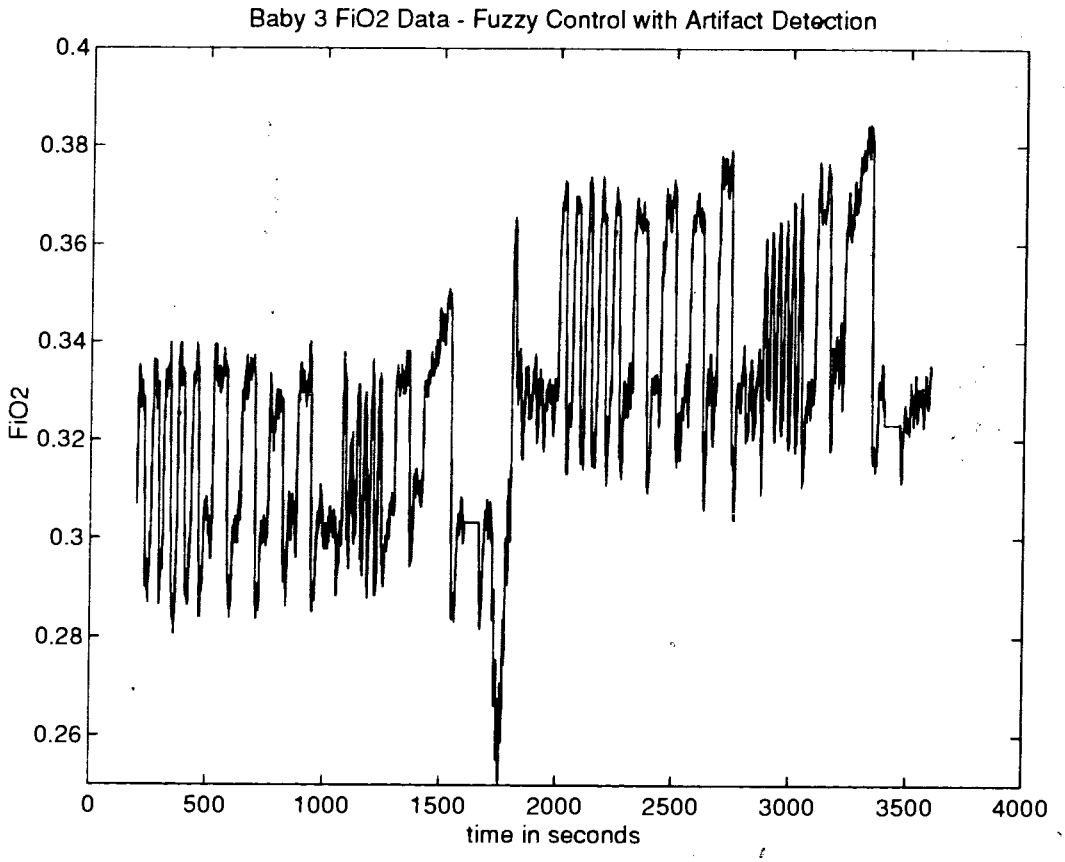

Figure 74. Baby 3 FiO_2 Plot - FLA Control

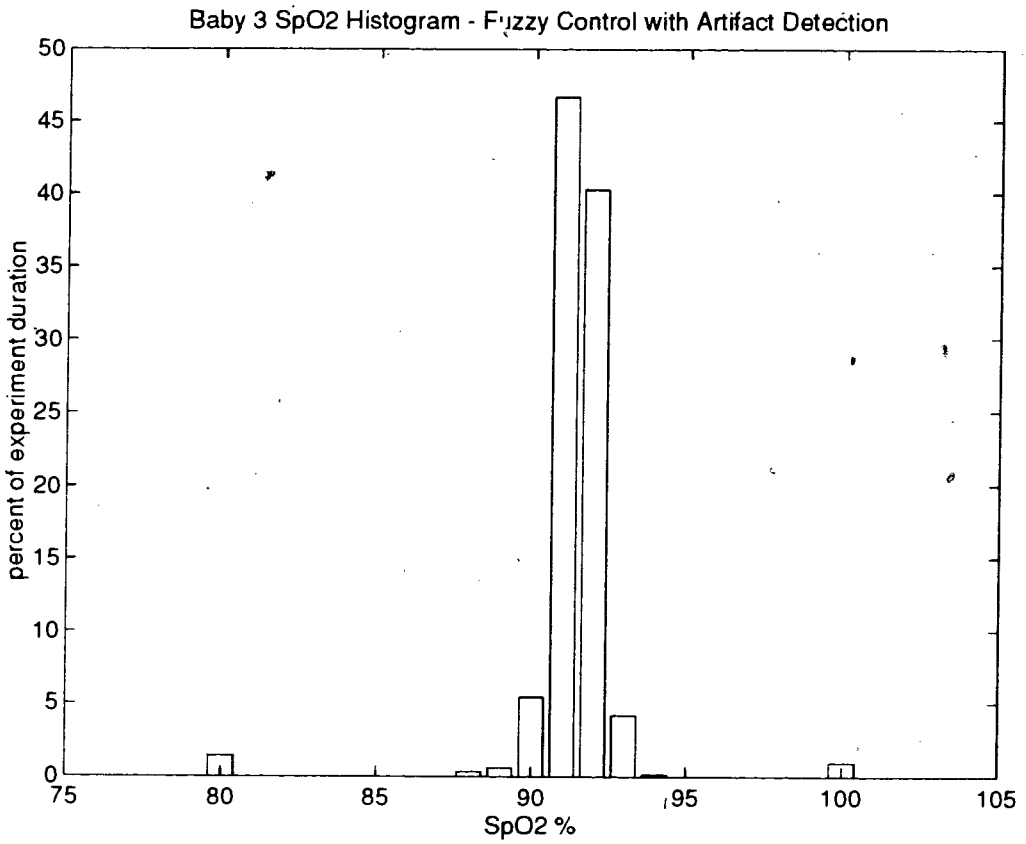

Figure 75. Baby 3 SpO_2 Histogram - FLA Control - *mean = 91.46% SpO_2; standard deviation = 0.66% SpO_2.*

5.5 Total Controller Performance.

Table XIV lists the average target performance of the controllers and is produced by averaging the percents of experiment duration spent at +/- 0.5% and +/- 1.5% SpO_2 of target. The automatic controllers provided an improved target performance over manual mode with the FLA controller providing the best. Listed in Table XV are the average normoxemic performances and the FLA controller is best. Note that the PID controller, on average, did not improve normoxemic performance over manual mode but with regards to target performance it did. This implies that the PID controller's false response to artifact caused it to push the model out of normoxemia and, after the artifact, quickly back to target. The Baby 1 model had many artifact events and the PID normoxemic performance is the worst of all four modes. The fuzzy logic controller provided, on average better target and normoxemic performance than the PID controller and was as good as manual modes. Overall, the fuzzy logic controller with artifact detection provided the best target and normoxemic performance.

Table XIV. Average Target Performance of Controllers

Controller	% of experiment duration	
	+/- 0.5% SpO_2	+/- 1.5% SpO_2
Manual	32.14	68.70
PID	42.50	75.64
FL	43.62	81.81
FLA	46.08	87.73

Table XV. Average Normoxemic Performance of Controllers

Controller	% of experiment duration		
	Hypoxemic	Normoxemic	Hyperoxemic
Manual	5.30	92.76	1.94
PID	2.60	90.47	6.93
FL	5.72	92.82	1.46
FLA	2.66	97.34	0

The FLA controller was within +/- 0.5% SpO_2 of target 13.94% longer than manual mode and, over 3 hours, this represents an extra 25.09 minutes. Over a 24 hour period we would get an extra 200.74 minutes (>3 hours) closer to target than manual mode. Looking at performance in terms of +/- 1.5% SpO_2 of target, the FLA controller was better than manual mode, on average, by 19.03% which over a 3 hour period translates into 34.25 minutes of improved O_2 therapy. This means that for a 24 hour period, the FLA controller may keep the models within +/- 1.5% of target 274.03 minutes (4.5 hours) more than manual mode. If the model was run for two weeks - O_2 therapy is often required on infants for this period - the model under FLA control would stay within +/- 1.5% SpO_2 of target 63.94 hours (2.66 days) more than that of manual mode. Of course, one would have to assume that the baby retained the physiological behaviour of only the three models during this period. With respect to normoxemic performance, the FLA controller spent 4.58% more time in normoxemia than manual mode. This translates to an extra 65.95 minutes per day; or 15.39 hours per two weeks.

Manual mode tends to keep the infant in normoxemia for a large (>90%) duration of the O_2 therapy session. The SpO_2 histograms show two trends. If the model is at target (within +/- 0.5% SpO_2) most of the time in manual control, as in Baby 2, the automatic controllers will only slightly increase this time but will tighten the distribution and increase (> 20%) the amount of time within +/- 1.5% SpO_2 of target. The second trend is shown in Baby 3, a model in which manual mode produces a small duration at target but a large portion within +/- 1.5% SpO_2 of target. In this case, the automatic controllers only slightly increase the +/- 1.5% SpO_2 duration but greatly (> 50%) increase the amount of time spent at target.

The data suggests that the fuzzy logic controllers are better than manual mode at keeping the model close to target, but only as good or slightly better at keeping the model in normoxemia. Some readers may propose that, if normoxemia is only required in the clinical setting, the controller is not necessary. The author disagrees with this point for the following reasons:

Assistant to Nursery Staff

The controller can augment manual O_2 therapy. Just because, in manual mode, a few FiO_2 increments are required, it doesn't mean that the neonate is ignored. Clinical staff must always be aware of a neonate's SpO_2 levels which can be distracting when trying to perform other duties.

Does not Degrade O_2 Therapy

The 3 automatic controllers did not make a good situation (patient within normoxemia most of the time) worse. This type of performance give the nursery staff confidence in the instrument and a willingness to allow it to manage more labile neonates.

Research into Specific SpO_2 Targets

Automatic controller can provide a tight error band width around a specific target. This can allow researchers to explore the effect of various SpO_2 levels. What is an optimal SpO_2 setting? Should SpO_2 set points be shifted with changes in a patient's condition? Can specific SpO_2 levels be correlated with BPD, ROP, etc.? These are only a few of the types of questions that can be explored using automatic oxygen therapy.

Labile Babies

The neonatal models presented in this thesis are representative of stable and unstable infants that generally stay within normoxemia. What about infants that are constantly swinging in and out of normoxemia? The PID controller used in this thesis was validated previously in the nursery environment (Morozoff, 1994). The results of this PID controller showed that it performed better (with respect to target and normoxemic performance) than manual O_2 therapy on stable and labile neonates. This implies that the fuzzy logic controllers, since they performed better than manual and PID control in the models, may also perform better than the two in the clinical setting on the same type of patients.

5.6 Summary

The four controllers - manual, PID, fuzzy logic and fuzzy logic with artifact detection - are applied to each neonatal model. SpO_2 plots, FiO_2 plots and SpO_2 histograms for each of the 12 experiments are presented. At target is defined as target +/- 0.5% SpO_2. Close to target is defined as target +/- 1.5% SpO_2. Target performance is related to the percent of experiment duration spent at and close to target. Normoxemic performance is a function of the percent of experiment spent in normoxemia - 90% to 95% SpO_2.

Fuzzy logic control with artifact detection consistently provided an improvement in target and normoxemic performance over the other three. Even though manual control provided a good distribution of time spent within normoxemia (90% - 95% SpO_2), the automatic controllers improved either the percent of time spent at or close to target.

The PID controller provided improved target performance over manual O_2 therapy in the model and, earlier, in the nursery. Since the fuzzy logic and fuzzy logic with artifact detection provided better target and normoxemic performance than the PID controller, the author suggests that the fuzzy controllers will perform better than manual mode in the nursery environment.

6.0 SUMMARY AND CONCLUSIONS

Premature babies are often born with underdeveloped lungs and require the administration of elevated levels of oxygen through mechanical ventilation. This process is known as oxygen therapy and clinical staff often use the output signal from a pulse oximeter, SpO_2, as an indirect indicator of tissue oxygenation. A mechanical air/oxygen gas blender is used to administer a percentage of fractional inspired oxygen, FiO_2. Hypoxemia may result when SpO_2 levels indicate low tissue oxygenation and may lead to permanent brain damage if frequent and prolonged. High levels of blood oxygen saturation, as indicated by high SpO_2, may lead to bronchopulmonary dysplasia (chronic lung disease) and/or retinopathy of prematurity (retinal damage). Normoxemia is a "safe" range of SpO_2 and may be defined as 90% to 95% saturation. Researchers have produced automatic SpO_2 controllers but this thesis is the first known analysis of one that uses a fuzzy logic based algorithm.

As oxygen moves from the mouth to the lungs its partial pressure drops. At the alveoli it diffuses across the lung walls into the pulmonary capillary blood where a small portion is dissolved. The majority of the oxygen is bonded to hemoglobin, related to the partial pressure of O_2 in the blood by the oxygen dissociation curve. The SaO_2, or blood oxygen saturation, is a measure that indicates the percentage of total hemoglobin bonded with oxygen. A computer model of this oxygen transport system was developed and contains a 4 compartment respiratory system linked to a 13 compartment cardiovascular circuit. The model was first developed for an adult and then scaled to represent a neonate using empirical data and

mammalian scaling functions. Three one hour supervisory programs were written to represent 3 neonate types: Baby 1 - stable but active; Baby 2 - unstable and not active; Baby 3 - unstable, not active and changing oxygen affinity.

Four controllers were developed - manual, PID, fuzzy logic (FL) and fuzzy logic with artifact detection (FLA). Manual mode was designed to represent actual clinical oxygen therapy where the emphasis is on keeping the infant within normoxemia rather than at a specific target. The PID controller gains were set from empirical values that were also confirmed by the literature. A non-linear fuzzy logic controller was developed around 35 rules. It uses two inputs, "error" and "error_rate" to formulate a single output, "FiO2_increment", which is integrated to produce an FiO_2 setting for the blender. The fuzzy logic controller with artifact detection consists of the FL controller augmented with a third input, "artifact", which is defined as the difference between the filtered and non-filtered SpO_2 signals. When "artifact" is detected (greater than 3% to 4% or less than -7% to -8%), the FLA controller ignores the inputs and makes no FiO2 adjustments until the "artifact" is not evident.

Each control algorithm was applied to each of the three neonatal models and the resulting data showed that the fuzzy logic controller with artifact detection provided the best performance. Target performance is measured by the percent of experiment duration at target (+/- 0.5% SpO_2) and close to target (+/- 1.5% SpO_2). These were increased, on average, by 12% and 13% respectively by the automatic controllers over manual mode. The PID controller produced better target performance manual control and the fuzzy logic controller was better

than both. Applied to a neonatal model with minimal artifact, the FLA controller provided, understandably, only a minor target performance improvement over the FL controller. Normoxemic performance is measured by the percent of experiment duration which the model stays within normoxemia (90% to 95% SpO_2). The PID controller on average, provided a slightly worse normoxemic performance than manual mode. Fuzzy logic control had as good a normoxemic performance as manual mode and the FLA controller was better than both. In summary, the fuzzy logic controller with artifact detection provided the best target and normoxemic performance on all three neonatal models.

The PID controller is based on one that produced good results - better target and normoxemic performance than manual control - in the clinical setting on a variety of neonates. Since the fuzzy logic controllers were better than the PID controller on the models, the author suggests that they may also perform better than manual mode in the nursery.

The controllers developed in this thesis can only be as good as the model. For this reason, the author feels that the focus of further development should be on improving the neonatal model. The addition of pulsatile blood flow may allow researchers to study the effect of heart rate on SaO_2 and SpO_2. If the model was packaged and disseminated to the medical community, perhaps medical personnel could produce new and varied test scripts for controller verification.

Further development of the controller is also required to fine tune the fuzzy logic algorithm. Perhaps the addition of inputs such as heart rate, motion detection, etc., will improve artifact

detection. Exploring supervisory and adaptive systems may produce controllers that can adapt to a neonates changing physiology. The author also believes that validating the fuzzy controllers in the clinical setting may provide further information towards improving both the neonatal model and controller algorithms.

Appendix A. Neonatal Model Initialisation Program.

```
% Initnn1.m - nn1.m initialization program
% Sept. 16, 1996
% run this m-file before running the simulink program
%
% This model is built from two sub-systems, the first is the pulmonary model and
% is based on the pulm1.m file. The second is the blood circuation system. It is
% different from earlier versions in that this model uses the SvO2
% value in its control loop. It also uses a default 10% shunt across the lungs to
% represent the pressure drop there. With the O2 consumption set at about 20%
% we get SaO2 = 96% and SvO2 = 77%
%
% "nn1.m" is essentually the same as "pulmcd3.m" except that this model has
% been altered to accomadate a neonates physiology. Key parameters include
% breathing rate, lung volume, compliance, resistance, heart rate, blood
% velocity, cardiac chamber sizes, etc.

% the following are global variables that are effected by shunting conditions
%
% SHUNT_1  SHUNT_2  SHUNT_3

% The following constants are used with the neonatal pulmonary model
%
% mouth compartment
R1 = 14.62;
C1 = 0.000013;
%R1 = 1.0;
%C1 = 0.001;
Q1U = 0.790;
Q1IC = 0.792;
invC1 = 1/C1;
invR1 = 1/R1;

% trachea compartment
R2 = 4.825;
C2 = 0.00004;
%R2 = 0.33;
%C2 = 0.002;
Q2U = 0.160;
Q2IC = 0.193;
invC2 = 1/C2;
invR2 = 1/R2;

% bronchi compartment
R3 = 4.385;
C3 = 0.00013;
%R3 = 0.3;
%C3 = 0.007;
Q3U = 0.350;
Q3IC = 0.494;
invC3 = 1/C3;
invR3 = 1/R3;
```

```
% alveoli compartment
R4 = 1.17;
C4 = 0.002;
%R4 = 0.08;
%C4 = 0.100;
Q4U = 7.87;
Q4IC = 10;
invC4 = 1/C4;
invR4 = 1/R4;

% The following constants are used with the pulmonary adult model
%
% mouth compartment
% R1 = 1.0;
% C1 = 0.0013;
% Q1U = 40;
% Q1IC = 40.325;
% invC1 = 1/C1;
% invR1 = 1/R1;

% trachea compartment
% R2 = 0.33;
% C2 = 0.004;
% Q2U = 8;
% Q2IC = 9.8;
% invC2 = 1/C2;
% invR2 = 1/R2;

% bronchi compartment
% R3 = 0.3;
% C3 = 0.013;
% Q3U = 18;
% Q3IC = 25;
% invC3 = 1/C3;
% invR3 = 1/R3;

% alveoli compartment
% R4 = 0.08;
% C4 = 0.2;
% Q4U = 400;
% Q4IC = 508;
% invC4 = 1/C4;
% invR4 = 1/R4;

%
% Rideout's concentration calculations for a 10 compartment model of the
% blood circulation system with three shunts - a pulmonary shunt between
% compartments DP1 and DP2 and two right to left shunts between compartments
% 7 and 3 and 0 and 4
%
% Note that the input and output flows, FP and FA are small compared to the total
% blood flow, FB, of the system. FB, for a neonate this is about 16.7 ml/s while the
```

```
% rate of O2 uptake for a 1.5 Kg neonate is about 0.25 ml/s.
%
% See Page 139-149 of his text and see Simulink program ridesim3.m for a schematic
%
% Compartment 0 => right ventrical (mixing)
% Compartment 1 => pulmonary artery (mixing)
% Compartment DP1 => pulmonary capillaries (delay)
% Compartment DP2 => pulmonary capillaries (delay)
% Compartment 2 => pulmonary vein (mixing)
% Compartment 3 => left ventrical (mixing)
% Compartment 4 => left aorta (mixing)
% Compartment 5 => systemic artery (mixing)
% Compartment 6 => systemic vein (mixing)
% Compartment 7 => right atrium (mixing)

% Compartment time constants - they should sum to about 9 seconds
% Dawson's book was used to calculate the volumes as a function of
% the percentages of adult values.
%

adult_circulation_time = 40.0;
neonate_circulation_time = 9.0;

% time constants are equal to volume/flow
%
% Volumes in ml.

global VOLUME_CHAMBER_0;
global VOLUME_CHAMBER_1;
global VOLUME_CHAMBER_2;
global VOLUME_CHAMBER_3;
global VOLUME_CHAMBER_4;
global VOLUME_CHAMBER_5;
global VOLUME_CHAMBER_6;
global VOLUME_CHAMBER_7;
global VOLUME_CHAMBER_PC_IN;
global VOLUME_CHAMBER_PC_OUT;

% neonate values calculated by pro-rating the time constants from adult
% values. From neonate time constants, Volume = T*FB

VOLUME_CHAMBER_0 = 4.68;
VOLUME_CHAMBER_1 = 9.39;
VOLUME_CHAMBER_2 = 4.68;
VOLUME_CHAMBER_PC_IN = 9.40;
VOLUME_CHAMBER_PC_OUT = 9.40;
VOLUME_CHAMBER_3 = 4.68;
VOLUME_CHAMBER_4 = 28.22;
VOLUME_CHAMBER_5 = 7.51;
VS1 = 15.03;
VS2 = 15.03;
VOLUME_CHAMBER_6 = 37.58;
```

```
VOLUME_CHAMBER_7 = 4.68;
VOLUME_CHAMBER_TISSUE = 30.06;  % tissue volume

% adult values
% VOLUME_CHAMBER_0 = 125;
% VOLUME_CHAMBER_1 = 250;
% VOLUME_CHAMBER_2 = 125;
% VOLUME_CHAMBER_PC_IN = 250;
% VOLUME_CHAMBER_PC_OUT = 250;
% VOLUME_CHAMBER_3 = 125;
% VOLUME_CHAMBER_4 = 750;
% VOLUME_CHAMBER_5 = 200;
% VS1 = 400;
% VS2 = 400;
% VOLUME_CHAMBER_6 = 1000;
% VOLUME_CHAMBER_7 = 125;
% VOLUME_CHAMBER_TISSUE = 800;  % tissue volume

% Input frequency
FREQ = 0.417 % neonate at 25 bpm
% FREQ = 0.60;  % neonate value 36 bpm
% FREQ = 0.23;  % adult value
PI = 3.1415927;
W = 2*PI*FREQ;
% Amplitude = 3600; % neonate pressure amplitude - too high]
% Amplitude = 3000; % neonate pressure amplitude
Amplitude = 2200; % neonate pressure amplitude - close but a bit low
%Amplitude = 800 % neonate pressure amplitude
%Amplitude = 1200; % adult pressure amplitude
Offset = -120;

% fractional neonatal O2 variables

Q1XIC = 0.137;
Q2XIC = 0.039;
Q3XIC = 0.090;
Q4XIC = 1.624;

% fractional adult O2 variables
%
% Q1XIC = 7;
% Q2XIC = 2.0;
% Q3XIC = 4.6;
% Q4XIC = 83;

FB = 16.7;      % blood flow in ml/sec.
%FB = 100;      % adult value
global MAXX;
MAXX = 0.224;  % max volume of O2 per litre of blood
%PVX = 40;     % pumonary venous O2 pressure, 8
%PVX = 45;
PVX = 35;
```

```
PATM=760;    % Atmospheric pressure in mmHg

% neonate  dissociation curve
PAO2 = [0.0, 1.1, 3.66, 12.8, 18.3, 27, 32, 37, 40.8,  48,  60, 300, 800];
SAO2 = [0.0, 3.0, 10,   33,   50,   70, 80, 85, 90,    95,  98, 100, 100];

% pulmcd3.m adult dissociation curve
% PAO2 = [0.0, 5.0, 10, 20, 30, 40, 50.0, 60, 80, 100, 150, 200,  300];
% SAO2 = [0.0, 3.0, 10, 33, 57, 74, 85.0, 94, 96.5,  98,  99, 99.5, 100];

% original adult dissociation curve
%PAO2 = [0.0, 5.0, 10, 20, 30, 40, 50.0, 60, 80, 90, 100, 150, 200,  300];
%SAO2 = [0.0, 3.0, 10, 33, 57, 74, 82.5, 89, 95, 96.5,  98,  99, 99.5, 100];

% Rideout's adult curve
%PAO2 = [0.0, 5.0, 10, 20, 30, 40, 50.0, 60, 80, 90, 100, 150, 200];
%SAO2 = [0.0, 3.0, 10, 33, 57, 74, 82.5, 89, 95, 96,  98,  99, 99.5];

%
% Shunts
% S1 represents percent of flow divided by 100% that goes from right atrium
%   to left atrium via the foramen ovale => 0.46 in unborn neonate
% S2 represents percent of flow divide by 100% that goes from right ventrical
%   to aorta via the ductus arteriosus => 0.75 in unborn neonate.
% S3 represents percent of flow divided by 100% that bypasses the lung or
%   goes through un-oxegenated capillaries.
%
% With the addition of shunts, the input flows to chambers change, and thus so
% does the time constant.
%
% Initial or baseline shunts
%

global SHUNT_1_BASELINE;
global SHUNT_2_BASELINE;
global SHUNT_3_BASELINE;
SHUNT_1_BASELINE = 0.0;
SHUNT_2_BASELINE = 0.0;
SHUNT_3_BASELINE = 0.1;

% times at which shunts change
%S3_start_1 = 200;
%S3_end_1   = 300;
%S3_shift_1 = 0.4;

global SHUNT_1;
global SHUNT_2;
global SHUNT_3;

SHUNT_1 = 0.0;
SHUNT_2 = 0.0;
SHUNT_3 = 0.1;
```

```
% Time constants are a function of input flow T = V/F
%

global FLOW_CHAMBER_0;
global FLOW_CHAMBER_1;
global FLOW_CHAMBER_1L;
global FLOW_CHAMBER_1S;
global FLOW_CHAMBER_2;
global FLOW_CHAMBER_3;
global FLOW_CHAMBER_4;
global FLOW_CHAMBER_5;
global FLOW_CHAMBER_6;
global FLOW_CHAMBER_7;
global FLOW_5_GAIN

FLOW_CHAMBER_4 = FB;
FLOW_CHAMBER_5 = FB;
FLOW_CHAMBER_6 = FB;
FLOW_CHAMBER_7 = FLOW_CHAMBER_6;
FLOW_CHAMBER_0 = (1-SHUNT_1)*FLOW_CHAMBER_7;
FLOW_CHAMBER_1 = (1-SHUNT_2)*FLOW_CHAMBER_0;
FLOW_CHAMBER_1L = (1-SHUNT_3)*FLOW_CHAMBER_1;
FLOW_CHAMBER_1S = SHUNT_3*FLOW_CHAMBER_1;
FLOW_CHAMBER_2 = FLOW_CHAMBER_1;
FLOW_CHAMBER_3 = FLOW_CHAMBER_2 + (SHUNT_1*FLOW_CHAMBER_7);
FLOW_CHAMBER_4 = FLOW_CHAMBER_3 + (SHUNT_2*FLOW_CHAMBER_0);
FLOW_5_GAIN = 0.01*MAXX*FLOW_CHAMBER_1L;

global TIME_DELAY_PC_IN;
global TIME_DELAY_PC_OUT;

TIME_DELAY_PC_IN = VOLUME_CHAMBER_PC_IN/FLOW_CHAMBER_1; % Pulmonary
capillary delay
TIME_DELAY_PC_OUT = VOLUME_CHAMBER_PC_OUT/FLOW_CHAMBER_1;
T0 = VOLUME_CHAMBER_0/FLOW_CHAMBER_0;
T1 = VOLUME_CHAMBER_1/FLOW_CHAMBER_1;
T2 = VOLUME_CHAMBER_2/FLOW_CHAMBER_2;
T3 = VOLUME_CHAMBER_3/FLOW_CHAMBER_3;
T4 = VOLUME_CHAMBER_4/FLOW_CHAMBER_4;
T5 = VOLUME_CHAMBER_5/FLOW_CHAMBER_5;
T6 = VOLUME_CHAMBER_6/FLOW_CHAMBER_6;
T7 = VOLUME_CHAMBER_7/FLOW_CHAMBER_7;
Tt = VOLUME_CHAMBER_TISSUE/FLOW_CHAMBER_5;

% invert for simulation
global TIME_CONSTANT_FC0i;
global TIME_CONSTANT_FC1i;
global TIME_CONSTANT_FC2i;
global TIME_CONSTANT_FC3i;
global TIME_CONSTANT_FC4i;
global TIME_CONSTANT_FC5i;
```

```
global TIME_CONSTANT_FC6i;
global TIME_CONSTANT_FC7i;
global TIME_CONSTANT_FCti;

TIME_CONSTANT_FC0i = 1/T0;
TIME_CONSTANT_FC1i = 1/T1;
TIME_CONSTANT_FC2i = 1/T2;
TIME_CONSTANT_FC3i = 1/T3;
TIME_CONSTANT_FC4i = 1/T4;
TIME_CONSTANT_FC5i = 1/T5;
TIME_CONSTANT_FC6i = 1/T6;
TIME_CONSTANT_FC7i = 1/T7;
TIME_CONSTANT_FCti = 1/Tt;

% Tissue compartment
% Oxygen uptake = 10 * B^0.75 (ml/min) where B is body weight in Kgm

%k20 = 24.4 % OK for 70 kg adult with 10% pulmonary shunt (S3)
% k20 = FB * 0.2436; % original value
k20 = FB * 0.10;
k20i = k20/VOLUME_CHAMBER_TISSUE
%Ptout = k20*PATM/FB;
```

Appendix B. Neonatal Model Supervisory Programs

```
function [sys, x0] = epm1_b1(t,x,u,flag)

% This S-function takes the time and makes changes to the system model by
% adjusting the neonates shunting values or adding motion artifact. The
% duration of the test is one hour (3600 seconds).

if abs(flag) == 1
  % return derivative
  sys = 1;
elseif abs(flag) == 3
  % return outputs
  if ( u == 50 )
    set_param('epm1/Neonate/circulation/S3_input','value', '0.20');
    set_param('epm1/Neonate/circulation/S2_input','value', '0.00');
    set_param('epm1/Neonate/circulation/S1_input','value', '0.00');
  end;
  if ( u == 200 )
    set_param('epm1/Pulse Oximeter/MA amplitude','gain', '-1.0');
  end;
  if (u == 230)
    set_param('epm1/Pulse Oximeter/MA amplitude','gain', '0.0');
  end;
  if (u == 360)
    set_param('epm1/Pulse Oximeter/MA amplitude','gain', '1.0');
  end;
  if (u == 420)
    set_param('epm1/Pulse Oximeter/MA amplitude','gain', '0.0');
  end;
  if ( u == 600 )
    set_param('epm1/Pulse Oximeter/MA amplitude','gain', '-1.0');
  end;
  if (u == 630)
    set_param('epm1/Pulse Oximeter/MA amplitude','gain', '2.0');
  end;
  if (u == 660)
    set_param('epm1/Pulse Oximeter/MA amplitude','gain', '0.0');
  end;
  if (u == 900)
    set_param('epm1/Pulse Oximeter/MA amplitude','gain', '2.0');
  end;
  if (u == 930)
    set_param('epm1/Pulse Oximeter/MA amplitude','gain', '-1.0');
  end;
  if (u == 960)
    set_param('epm1/Pulse Oximeter/MA amplitude','gain', '0.0');
  end;
  if (u == 1100)
    set_param('epm1/Neonate/circulation/S3_input','value', '0.30');
  end;

  if ( u == 1200 )
    set_param('epm1/Pulse Oximeter/MA amplitude','gain', '-1.0');
```

```
end;
if (u == 1260)
  set_param('epm1/Pulse Oximeter/MA amplitude','gain', '0.0');
end;
if (u == 1500)
  set_param('epm1/Pulse Oximeter/MA amplitude','gain', '1.0');
end;
if (u == 1560)
  set_param('epm1/Pulse Oximeter/MA amplitude','gain', '0.0');
end;
if ( u == 1800 )
  set_param('epm1/Pulse Oximeter/MA amplitude','gain', '-1.0');
end;
if (u == 1830)
  set_param('epm1/Pulse Oximeter/MA amplitude','gain', '2.0');
end;
if (u == 1860)
  set_param('epm1/Pulse Oximeter/MA amplitude','gain', '0.0');
end;

if (u == 2100)
  set_param('epm1/Pulse Oximeter/MA amplitude','gain', '2.0');
end;
if (u == 2130)
  set_param('epm1/Pulse Oximeter/MA amplitude','gain', '-1.0');
end;
if (u == 2160)
  set_param('epm1/Pulse Oximeter/MA amplitude','gain', '0.0');
end;
if (u == 2300)
  set_param('epm1/Neonate/circulation/S3_input','value', '0.40');
end;

if ( u == 2400 )
  set_param('epm1/Pulse Oximeter/MA amplitude','gain', '-1.0');
end;
if (u == 2460)
  set_param('epm1/Pulse Oximeter/MA amplitude','gain', '0.0');
end;
if (u == 2700)
  set_param('epm1/Pulse Oximeter/MA amplitude','gain', '1.0');
end;
if (u == 2760)
  set_param('epm1/Pulse Oximeter/MA amplitude','gain', '0.0');
end;
if ( u == 3000 )
  set_param('epm1/Pulse Oximeter/MA amplitude','gain', '-1.0');
end;
if (u == 3030)
  set_param('epm1/Pulse Oximeter/MA amplitude','gain', '2.0');
end;
if (u == 3060)
```

```
    set_param('epm1/Pulse Oximeter/MA amplitude','gain', '0.0');
   end;

   if (u == 3300)
    set_param('epm1/Pulse Oximeter/MA amplitude','gain', '2.0');
   end;
   if (u == 3330)
    set_param('epm1/Pulse Oximeter/MA amplitude','gain', '-1.0');
   end;
   if (u == 3360)
    set_param('epm1/Pulse Oximeter/MA amplitude','gain', '0.0');
   end;

  sys = u;
elseif flag == 0
  % return sizes and initial values
  sys = [1,0,1,1,0,1];
  x0 = 0.1;
else
  sys = [];
end
```

```
function [sys, x0] = epm1_b2(t,x,u,flag)

% This S-function takes the time and makes changes to the system model by
% adjusting the neonates shunting values or adding motion artifact. The
% duration of the test is one hour (3600 seconds).

if abs(flag) == 1
  % return derivative
  sys = 1;
elseif abs(flag) == 3
  % return outputs
  if ( u == 50 )
    set_param('epm1/Neonate/circulation/S3_input','value', '0.30');
    set_param('epm1/Neonate/circulation/S2_input','value', '0.05');
    set_param('epm1/Neonate/circulation/S1_input','value', '0.00');
  end;
  if ( u == 200 )
    set_param('epm1/Neonate/circulation/S3_input','value', '0.10');
  end;
  if ( u == 260 )
    set_param('epm1/Neonate/circulation/S3_input','value', '0.30');
  end;
  if ( u == 380 )
    set_param('epm1/Neonate/circulation/S2_input','value', '0.20');
  end;
  if ( u == 440 )
    set_param('epm1/Neonate/circulation/S2_input','value', '0.05');
  end;
  if ( u == 560 )
    set_param('epm1/Neonate/circulation/S2_input','value', '0.20');
  end;
  if ( u == 590 )
    set_param('epm1/Neonate/circulation/S2_input','value', '0.05');
  end;
  if ( u == 620 )
    set_param('epm1/Neonate/circulation/S2_input','value', '0.20');
  end;
  if ( u == 680 )
    set_param('epm1/Neonate/circulation/S2_input','value', '0.05');
  end;
  if ( u == 710 )
    set_param('epm1/Neonate/circulation/S2_input','value', '0.20');
  end;
  if ( u == 770 )
    set_param('epm1/Neonate/circulation/S2_input','value', '0.05');
  end;
  if ( u == 830 )
    set_param('epm1/Neonate/circulation/S2_input','value', '0.20');
  end;
  if ( u == 860 )
    set_param('epm1/Neonate/circulation/S2_input','value', '0.05');
  end;
```

```
if ( u == 1000 )
  set_param('epm1/Pulse Oximeter/MA amplitude','gain', '-1.0');
  set_param('epm1/Neonate/circulation/S2_input','value', '0.20');
end;
if (u == 1060)
  set_param('epm1/Pulse Oximeter/MA amplitude','gain', '0.0');
end;
if (u == 1460)
  set_param('epm1/Pulse Oximeter/MA amplitude','gain', '-1.0');
end;
if (u == 1520)
  set_param('epm1/Pulse Oximeter/MA amplitude','gain', '0.0');
end;
if (u == 1700)
  set_param('epm1/Pulse Oximeter/MA amplitude','gain', '1.0');
end;
if (u == 1790)
  set_param('epm1/Pulse Oximeter/MA amplitude','gain', '0.0');
end;
if ( u == 2000 )
  set_param('epm1/Pulse Oximeter/MA amplitude','gain', '1.0');
  set_param('epm1/Neonate/circulation/S3_input','value', '0.10');
end;
if (u == 2030)
  set_param('epm1/Pulse Oximeter/MA amplitude','gain', '0.0');
end;
if (u == 2150)
  set_param('epm1/Pulse Oximeter/MA amplitude','gain', '-1.0');
  set_param('epm1/Neonate/circulation/S3_input','value', '0.30');
end;
if (u == 2180)
  set_param('epm1/Pulse Oximeter/MA amplitude','gain', '0.0');
end;
if ( u == 2360 )
  set_param('epm1/Neonate/circulation/S2_input','value', '0.05');
end;


if (u == 2540)
  set_param('epm1/Pulse Oximeter/MA amplitude','gain', '1.0');
  set_param('epm1/Neonate/circulation/S3_input','value', '0.10');
end;
if (u == 2600)
  set_param('epm1/Pulse Oximeter/MA amplitude','gain', '0.0');
end;
if (u == 2720)
  set_param('epm1/Neonate/circulation/S3_input','value', '0.30');
  set_param('epm1/Neonate/circulation/S2_input','value', '0.20');
end;
if (u == 2960)
  set_param('epm1/Pulse Oximeter/MA amplitude','gain', '-1.0');
```

```
  end;
  if (u == 3000)
    set_param('epm1/Pulse Oximeter/MA amplitude','gain', '0.0');
  end;
  if (u == 3180)
    set_param('epm1/Pulse Oximeter/MA amplitude','gain', '1.0');
  end;
  if (u == 3210)
    set_param('epm1/Pulse Oximeter/MA amplitude','gain', '0.0');
  end;
  if (u == 3390)
    set_param('epm1/Neonate/circulation/S2_input','value', '0.05');
  end;
  if (u == 3420)
    set_param('epm1/Neonate/circulation/S2_input','value', '0.20');
  end;
  if (u == 3450)
    set_param('epm1/Neonate/circulation/S2_input','value', '0.05');
  end;
  if (u == 3480)
    set_param('epm1/Neonate/circulation/S2_input','value', '0.20');
  end;
  if (u == 3510)
    set_param('epm1/Neonate/circulation/S2_input','value', '0.05');
  end;
  if (u == 3540)
    set_param('epm1/Neonate/circulation/S2_input','value', '0.20');
  end;

  sys = u;
elseif flag == 0
  % return sizes and initial values
  sys = [1,0,1,1,0,1];
  x0 = 0.1;
else
  sys = [];
end
```

```
function [sys, x0] = epm1_b3(t,x,u,flag)

% This S-function takes the time and makes changes to the system model by
% adjusting the neonates shunting values or adding motion artifact. The
% duration of the test is one hour (3600 seconds).
global CONTROL_MODE;

if abs(flag) == 1
  % return derivative
  sys = 1;
elseif abs(flag) == 3
  % return outputs
  if ( u == 1 )
    set_param('epm1/Neonate/respiration/alveoli O2/DC','Input_Values', 'PAO2', 'Output_Values','SAO2');
  end;
  if ( u == 50 )
    set_param('epm1/Neonate/circulation/S3_input','value', '0.20');
    set_param('epm1/Neonate/circulation/S2_input','value', '0.10');
    set_param('epm1/Neonate/circulation/S1_input','value', '0.00');
  end;
  if ( u == 200 )
    set_param('epm1/Neonate/circulation/S2_input','value', '0.30');
  end;
  if ( u == 230 )
    set_param('epm1/Neonate/circulation/S2_input','value', '0.10');
  end;
  if ( u == 260 )
    set_param('epm1/Neonate/circulation/S2_input','value', '0.30');
  end;
  if ( u == 290 )
    set_param('epm1/Neonate/circulation/S2_input','value', '0.10');
  end;
  if ( u == 310 )
    set_param('epm1/Neonate/circulation/S2_input','value', '0.30');
  end;
  if ( u == 340 )
    set_param('epm1/Neonate/circulation/S2_input','value', '0.10');
  end;
  if ( u == 370 )
    set_param('epm1/Neonate/circulation/S2_input','value', '0.30');
  end;
  if ( u == 400 )
    set_param('epm1/Neonate/circulation/S2_input','value', '0.10');
  end;
  if ( u == 430 )
    set_param('epm1/Neonate/circulation/S2_input','value', '0.30');
  end;

  if ( u == 460 )
    set_param('epm1/Neonate/circulation/S2_input','value', '0.10');
  end;
  if ( u == 520 )
```

```
  set_param('epm1/Neonate/circulation/S2_input','value', '0.30');
 end;
 if ( u == 580 )
  set_param('epm1/Neonate/circulation/S2_input','value', '0.10');
 end;
 if ( u == 640 )
  set_param('epm1/Neonate/circulation/S2_input','value', '0.30');
 end;
 if ( u == 700 )
  set_param('epm1/Neonate/circulation/S2_input','value', '0.10');
 end;
 if ( u == 760 )
  set_param('epm1/Neonate/circulation/S2_input','value', '0.30');
 end;
 if ( u == 820 )
  set_param('epm1/Neonate/circulation/S2_input','value', '0.10');
 end;
 if ( u == 880 )
  set_param('epm1/Neonate/circulation/S2_input','value', '0.30');
 end;
 if ( u == 940 )
  set_param('epm1/Neonate/circulation/S2_input','value', '0.10');
 end;

 if ( u == 1075 )
  set_param('epm1/Neonate/circulation/S2_input','value', '0.30');
 end;
 if ( u == 1090)
  set_param('epm1/Neonate/circulation/S2_input','value', '0.10');
 end;
 if ( u == 1105 )
  set_param('epm1/Neonate/circulation/S2_input','value', '0.30');
 end;
 if ( u == 1120)
  set_param('epm1/Neonate/circulation/S2_input','value', '0.10');
 end;
 if ( u == 1135 )
  set_param('epm1/Neonate/circulation/S2_input','value', '0.30');
 end;
 if ( u == 1150)
  set_param('epm1/Neonate/circulation/S2_input','value', '0.10');
 end;
 if ( u == 1165 )
  set_param('epm1/Neonate/circulation/S2_input','value', '0.30');
 end;
 if ( u == 1180)
  set_param('epm1/Neonate/circulation/S2_input','value', '0.10');
 end;
 if ( u == 1195 )
  set_param('epm1/Neonate/circulation/S2_input','value', '0.30');
 end;
 if ( u == 1210)
```

```
    set_param('epm1/Neonate/circulation/S2_input','value', '0.10');
   end;
   if ( u == 1225 )
    set_param('epm1/Neonate/circulation/S2_input','value', '0.30');
   end;
   if ( u == 1240)
    set_param('epm1/Neonate/circulation/S2_input','value', '0.10');
   end;
   if ( u == 1300 )
    set_param('epm1/Neonate/circulation/S2_input','value', '0.30');
   end;
   if ( u == 1360 )
    set_param('epm1/Neonate/circulation/S3_input','value', '0.05');
   end;
   if ( u == 1420 )
    set_param('epm1/Neonate/circulation/S3_input','value', '0.20');
   end;
   if ( u == 1540 )
    set_param('epm1/Neonate/circulation/S2_input','value', '0.10');
   end;
   if ( u == 1600 )
    set_param('epm1/Pulse Oximeter/MA amplitude','gain', '1.0');
   end;
   if (u == 1660)
    set_param('epm1/Pulse Oximeter/MA amplitude','gain', '0.0');
   end;
   if (u == 1720)
    set_param('epm1/Pulse Oximeter/MA amplitude','gain', '-1.0');
   end;
   if (u == 1800)
    set_param('epm1/Pulse Oximeter/MA amplitude','gain', '0.0');
    set_param('epm1/Neonate/respiration/alveoli O2/DC','Input_Values', 'PAO2a',
'Output_Values','SAO2a');
   end;

   if ( u == 2000 )
    set_param('epm1/Neonate/circulation/S2_input','value', '0.30');
   end;
   if ( u == 2030 )
    set_param('epm1/Neonate/circulation/S2_input','value', '0.10');
   end;
   if ( u == 2060 )
    set_param('epm1/Neonate/circulation/S2_input','value', '0.30');
   end;
   if ( u == 2090 )
    set_param('epm1/Neonate/circulation/S2_input','value', '0.10');
   end;
   if ( u == 2110 )
    set_param('epm1/Neonate/circulation/S2_input','value', '0.30');
   end;
   if ( u == 2140 )
    set_param('epm1/Neonate/circulation/S2_input','value', '0.10');
```

```
end;
if ( u == 2170 )
  set_param('epm1/Neonate/circulation/S2_input','value', '0.30');
end;
if ( u == 2200 )
  set_param('epm1/Neonate/circulation/S2_input','value', '0.10');
  set_param('epm1/FiO2','value','0.35');
end;
if ( u == 2230 )
  set_param('epm1/Neonate/circulation/S2_input','value', '0.30');
end;

if ( u == 2260 )
  set_param('epm1/Neonate/circulation/S2_input','value', '0.10');
end;
if ( u == 2320 )
  set_param('epm1/Neonate/circulation/S2_input','value', '0.30');
end;
if ( u == 2380 )
  set_param('epm1/Neonate/circulation/S2_input','value', '0.10');
end;
if ( u == 2440 )
  set_param('epm1/Neonate/circulation/S2_input','value', '0.30');
end;
if ( u == 2500 )
  set_param('epm1/Neonate/circulation/S2_input','value', '0.10');
end;
if ( u == 2560 )
  set_param('epm1/Neonate/circulation/S2_input','value', '0.30');
end;
if ( u == 2620 )
  set_param('epm1/Neonate/circulation/S2_input','value', '0.10');
end;
if ( u == 2680 )
  set_param('epm1/Neonate/circulation/S2_input','value', '0.30');
end;
if ( u == 2740 )
  set_param('epm1/Neonate/circulation/S2_input','value', '0.10');
end;

if ( u == 2875 )
  set_param('epm1/Neonate/circulation/S2_input','value', '0.30');
end;
if ( u == 2890)
  set_param('epm1/Neonate/circulation/S2_input','value', '0.10');
end;
if ( u == 2905 )
  set_param('epm1/Neonate/circulation/S2_input','value', '0.30');
end;
if ( u == 2920)
  set_param('epm1/Neonate/circulation/S2_input','value', '0.10');
end;
```

```
    if ( u == 2935 )
     set_param('epm1/Neonate/circulation/S2_input','value', '0.30');
    end;
    if ( u == 2950)
     set_param('epm1/Neonate/circulation/S2_input','value', '0.10');
    end;
    if ( u == 2965 )
     set_param('epm1/Neonate/circulation/S2_input','value', '0.30');
    end;
    if ( u == 2980)
     set_param('epm1/Neonate/circulation/S2_input','value', '0.10');
    end;
    if ( u == 2995 )
     set_param('epm1/Neonate/circulation/S2_input','value', '0.30');
    end;
    if ( u == 3010)
     set_param('epm1/Neonate/circulation/S2_input','value', '0.10');
    end;
    if ( u == 3025 )
     set_param('epm1/Neonate/circulation/S2_input','value', '0.30');
    end;
    if ( u == 3040)
     set_param('epm1/Neonate/circulation/S2_input','value', '0.10');
    end;
    if ( u == 3100 )
     set_param('epm1/Neonate/circulation/S2_input','value', '0.30');
    end;
    if ( u == 3160 )
     set_param('epm1/Neonate/circulation/S3_input','value', '0.05');
    end;
    if ( u == 3220 )
     set_param('epm1/Neonate/circulation/S3_input','value', '0.20');
    end;
    if ( u == 3340 )
     set_param('epm1/Neonate/circulation/S2_input','value', '0.10');
    end;
    if ( u == 3400 )
     set_param('epm1/Pulse Oximeter/MA amplitude','gain', '1.0');
    end;
    if (u == 3460)
     set_param('epm1/Pulse Oximeter/MA amplitude','gain', '0.0');
    end;

   sys = u;
elseif flag == 0
   % return sizes and initial values
   sys = [1,0,1,1,0,1];
   x0 = 0.1;
else
   sys = [];
end
```

Appendix C. Closed Loop Initialisation Program

```
% Initepm1.m - epm1.m initialization program
% Sept. 24, 1996
% run this m-file before running the simulink program
%
% This model is built from two sub-systems, the first is the pulmonary model and
% is based on the pulm1.m file. The second is the blood circuation system. It is
% different from earlier versions in that this model uses the SvO2
% value in its control loop. It also uses a default 10% shunt across the lungs to
% represent the pressure drop there. With the O2 consumption set at about 20%
% we get SaO2 = 96% and SvO2 = 77%
%
% "epm1.m" is a model consisting of the blender, neonate and pulse oximeter
% models extracted from files "bend1.m", "nn1a.m" and "pulse1.m".

% the following are global variables that are effected by shunting conditions
%
% SHUNT_1  SHUNT_2  SHUNT_3

% The following constants are used with the neonatal pulmonary model
%
% mouth compartment
R1 = 14.62;
C1 = 0.000013;
%R1 = 1.0;
%C1 = 0.001;
Q1U = 0.790;
Q1IC = 0.792;
invC1 = 1/C1;
invR1 = 1/R1;

% trachea compartment
R2 = 4.825;
C2 = 0.00004;
%R2 = 0.33;
%C2 = 0.002;
Q2U = 0.160;
Q2IC = 0.193;
invC2 = 1/C2;
invR2 = 1/R2;

% bronchi compartment
R3 = 4.385;
C3 = 0.00013;
%R3 = 0.3;
%C3 = 0.007;
Q3U = 0.350;
Q3IC = 0.494;
invC3 = 1/C3;
invR3 = 1/R3;

% alveoli compartment
R4 = 1.17;
```

```
C4 = 0.002;
%R4 = 0.08;
%C4 = 0.100;
Q4U = 7.87;
Q4IC = 10;
invC4 = 1/C4;
invR4 = 1/R4;

% The following constants are used with the pulmonary adult model
%
% mouth compartment
% R1 = 1.0;
% C1 = 0.0013;
% Q1U = 40;
% Q1IC = 40.325;
% invC1 = 1/C1;
% invR1 = 1/R1;

% trachea compartment
% R2 = 0.33;
% C2 = 0.004;
% Q2U = 8;
% Q2IC = 9.8;
% invC2 = 1/C2;
% invR2 = 1/R2;

% bronchi compartment
% R3 = 0.3;
% C3 = 0.013;
% Q3U = 18;
% Q3IC = 25;
% invC3 = 1/C3;
% invR3 = 1/R3;

% alveoli compartment
% R4 = 0.08;
% C4 = 0.2;
% Q4U = 400;
% Q4IC = 508;
% invC4 = 1/C4;
% invR4 = 1/R4;

%
% Rideout's concentration calculations for a 10 compartment model of the
% blood circulation system with three shunts - a pulmonary shunt between
% compartments DP1 and DP2 and two right to left shunts between compartments
% 7 and 3 and 0 and 4
%
% Note that the input and output flows, FP and FA are small compared to the total
% blood flow, FB, of the system. FB, for a neonate this is about 16.7 ml/s while the
% rate of O2 uptake for a 1.5 Kg neonate is about 0.25 ml/s.
%
```

```
% See Page 139-149 of his text and see Simulink program ridesim3.m for a schematic
%
% Compartment 0 => right ventrical (mixing)
% Compartment 1 => pulmonary artery (mixing)
% Compartment DP1 => pulmonary capillaries (delay)
% Compartment DP2 => pulmonary capillaries (delay)
% Compartment 2 => pulmonary vein (mixing)
% Compartment 3 => left ventrical (mixing)
% Compartment 4 => left aorta (mixing)
% Compartment 5 => systemic artery (mixing)
% Compartment 6 => systemic vein (mixing)
% Compartment 7 => right atrium (mixing)

% Compartment time constants - they should sum to about 9 seconds
% Dawson's book was used to calculate the volumes as a function of
% the percentages of adult values.
%

adult_circulation_time = 40.0;
neonate_circulation_time = 9.0;

% time constants are equal to volume/flow
%
% Volumes in ml.

global VOLUME_CHAMBER_0;
global VOLUME_CHAMBER_1;
global VOLUME_CHAMBER_2;
global VOLUME_CHAMBER_3;
global VOLUME_CHAMBER_4;
global VOLUME_CHAMBER_5;
global VOLUME_CHAMBER_6;
global VOLUME_CHAMBER_7;
global VOLUME_CHAMBER_PC_IN;
global VOLUME_CHAMBER_PC_OUT;

% neonate values calculated by pro-rating the time constants from adult
% values. From neonate time constants, Volume = T*FB

VOLUME_CHAMBER_0 = 4.68;
VOLUME_CHAMBER_1 = 9.39;
VOLUME_CHAMBER_2 = 4.68;
VOLUME_CHAMBER_PC_IN = 9.40;
VOLUME_CHAMBER_PC_OUT = 9.40;
VOLUME_CHAMBER_3 = 4.68;
VOLUME_CHAMBER_4 = 28.22;
VOLUME_CHAMBER_5 = 7.51;
VS1 = 15.03;
VS2 = 15.03;
VOLUME_CHAMBER_6 = 37.58;
VOLUME_CHAMBER_7 = 4.68;
VOLUME_CHAMBER_TISSUE = 30.06;  % tissue volume
```

```
% adult values
% VOLUME_CHAMBER_0 = 125;
% VOLUME_CHAMBER_1 = 250;
% VOLUME_CHAMBER_2 = 125;
% VOLUME_CHAMBER_PC_IN = 250;
% VOLUME_CHAMBER_PC_OUT = 250;
% VOLUME_CHAMBER_3 = 125;
% VOLUME_CHAMBER_4 = 750;
% VOLUME_CHAMBER_5 = 200;
% VS1 = 400;
% VS2 = 400;
% VOLUME_CHAMBER_6 = 1000;
% VOLUME_CHAMBER_7 = 125;
% VOLUME_CHAMBER_TISSUE = 800;  % tissue volume

% Input frequency
FREQ = 0.417 % neonate at 25 bpm
% FREQ = 0.60;  % neonate value 36 bpm
% FREQ = 0.23;  % adult value
PI = 3.1415927;
W = 2*PI*FREQ;
% Amplitude = 3600; % neonate pressure amplitude - too high]
% Amplitude = 3000; % neonate pressure amplitude
% Amplitude = 2200; % neonate pressure amplitude - close but a bit low
Amplitude = 1200; % emulate an ill neonate with FiO2 = 30% +/-
%Amplitude = 800 % neonate pressure amplitude
%Amplitude = 1200; % adult pressure amplitude
Offset = -120;

% fractional neonatal O2 variables

Q1XIC = 0.137;
Q2XIC = 0.039;
Q3XIC = 0.090;
Q4XIC = 1.624;

% fractional adult O2 variables
%
% Q1XIC = 7;
% Q2XIC = 2.0;
% Q3XIC = 4.6;
% Q4XIC = 83;

FB = 16.7;      % blood flow in ml/sec.
%FB = 100;      % adult value
global MAXX;
MAXX = 0.224;  % max volume of O2 per litre of blood
%PVX = 40;      % pumonary venous O2 pressure, 8
%PVX = 45;
PVX = 35;
%SvO2X = 82;    % used at start-up to remove transient
```

```
SvO2X = 86;
PATM = 760;    % Atmospheric pressure in mmHg

% neonate  dissociation curve
PAO2 = [0.0, 1.1, 3.66, 12.8, 18.3, 27, 32, 37, 40.8,  48,  60, 200,  300, 800];
SAO2 = [0.0, 3.0, 10,   33,   50,   70, 80, 85, 90,    95,  98, 99.5, 100, 100];

% pulmcd3.m adult dissociation curve
PAO2a = [0.0, 5.0, 10, 20, 30, 40, 50.0, 60, 80, 100, 150, 200,  300, 800];
SAO2a = [0.0, 3.0, 10, 33, 57, 74, 85.0, 94, 96.5,  98,  99, 99.5, 100, 100];

% original adult dissociation curve
%PAO2 = [0.0, 5.0, 10, 20, 30, 40, 50.0, 60, 80, 90, 100, 150, 200,  300];
%SAO2 = [0.0, 3.0, 10, 33, 57, 74, 82.5, 89, 95, 96.5,  98,  99, 99.5, 100];

% Rideout's adult curve
%PAO2 = [0.0, 5.0, 10, 20, 30, 40, 50.0, 60, 80, 90, 100, 150, 200];
%SAO2 = [0.0, 3.0, 10, 33, 57, 74, 82.5, 89, 95, 96,  98,  99, 99.5];

%
% Shunts
% S1 represents percent of flow divided by 100% that goes from right atrium
%    to left atrium via the foramen ovale => 0.46 in unborn neonate
% S2 represents percent of flow divide by 100% that goes from right ventrical
%    to aorta via the ductus arteriosus => 0.75 in unborn neonate.
% S3 represents percent of flow divided by 100% that bypasses the lung or
%    goes through un-oxegenated capillaries.
%
% With the addition of shunts, the input flows to chambers change, and thus so
% does the time constant.
%
% Initial or baseline shunts
%

global SHUNT_1_BASELINE;
global SHUNT_2_BASELINE;
global SHUNT_3_BASELINE;
SHUNT_1_BASELINE = 0.0;
SHUNT_2_BASELINE = 0.0;
SHUNT_3_BASELINE = 0.1;

global SHUNT_1;
global SHUNT_2;
global SHUNT_3;

SHUNT_1 = 0.0;
SHUNT_2 = 0.0;
SHUNT_3 = 0.1;

% Time constants are a function of input flow T = V/F
%
```

```
global FLOW_CHAMBER_0;
global FLOW_CHAMBER_1;
global FLOW_CHAMBER_1L;
global FLOW_CHAMBER_1S;
global FLOW_CHAMBER_2;
global FLOW_CHAMBER_3;
global FLOW_CHAMBER_4;
global FLOW_CHAMBER_5;
global FLOW_CHAMBER_6;
global FLOW_CHAMBER_7;
global FLOW_5_GAIN

FLOW_CHAMBER_4 = FB;
FLOW_CHAMBER_5 = FB;
FLOW_CHAMBER_6 = FB;
FLOW_CHAMBER_7 = FLOW_CHAMBER_6;
FLOW_CHAMBER_0 = (1-SHUNT_1)*FLOW_CHAMBER_7;
FLOW_CHAMBER_1 = (1-SHUNT_2)*FLOW_CHAMBER_0;
FLOW_CHAMBER_1L = (1-SHUNT_3)*FLOW_CHAMBER_1;
FLOW_CHAMBER_1S = SHUNT_3*FLOW_CHAMBER_1;
FLOW_CHAMBER_2 = FLOW_CHAMBER_1;
FLOW_CHAMBER_3 = FLOW_CHAMBER_2 + (SHUNT_1*FLOW_CHAMBER_7);
FLOW_CHAMBER_4 = FLOW_CHAMBER_3 + (SHUNT_2*FLOW_CHAMBER_0);
FLOW_5_GAIN = 0.01*MAXX*FLOW_CHAMBER_1L;

global TIME_DELAY_PC_IN;
global TIME_DELAY_PC_OUT;

TIME_DELAY_PC_IN = VOLUME_CHAMBER_PC_IN/FLOW_CHAMBER_1; % Pulmonary
capillary delay
TIME_DELAY_PC_OUT = VOLUME_CHAMBER_PC_OUT/FLOW_CHAMBER_1;
T0 = VOLUME_CHAMBER_0/FLOW_CHAMBER_0;
T1 = VOLUME_CHAMBER_1/FLOW_CHAMBER_1;
T2 = VOLUME_CHAMBER_2/FLOW_CHAMBER_2;
T3 = VOLUME_CHAMBER_3/FLOW_CHAMBER_3;
T4 = VOLUME_CHAMBER_4/FLOW_CHAMBER_4;
T5 = VOLUME_CHAMBER_5/FLOW_CHAMBER_5;
T6 = VOLUME_CHAMBER_6/FLOW_CHAMBER_6;
T7 = VOLUME_CHAMBER_7/FLOW_CHAMBER_7;
Tt = VOLUME_CHAMBER_TISSUE/FLOW_CHAMBER_5;

% invert for simulation
global TIME_CONSTANT_FC0i;
global TIME_CONSTANT_FC1i;
global TIME_CONSTANT_FC2i;
global TIME_CONSTANT_FC3i;
global TIME_CONSTANT_FC4i;
global TIME_CONSTANT_FC5i;
global TIME_CONSTANT_FC6i;
global TIME_CONSTANT_FC7i;
global TIME_CONSTANT_FCti;
```

```
TIME_CONSTANT_FC0i = 1/T0;
TIME_CONSTANT_FC1i = 1/T1;
TIME_CONSTANT_FC2i = 1/T2;
TIME_CONSTANT_FC3i = 1/T3;
TIME_CONSTANT_FC4i = 1/T4;
TIME_CONSTANT_FC5i = 1/T5;
TIME_CONSTANT_FC6i = 1/T6;
TIME_CONSTANT_FC7i = 1/T7;
TIME_CONSTANT_FCti = 1/Tt;

% Tissue compartment
% k20 = 24.4 % OK for 70 kg adult with 10% pulmonary shunt (S3)
% k20 = FB * 0.2436; % original value
k20 = FB * 0.10;
k20i = k20/VOLUME_CHAMBER_TISSUE

% for histograms
xbin = [80,81,82,83,84,85,86,87,88,89,90,91,92,93,94,95,96,97,98,99,100];

% for types of control 1 = manual, 0 = none, PID or Fuzzy
global CONTROL_MODE;
CONTROL_MODE = 0;

set_param('epm1/Neonate/circulation/S1_input','value','0.05');
set_param('epm1/Neonate/circulation/S2_input','value','0.05');
set_param('epm1/Neonate/circulation/S3_input','value','0.20');
%set_param('epm1/Neonate/circulation/S1_input','value','0.0');
%set_param('epm1/Neonate/circulation/S2_input','value','0.0');
%set_param('epm1/Neonate/circulation/S3_input','value','0.10');
set_param('epm1/FiO2','value','30');
set_param('epm1/Neonate/respiration/alveoli O2/DC','Input_Values','PAO2','Output_Values','SAO2');
set_param('epm1/Pulse Oximeter/MA amplitude','gain','0.0')
```

LIST OF REFERENCES

American Academy of Pediatrics and American College of Ostetricians and Gynocologists. *Guidelines for Perinatal Care*, 3rd. ed., 1992.

American Academy of Pediatrics and American College of Ostetricians and Gynocologists. *Guidelines for Perinatal Care*, 2nd. ed., 1983.

Association for the Advancement of Medical Instrumentation, 29th Annual Meeting & Exposition, Washington DC, 1993.

Avery ME, Taeusch HW Jr. (eds.). *Schaffer's Diseases of the Newborn*, Toronto: WB Saunders Co., pp. 110-119, 1984.

Bancalari E, Abdenour GE, Feller R, Gannon J."Bronchopulmonary Dysplasia: Clinical presentaion," *Journal Pediatrics*, 95: p.819, 1979.

Bancalari E, Flynn J, Goldberg RN, Bawol R, Cassady J, Schiffman J, Feuer W, Roberts J,Gillings D, Sim E."Influence of transcutaneous oxygen monitoring on the incidence of retnopathy of prematurity," *Pediatrics*, 79: pp.663-669, 1987.

Bard H, Teasdale F. "Red cell affinity, hemoglobin type, 2,3-diphosphoglycerate, and pH as a function of fetal development" *Pedeatrics*, 64: pp.483-487, 1979.

Beddis IR, Collins P, Levy NM, Godfrey S, Silverman."New technique for servocontrol of arterial oxygen tension in preterm infants," *Arch Dis Child*, 54: pp.278-280, 1979.

Bucher H, Franconi S, Baeckert P, Duc G. "Hyperoxemia in newborn infants: detection by pulse oximetry," *Pediatrics*, 2: pp.226-230,1989.

Cook CD, Sutherland JM, Segal S, Cherry RB, Mead J, McIlroy MC and Smith CA. "Studies of respiratory physiology in the newborn infant III. Measurements of the mechanics of respiration," *J. Clin. Investig.* 36: p.440, 1957.

Cook CD, Helliesen PJ and Agathon S. "Relation between mechanics of respiration, lung size and body size from birth to young adulthood," J.Appl. Physiol. 13(3): pp. 349-352, 1958.

Dawson TH. Engineering Design of the Cardiovascular System of Mammals. Prentice Hall, Inc., New Jersey, 1991.

Defares JG, Derksen HE and Duyff JW. "Cerebral blood flow in the regulation of respiration," *Acta Physiol. Parmacol. Neerl.*, 9: pp. 327-360, 1960.

Delivoria-Papadopoulos M, Roncevic NP and Oski FA. "Postnatal changes in oxygen transport of term, premature, and sick infants. The role of red cell 2,3-diphospoglycerate and adult hemoglobin," *Ped. Res.* 5: p.235, 1971.

Driankov D, Hellendoorn H and Reinfrank M. An Introduction to Fuzzy Control. Springer-Verlag, Santa Clara, 1996.

Dudell G, Cornish JD, Bartlett RH."What constitutes adequate oxygenation?," *Pediatrics*, 85(1): pp.39-41, 1990.

Durbin GM. "Reasons for monitoring arterial oxygen in the neonate" *Oxygen Measurements in Biology and Medicine*, Toronto: Butterworth & Co., pp.259-268, 1975.

Emond D, Lachance C, Gagnon J, Bard H. "Arterial partial pressure of oxygen required to achieve 90% saturation of hemoglobin in very low birth weight newborns," *Pediatrics*, 91(3): pp.602-604, 1993.

Fanaroff AA, Martin RJ, Merkatz IR, eds. *Behrman's Neonatal-Perinatal Medicine: Diseases of the Fetus and Infant.* Toronto:The C.V.Mosby Co., 1983.

Ferrara TB, Hoekstra RE, Couser RJ, Gaziano EP, Calvin SE, Payne NR, Fangman JJ. "Survival and follow-up of infants born at 23 to 26 weeks of gestational age: Effects of surfactant therapy", *Journal Pediatr*, 124: pp.119-124, 1994.

Flynn JT, Bancalari E, Snyder ES, Goldberg RN, Feuer W, Cassady J, Schiffman J, Feldman HI, Bachynski B, Buckley E, Roberts J and Gillings D, "A cohort study of transcutaneous oxygen tension and the incidence and severity of retinopathy of prematurity," *New England Journal of Medicine*, 326: pp. 1050-1054, 1992.

Freed MD. "Cardiac Dysrythmias", *Schaffer's Diseases of the Newborn*, eds. M.E.Avery and H.W.Taeusch, Toronto:WB Saunders Co., pp. 304-308, 1984.

Gibson DL, Sheps SB, Uh SH, Schechter MT, McCormic AQ."Retnopathy of prematurity-induced blindness: birth weight-specific survival and the new epidemic," *Pediatrics*, 86(3): pp.405-412, 1990.

Gray JS. "The multiple factor theory of the control of respiratory ventilation," *Science*, 103: pp. 739-744, 1946.

Grodins FS. "Analysis of factors concerned in regulation of breathing in exercise," *Physiol. Rev.*, 30: pp. 220-239, 1950.

Grodins FS, Gray JS, Schroeder KR, Norins AL and Jones RW. "Respiratory responses to CO_2 inhilation. A theoretical study of a non-linear biological," *J. Appl. Physiol.*, 7: pp. 283-308, 1954.

Grodins FS. Control Theory and Biological Systems. Columbia Univ. Press, New York, 1963.

Hacisalihzade SS."Biomedical applications of control engineering," *IEEE Control Systems*, 12(6): pp.4-5, 1992.

Hahn CEW, Foex P."A recent development in the technique of dynamically plotting the oxyhaemoglobin dissociation curve in vitro with associated improvement in PO_2 electrode performance" *Oxygen Measurements in Biology and Medicine*, Butterworth & Co., Toronto, pp.45-68, 1975.

Hay WW, Thilo E, Curlander JB. "Pulse oximetry in neonatal medicine" *Clin in Perinatol*, 18(3): pp.441-472, 1979.

Horgan JD and Lange RL. "Digital computer simulation of the human respiratory system," *IEEE Intern. Conv. Record II*, 9: pp. 149-158, 1963.

Horgan JD and Lange RL. "Computer simulation of the respiratory response to the cerebrospinal fluid PCO_2 in the cat," *Biophys. Journal*, 8: pp. 935-945, 1965.

Kari MA, Hallman M, Eronen M, Teramo K, Virtanen M, Koivisto M, Ikonen RS. "Prenatal dexamethosone treatment in conjunction with rescue therapy of human surfactant: A randomized placebo-controlled multi-center study", *Pediatrics*, 93: pp.730-736, 1994.

Kinsey VE, "Retrolental fibroplasia: cooperative study of retrolental fibroplasia and the use of oxygen," *Arch Opthalmol*, 56: p.481, 1956.

Kraus AN, Klain DB, Dahms B and Auld PA. "Vital capacity in premature infants," *Amer. Rev. Resp. Dis.* 108: p.1361, 1973.

Linkens DA and Mahfouf M. "Fuzzy logic knowledge-based control for muscle relaxant anaesthesia," *Proc IFAC Symp. Modelling & Control in Medicine*, Venice, Italy, pp. 185-190, 1988.

Linkens DA, "Adaptive and intelligent control in anesthesia," *IEEE Control Systems*, 12(6): pp. 6-11, 1992.

MacDonald, AD. "Cerebral palsy in children of very low birthweight" *Archs Dis Childh*, 38: p.570, 1963.

Mamdani EH, Assilian S."An experiment in linguistic synthesis with a fuzzy logic controller," *International Journal of Machine Studies*, 7(1): pp. 1-13, 1975.

Mason DG, Linkens DA, Abbod MF, Edwards ND and Reilly CS."Automated Delivery of muscle relaxants using fuzzy logic control," *IEEE Eng. in Med. and Biology*, 13(5): pp. 678-686.

Mathworks, Inc. MATLAB. Natick, Mass. 1995.

Meier R, Nieuwland J, Zbinden AM and Hacisalihzade SS."Fuzzy logic control of blood pressure during anesthesia," *IEEE Control Systems*, 12(6): pp. 12-17, 1992.

MicroSoft, Inc. Windows 3.10. Redmond, Wash. 1993.

Milhorn HT Jr. and Guyton AC. "An analog computer analysis of Cheyne-Stokes breathing," *J. Appl. Physiol.*, 20: pp. 328-338, 1965.

Milhorn HT Jr., Benton R, Rose R and Guyton AC. "A mathematical model of the human respiratory control system," *Biophys. Journal*, 5: pp. 27-46, 1965.

Milhorn HT Jr. The Application of Control Theory to Physiological Systems. W.B.Saunders Co. Philadelphia, 1966.

Morozoff EP, Evans RW. "Closed loop control of SaO_2 levels in neonates," *Proc 26th Annual Meeting of the Association for the Advancement of Medical Instrumentation.* Washington, p.65., 1991.

Morozoff EP, Evans RW."Closed loop control of SaO_2 in the neonate," *Biomed Instrum Technol*, 26(2): pp.117-123, 1992.

Morozoff EP, Evans RW, Smyth JA."Automatic control of blood oxygen saturation in premature infants," in *Proc of 2nd IEEE Conf on Control Appl*, pp.415-420, 1993.

Morozoff EP, Smyth JA, Evans RW. "Automatic SaO_2 control using adaptive modelling," *Proc 20th Conf. of Canadian Med. Biol. Eng. Soc.*, Vancouver, p.144, 1994.

Northway WH, Rosan Jr. RC, Porter DY. "Pulmonary disease following respiratory therapy" *New England Journal of Medicine*, 276: p.357, 1967.

Oshita S, Nakakimura K, Sakabe T."Hypertension control during anesthesia," *IEEE Eng. in Med. and Biology*, 13(5): pp. 667-670, 1994.

Payne JW, "Retinopathy of prematurity", *Schaffer's Diseases of the Newborn*, eds. M.E.Avery and H.W.Taeusch, Toronto: WB Saunders Co., pp. 909-914., 1984.

Poets CF, Southall DP."Noninvasive monitoring of oxygenation in infants and children: practical considerations and areas of concern," *Pediatrics*, 93(5): pp.737-746, 1994.

Polgar G. "Airway resistance in the newborn infant. Preliminary Comunication," *J. Ped.* 59: p.915, 1961.

Polgar G, Kong G. "The nasal resistance of newborn infants," *J. Ped.* 67: p. 557, 1965

Praud JP, Carofilis A, Bridely F, Lacaille F, Dehan M, Gaultier CL. "Accuracy of two wave pulse oximetry in neonates and infants," *Pediatric Pulm*, 6: pp.180-182, 1989.

Richardson P. Lung Mechanics: a discussion of methods for measurements in newborn infants. ARKOS. Los Angeles, CA. Curant Communications Inc., 1989.

Rideout VC. Mathematical and Computer Modelling of Physiological Systems. Prentice Hall, Inc. New Jersey, 1991.

Rolfe P."Intra-vascular oxygen sensors for neonatal monitoring," *IEEE Eng in Med and Biology*, 13(3): pp.336-346, 1994.

Ross J. Jr. "Cardiovascular System", In: Best and Taylor's Physiological Basis of Medicine. JB West (ed.), Williams & Wilkins, Los Angeles, pp. 108-332, 1985.

Saito K, Honda Y and Hasamura N. "Evaluation of respiratory response to changes in PCO2 and hydrogen ion concentration of arterial blood in rabbits and dogs," *Japan Journal Physiol.*, 10: pp. 634-645, 1960.

Scarpelli EM. Pulmonary Physiology of the Fetus Newborn and Child. Lea & Febiger, Philadelphia, 1975.

Severinghaus JW. "Simple, accurate equations for human blood O_2 dissociation computations" *Journal Appl Physiol*, 46(3): pp.599-602, 1979.

Sheppard CW. "The theory of the study of transfer within a multicompartment system using isotropic tracers," *J. Appl. Physics*, 19: p. 70, 1948.

Sheppard LC. "Computer control of the infusion of vasoactive drugs," *Ann of Biomed Engineering*, 20: pp. 431- 444, 1980.

Soller BR."Design of intravascular fiber optic blood gas sensors," *IEEE Eng. in Med. and Biology*, 13(3): pp.327-335, 1994.

Stahl WR. "Scaling of respiratory variables in mammals," *J. Appl. Physiology*, 22(3): pp. 453-460. 1967.

Sugeno M. Industrial Applications of Fuzzy Control. Elsevier Science Pub. Co., 1985.

Taube J."Automatic control of neonatal fractional inspired oxygen," Thesis, Drexel University, 1989.

Tehrani FT, Bazar AR."An automated control system for oxygen therapy of newborn infants," in *Proc IEEE EMBES '91*, pp.2180-2182, 1991.

Terry TL, "Extreme prematurity and fibroblastic overgrowth of persistent vascular sheath behind each crystalline lens. Preliminary Report," *Am Journal Opthalmol.*, 25: p.203, 1942.

Van Marter LJ, Leviton A, Kuban KCK, Pagano M, Allred EN. "Maternal glucocorticoid therapy and reduced risk of bronchopulmonary dysplasia", *Pediatrics*, 86: pp.331-336, 1990.

Way WL, Costley EC, Way EC."Respiratory sensitivety of the newborn infant to meperidine and morphine. *Clin Pharmocol Ther*, 6: p 454, 1965.

West JB (ed.). Bioengineering Aspects of the Lung. Marcel Dekker Inc., New York, 1977.

West JB. "Respiration", In: Best and Taylor's Physiological Basis of Medicine. JB West (ed.), Williams & Wilkins, Los Angeles, pp. 546-632, 1985.

Wood WG, Weatherall DJ. "Haemoglobin synthesis during foetal development," *Nature*, 244: p.162, 1973.

Wilkinson MH, Berger PJ, Blanch N and Brodecky V. "Effect of veous oxygenation on arterial desaturation rate during repetative apneas in lambs," *Resp. Physiology*, 101: pp.321-331, 1995.

Yamamoto W and Hori T. "Phasic air movement model of the respiratory regulation and carbon-dioxide balance," *Computers Biomed. Res.*, 3: pp.699-717, 1970.

Ying H, Sheppard LC and Tucker."Expert-system based fuzzy control of arterial pressure by drug infusion," *Medical Progress through Technology*, 13: pp. 202-215, 1988.

Ying H, McEacherin M, Eddleman DW, Sheppard LC."Fuzzy Control of mean arterial pressure in postsurgical patients with sodium nitroprusside infusion," *IEEE Trans Biomed Eng*, 39:1060-1070, 1992.

Ying H, Sheppard LC. "Regulating Mean Arterial Pressure in Postsurgical Cardiac Patients," *IEEE Eng. in Med. and Biology*, 13(5):pp.671-677, 1994.

Zadeh LA. "Fuzzy sets," *Information and Control*, 8: pp. 338-353, 1965.

Zadeh LA. "Outline of a new approach to the analysis of complex systems and decision processes," *IEEE Transactions on Systems, Man*, and Cybernetics, 3(1): pp. 28-44, 1973.

Zadeh LA. "The concept of a linguistic variable and its application to approximate reasoning, Parts 1, 2, and 3," *Information Sciences*, 8: pp.199-249, 8: pp. 301-357, 9: pp. 43-80, 1975.